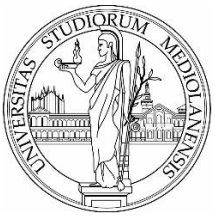

UNIVERSITÀ DEGLI STUDI DI MILANO

PhD Course in Veterinary and Animal Science

Cycle XXXI

COMPARATIVE EVALUATION OF PROGNOSTIC MARKERS IN CANINE AND FELINE MELANOMAS

PhD Candidate: Laura Nordio

R11408

Tutor: Prof. Chiara Giudice

Academic Year 2017-2018

SUMMARY

Abstract 1

BACKGROUND 5

Rationale of the project 5

Pathology of melanoma 7

Human and canine oral melanoma 11

Human and feline ocular melanoma 14

LTA4H, Leukotriene A4 Hydrolase 18

FXR1, Fragile X mental retardation-related protein 1 19

Metalloproteinases and tumor-matrix interactions 21

AIMS 26

I. VALIDATION OF ANTI-FXR1 ANTIBODIES IN CANINE NORMAL TISSUES AND MELANOCYTIC NEOPLASMS 27

Abstract 27

Introduction 27

Materials and methods 29

Results 32

Discussion 38

Conclusions 40

II. MOLECULAR AND IMMUNOHISTOCHEMICAL EXPRESSION OF LTA4H AND FXR1 IN CANINE ORAL MELANOMAS 42

Abstract 42

Introduction 42

Materials and methods 45

Results 50

Discussion 57

Conclusions 61

III. PRELIMINARY OBSERVATIONS ON MATRIX METALLOPROTEINASES IN CANINE ORAL MELANOMA: ASSOCIATION OF MMP-9 AND TIMP-2 WITH FXR1 IMMUNOHISTOCHEMICAL EXPRESSION AND CLINICAL OUTCOME 64

Abstract 64

Introduction 64

Materials and methods 66

Results 69

Discussion 73

Conclusions 75

IV. EXPRESSION OF MMP-9 AND TIMP-2 IN FELINE DIFFUSE IRIS MELANOMA AND CORRELATION WITH HISTOLOGICAL PARAMETERS OF MALIGNANCY 76

Abstract 76
Introduction 76
Materials and methods 78
Results 80
Discussion 85
Conclusions 89
V. CASE REPORT: EVIDENCES OF VASCULOGENIC MIMICRY IN A PALPEBRAL MELANOCYTOMA IN A DOG 90
Abstract 90
Introduction 90
Case report 91
Discussion and conclusions 93
GENERAL CONCLUSIONS 96
ACKNOWLEDGMENT 98
REFERENCES 99
LIST OF PHD ACTIVITIES AND PUBLICATIONS 112
ATTACHED PAPERS 118

Abstract

The present PhD project investigates animal spontaneous models of non-UV induced melanomas, namely canine oral melanoma and feline iris diffuse melanoma (FDIM), which shares unique similarities in biological behavior with human mucosal melanoma and human iris melanoma, respectively.

The project investigates selected markers related to the pathogenesis and prognosis of these tumors, i.e. gene and proteins that have been implicated in the progression and metastasis in human, canine and feline melanomas, such as Leukotriene A4 Hydrolase (LTA4H), Fragile X mental retardation-related protein 1 (FXR1) and matrix-metalloproteinases (MMPs). LTA4H is an enzyme of the arachidonic acid cascade, FXR1 is a RNA binding protein, MMPs a family of proteolytic enzymes of the extracellular matrix.

The specific aims of the project are:

1) the validation of anti-FXR1 antibodies in the canine species;
2) the investigation of the expression of LTA4H and FXR1 in canine oral melanoma;
3) the study of FXR1-induced modulation of MMPs in canine oral melanoma;
4) the study of MMPs and tumor-matrix interaction in feline diffuse iris melanoma.

1) Two different commercially available polyclonal anti-human FXR1 antibodies were validated for use in dogs. Western blot experiments highlighted the specificity of cross-reaction. Immunohistochemistry described for the first time the specific distribution of FXR1 protein in canine normal tissues, and then the expression of FXR1 in a pool of canine melanocytic tumors.
2) LTA4H and FXR1 genes and proteins expression was investigated in FFPE canine oral melanomas (histology and immunohistochemistry, n=36, from 32 dogs; RT-PCR, subset n=23; clinical follow-up, subset n=13). ΔCt expression values ranged 0.76-5.11 for *LTA4H* and 0.22-6.24 range for *FXR1* (out of range in 3 cases). The immunohistochemical expression of the proteins was evaluated as IRS-score (percentage of positive cells combined with intensity of the staining). IRS-score of LTA4H and FXR1 proteins did not correlate with the expression of the codifying genes.

LTA4H and FXR1 seemed not correlated with the known criteria of malignancy or with the clinical outcome, when available.

3) Since FXR1 belongs to a family of RNA binding protein able to modulate the mRNA coding for the proteolytic enzyme MMP-9, MMP-9 and its inhibitor TIMP-2 were investigated by immunohistochemistry in canine oral melanomas to assess the association of FXR1 with MMP-9 and the association of MMPs activity with the clinical outcome. MMP-9 expression seemed not associated with FXR1 in canine oral melanomas. Anyway, intense levels of MMP-9/TIMP-2 were observed in cases with high expression of FXR1 and with unfavorable clinical outcome in canine oral melanoma.
4) The expression of MMPs in FDIM was investigated. Immunohistochemical expression of MMP-9/TIMP-2 was investigated in 62 FDIM and results were compared with the histological grade and mitotic index. MMP-9 and TIMP-2 were expressed in 77.4% and 71.0% FDIM, respectively. Increasing MMP-9 and TIMP-2 paralleled with high histological grades and high mitotic index.

Riassunto

Il presente progetto di dottorato è volto allo studio di modelli animali di melanoma spontaneo non UV-indotto, nello specifico il melanoma orale del cane ed il melanoma irideo diffuso del gatto, che condividono caratteristiche uniche per comportamento biologico con i melanomi umani rispettivamente mucosale ed irideo.

Il progetto indaga marcatori associati con la patogenesi e la prognosi di questi tumori, ossia geni e proteine implicati nella progressione e nella metastasi dei melanomi di uomo, cane e gatto, come Leukotriene A4 Hydrolase (LTA4H), Fragile X mental retardation-related protein 1 (FXR1) e le metalloproteasi della matrice (MMP). LTA4H è un enzima della cascata dell'acido arachidonico, FXR1 è una RNA-binding protein, le MMP sono una famiglia di enzimi proteolitici della matrice extracellulare.

Gli obiettivi specifici del progetto sono:

1) la validazione di anticorpi anti-FXR1 nel cane;
2) lo studio dell'espressione di LTA4H e FXR1 nel melanoma orale del cane;
3) l'analisi della modulazione FXR1-indotta delle MMP nel melanoma orale del cane;
4) l'indagine delle MMP e delle interazioni tumore-matrice nel melanoma irideo diffuso di gatto.

1) Due anticorpi policlonali commerciali anti-FXR1 umano sono stati validati per l'uso nella specie canina. La western blot ha appurato la specificità del legame antigene-anticorpo. Con l'immunoistochimica, è stata descritta per la prima volta la distribuzione specifica della proteina FXR1 in tessuti normali di cane, successivamente testata anche in un gruppo di diversi tumori melanocitari di cane.
2) I geni e le proteine LTA4H e FXR1 sono stati analizzati in campioni di melanoma orale canino fissati in formalina e inclusi in paraffina (istologia ed immunoistochimica, n=36, da 32 cani; RT-PCR, sottogruppo n=23; dati clinici di sopravvivenza, sottogruppo n=13). I valori di espressione ΔCt variavano 0.76-5.11 per LTA4H e 0.22-6.24 per FXR1 (fuori dal range in 3 casi). L'espressione immunoistochimica delle proteine è stata valutata come punteggio IRS (percentuale di cellule

positive combinate con l'intensità). I punteggi IRS di LTA4H e FXR1 non erano correlati con l'espressione dei geni codificanti. LTA4H e FXR1 non erano correlati con i dati clinici di sopravvivenza, quando disponibili.

3) Inoltre, poiché FXR1 appartiene ad una famiglia di proteine in grado di modulare l'espressione di mRNA codificante per l'enzima proteolitico MMP-9, l'espressione immunoistochimica di MMP-9 e del suo inibitore TIMP-2 è stata studiata nel melanoma orale del cane, in modo da indagare l'assocazione dell'espressione di FXR1 con le MMP e l'associazione delle attività delle MMP con i dati di sopravvivenza. L'espressione di MMP-9 non è risultata associata con FXR1. Tuttavia, livelli intensi di MMP-9/TIMP-2 sono stati osservati nei casi di melanoma orale con espressione intensa di FXR1 e con esito clinico sfavorevole.
4) Infine, è stata studiata l'attività di MMP nel melanoma irideo diffuso del gatto (FDIM). Sessantadue casi di FDIM sono stati analizzati per studiare l'espressione di MMP-9/TIMP-2 in riferimento al grado istologico e all'indice mitotico dei tumori. MMP-9 e TIMP-2 erano espresse nel 77.4% e 71.0% dei FDIM, rispettivamente. Un'espressione crescente di MMP-9/TIMP-2 è stata correlata con gli alti gradi istologici e con alto indice mitotico.

BACKGROUND

Rationale of the project

Spontaneously occurring non-UV induced melanomas are relatively common in dogs and cats and may be considered spontaneous animal models of certain types of human melanoma. They arise and metastasize spontaneously, thus more likely reflecting the process of spontaneous tumorigenesis than experimentally-induced models. Melanoma is quite challenging to pathologists under both diagnostic and prognostic point of view

The melanocytic tumors investigated in the present project are canine oral melanoma and feline diffuse iris melanoma, which have been selected since they share marked biological similarities with the human mucosal melanoma and human iris melanoma, respectively.

Melanoma is an aggressive neoplasia, which, as in human beings as in cats and dogs, frequently recur and metastasize (Smith et al., 2002). Canine oral melanomas are highly heterogeneous and aggressive tumors (Smith et al., 2002). Similarly, in human medicine, oral melanomas are, in turn, considered a rare but aggressive variant of human melanoma (Mihajlovic et al., 2012). Both exhibit a similar malignant behavior, that includes biological aggressiveness, metastasizing tendency with poor prognosis, and specific mutations.

Feline diffuse iris melanoma (FDIM) is the most common feline primary intraocular tumor. FDIMs are usually malignant, even if slowly progressive (Dubielzig, 2017). Similarly, iris melanoma is the most common malignant neoplasm of the human iris (Demirci et al., 2002).

At the present day, the main issue for veterinary pathologists is the prognostic value of the histological diagnosis. After years of efforts in demonstrating histological features indicative of malignancy and metastatic behavior, the new frontier of study of tumors is the analysis of differential gene and protein expression. During last years, altered expression of specific genes, such as *LTA4H* and *FXR1,* has been demonstrated in a subset of human and canine uveal melanomas,

correlating with the biological behavior of the neoplasms (Malho et al., 2013). *FXR1* belongs to a family of mRNA binding protein that can target, among the others, the mRNA coding for MMP-9 (Metalloproteinase-9) (Castagnola et al., 2017). MMP-9, in turn, is an endopeptidase with proteolytic activity, whose ability to digest the extracellular matrix has been involved in the process of tumor invasion, in the wider scenario of the interaction between neoplastic cells and the so-called tumor microenvironment.

The present study analyzes samples from two models of non-UV induced melanoma, namely canine oral melanoma and feline diffuse iris melanomas, facing the topic with different approaches.

1) Pathogenesis: the project assesses if the activity of enzymes underlying tumor-matrix interactions is correlated with tumor progression (as it is in the analysis of metalloproteinases in canine oral melanomas and feline diffuse iris melanoma);
2) Prognosis: the project tests if the differential expression of specific target genes may be associated with clinical implications, thus bearing prognostic value (as it is in the study of the expression of LTA4H and FXR1 in canine oral melanomas);
3) Multidisciplinary approach: in a modern concept of diagnostic pathology, the histology is joined by immunohistochemical analyses and molecular biology techniques, capable to investigate molecules at different levels (eg. mRNA, protein).

Results of the present study are expected to enlarge the data available on melanoma in veterinary literature, to understand the molecular pathways involved in the pathogenesis of this kind of tumors, and to justify (or exclude) the use of selected prognostic markers, base for future therapeutic considerations or diagnostic tests.

Pathology of melanoma

Melanocytes are dendritic cells that origin from the neuroectodermal melanoblasts. During development, melanocytes colonize the skin, eye and, to a lesser degree, a broad range of other tissues throughout the body. They are found, in the adult, within the basal layer of the epidermis interspersed between basal keratinocytes. Melanin is normally packed in the cytoplasm inside melanosomes and transferred to keratinocytes (Smith et al., 2002). Melanoma may arise in any location where melanocytes are present, thus including the eye, mucosae, skin, leptomeninges, and some internal organs.

Human cutaneous melanoma (US incidence: 153.5 cases per million per year) represents the fifth most common tumor in the United States, whereas mucosal melanoma (US incidence: 2.2 cases per million per year) represents only 0.03% of all cancer (1.4% of all melanomas) (Mihajlovic et al., 2012; Spencer and Mehnert, 2016).

Initiation of melanoma in humans is due to mutations generated by UVA and UVB solar radiation, in 65% of cutaneous melanomas, or to driver oncogenic mutations (eg. *NRAS, BRAF, KIT*), associated with distinct morphologic melanoma subtypes (Shain and Bastian, 2016; Tímár et al., 2016).

The present project focuses on animal model of non-UV induced melanomas.

In humans, melanocytic neoplasms commonly evolve from precursors lesions, ranging from benign lesions, termed melanocytic naevi, to malignant ones: melanomas (Shain and Bastian, 2016; Tímár et al., 2016). On the opposite, little is known about initiation of most animal melanomas, although some genetic susceptibility due to great frequency of spontaneous mutations has been recognized. While most human melanomas evolve form precursor lesions, most animal melanomas are believed to arise *de novo* (Smith et al., 2002).

Histological morphology of melanoma (Figure 1) has a wide variety of presentation, both as degree of pigmentation and morphologic types (Smith et al., 2002). Different recognized cellular morphologies include (Smith et al., 2002):

- epitheliod type, with round discrete cells with abundant cytoplasm, round nucleus, prominent nucleolus;

- spindle type, with a cellular arrangement in stream and bundles;
- mixed type, consisting in a mixture of the previous types (epithelioid and spindle);
- balloon cell type, round cells with finely granular abundant cytoplasm;
- signet-ring type, with pleomorphic amelanotic cells with eccentric nucleus;
- adenoid-papillary form, with cells in acinar structures.

As far as tumor growth pattern, melanomas can be compound, that is the presence of both epithelial/epidermal and submucosal/dermal components, or submucosal/dermal only. "Junctional" refers to the proliferation of neoplastic cells at the interface between epithelium/epidermis and submucosa/dermis. "Pagetoid" refers to the presence of neoplastic cells, single or aggregated, within the upper levels of the epithelium/epidermis (Smith et al., 2002).

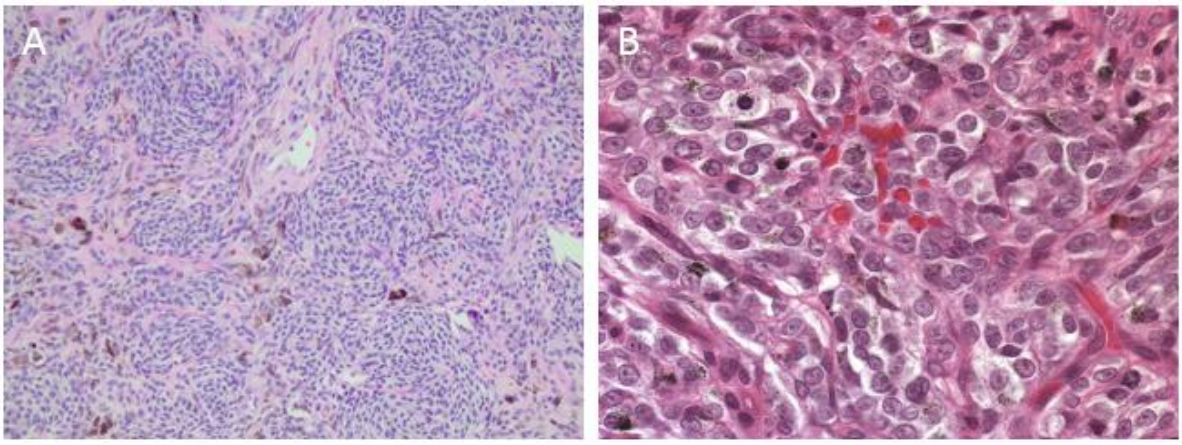

Figure 1- A) Dog, oral melanoma, spindle cell type. Neoplastic cells are spindle-shaped and arranged in concentric whorls and short interlacing bundles. H&E, 20x. B) Dog, oral melanoma, epithelioid cell type. There are lobules and packets of polygonal neoplastic melanocytes. H&E, 40x.

As previously mentioned, a diagnosis of melanoma can be tricky due to the wide amount of different morphology that this kind of tumors can adopt. Even more difficult can be the distinction between benign form, usually referred to as "melanocytoma", and the malignant form, usually called "melanoma" (Wilcock and Peiffer, 1986).

Several authors tried to investigate different histological and epidemiologic parameters searching for their prognostic significance. Spangler and Kass identified as negative determinants the mitotic index, nuclear atypia, tumor score, size of the tumor, presence of inflammation,

intralesional necrosis and the presence of metastasis (Spangler and Kass, 2006). Smedley and co-authors in a comparative review focused on the presence of metastasis, lymphatic invasion, mitotic index ≥ 4/10 high power field (HPF), nuclear atypia, degree of pigmentation (the higher the more favorable), level of infiltration and Ki67 index (Smedley et al., 2011). Bergin and colleagues suggested to evaluate the pigmentation together with nuclear atypia score, mitotic index, and Ki67 index (Bergin et al., 2011). Since all authors concluded with different findings or even conflicting results, there is still poor agreement about histological criteria to be commonly adopted in diagnostic pathology.

During the last years, more and more studies both in human and in veterinary medicine have been focusing on the research of genetic markers through the use of molecular analyses that are minimally invasive and can have a good predictive value (Malho et al., 2013; Onken et al., 2010, 2004; Poorman et al., 2015). Specific emphasis has been given to markers of potential development of metastatic disease. In human uveal melanoma, a highly aggressive subtype of melanoma in human beings, different studies have identified specific molecular/genetic profiles of tumors that allowed a molecular subdivision in two classes of neoplasm with different probabilities of tumor spread (Onken et al., 2010, 2004). Similarly, a project on canine uveal melanoma investigated prognostic biomarkers among a 12-discriminating gene set, and identified four genes *(HTR2B, FXR1, LTA4H, CDH1*) that demonstrated an increased expression in metastasizing melanomas (Malho et al., 2013).

Additional diagnostic test commonly adopted in the diagnosis of melanomas are immunohistochemical staining. Diagnostic markers include:

- PNL2: a still unidentified protein target, which reacts with normal and neoplastic melanocytes in benign and malignant lesions (Ramos-Vara et al., 2000; Giudice et al., 2010).
- Melan A: a melanocyte-differentiating protein recognized by tumor-infiltrating human cytotoxic T lymphocytes, highly specific since expressed by normal human melanocytes, benign nevi, melanomas, and, less frequently, desmoplastic human melanomas (Ramos-Vara et al., 2000; Giudice et al., 2010).

Other markers include: tyrosine reactive proteins 1 and 2; NSE (Neuron Specific Enolase); MITF-1, and S100, the latter being highly sensitive, but not specific (Smedley et al., 2011; Goldschmidt & Goldschmidt, 2017).

Human and canine oral melanoma

Human mucosal melanoma is a rare variant of human melanoma, representing about 0.03% of all tumors and 1.3% of all melanomas. Mucosal melanoma arises from mucosal epithelium of the respiratory, alimentary and genitourinary tracts, most commonly in the head and neck (55%), the anorectum (24%) and the vulvovaginal region (18%). The common anatomic locations are not associated with UV exposure, unlike cutaneous melanoma (Mihajlovic et al., 2012; Shain and Bastian, 2016; Spencer and Mehnert, 2016). Mucosal melanomas more frequently have a multifocal and amelanotic presentation (Ballester Sanchez et al., 2015). Among mucosal melanoma of the head and neck, 25-40% are located in the oral cavity. Oral melanoma is a rare tumor with incidence of 0.2 per billion. Timing of onset range between 50-80 years of age. Female and Japanese people are over-represented in the reported series (Mihajilovic et al., 2012). Oral melanoma arise especially in the large palate and upper alveolus, whereas other sites include mandibular gingiva, labial and buccal mucosa, and, extremely rare, floor of the mouth, tongue, tonsils, uvula and parotid gland (Spencer and Mehnert, 2016; Mihajilovic et al., 2012).

Up to one third of oral melanomas are usually preceded by pre-existing melanocytic lesions, like melanosis (Spencer and Mehnert, 2016). Differential diagnosis of oral melanoma includes melanosis, melanotic macule, and oral nevi (Mihajilovic et al., 2012).

Mucosal melanomas are often aggressive and have a poor prognosis, regardless of the stage (Spencer and Mehnert, 2016). Mucosal melanomas have the lowest percentage of 5-years survival (25%), compared to 80.8% of cutaneous and 74.6% of ocular counterparts (Mihajilovic et al., 2012). Oral tumors are usually malignant and often associated with early involvement of the lymph nodes; even with aggressive surgical removal, there is a high tendency toward recurrence and widespread disease (Spencer and Mehnert, 2016). Human oral melanomas share their aggressive behavior with canine oral melanoma, which in turn is associated with a poor prognosis (Atherton et al., 2016).

Melanocytic neoplasms are quite common in the **dog**, where they represent about 3% of all neoplasms and 7% of malignant neoplasia (being the most common tumor of the oral cavity). The

locations mostly affected by melanomas in the canine species are the oral cavity (56%), the lip (23%), the skin (11%), the digit (8%) and the eye (2%).

Melanoma is the most common malignant tumor of the oral cavity in dogs, other common tumor of the oral cavity including squamous cell carcinoma, fibrosarcoma, epulides and odontogenic tumors (Uzal et al., 2016). Irish Setter, Chihuahua, Golden Retriever, and Cocker Spaniel are highly susceptible to melanoma of the lip, whereas German Shepherd Dogs and Boxers are prone to develop oral mucosal melanoma (Smith et al., 2002). Melanoma usually affects older dogs, averaging 8-11 years (Smedley et al., 2011). Presenting signs of oral melanoma include dysphagia, ptyalism, bleeding, and, occasionally, pathological fracture of the mandible (Smith et al., 2002).

In the dog, melanoma arising in the oral cavity, as well as at muco-cutaneous junctions and subungueal bed, are traditionally believed to be malignant even independently from the histological morphology, because they are infiltrative, frequently recur after surgical excision and have a high metastatic rate (Smith et al., 2002). On the opposite, cutaneous and ocular melanocytic tumors have a much less aggressive behavior (Smith et al., 2002), unlike humans. Oral melanomas grow rapidly, are invasive, often recur after surgical resection and frequently (70-90%) metastasize, via lymphatic or blood vessels, to regional lymph nodes, lungs and viscera (Bergman, 2007; Smith et al., 2002). The reported median survival time spans 5-7 months (Gillard et al., 2014; Ramos-Vara et al., 2000; Spangler and Kass, 2006). However, also a subset of oral melanocytic tumors with more favorable clinical course and prolonged survival exists, as expected mainly in dogs with histologically well-differentiated melanocytic neoplasms (Bergin et al., 2011; Esplin, 2008; Poorman et al., 2015; Spangler and Kass, 2006).

Classical histological criteria of malignancy are poor indicators of metastatic behavior of the tumor: several works evaluated prognostic markers and possible threshold values (Bergin et al., 2011; Smedley et al., 2011; Spangler and Kass, 2006), but, due to different findings or even conflicting results, there is still poor agreement about histological criteria to commonly adopt in diagnostic pathology. At this time, there is no good way to predict the likely progression of disease in individual dogs.

Currently, there are no specific staging systems for oral melanomas, therefore, oral melanomas are usually staged according to the staging scheme proposed by Owen for oral neoplasms in general (Table 1). Surgical excision is the current recommended treatment for canine oral malignant melanomas. Additional therapies such as radiation therapy or chemotherapy generally are poorly beneficial, while new therapies such as xenogeneic DNA vaccines and tyrosine kinase inhibitors are being tested. Death is usually due to systemic metastases (Munday et al., 2017).

Table 1 - Current WHO classification for oral neoplasm of domestic animals: TMN classification and staging of oral neoplasms (Munday et al., 2017)

T. Tumor size or involvement
T1. Tumor <2 cm diameter.
T1a. No bone invasion
T1b. Bone invasion
T2. Tumor 2–4 cm diameter.
T2a. No bone invasion
T2b. Bone invasion
T3. Tumor >4 cm diameter.
T3a. No bone invasion
T3b. Bone invasion
N. Regional node involvement
N0. No evidence of involvement.
N1. Movable ipsilateral nodes.
N1a. Not considered to contain metastases
N1b. Considered to contain metastases
N2. Movable contralateral or bilateral nodes
N2a. Not considered to contain metastases
N2b. Considered to contain metastases
M. Distant metastasis
M0. No distant metastases
M1. Distant metastases

Human and feline ocular melanoma

Intra-ocular melanocytic neoplasms are classified based on the ocular anatomical site of onset (iris, choroid, ciliary bodies, corneo-scleral junction) and malignancy (melanocytomas or melanomas). Human intra-ocular melanocytic neoplasms may arise in the choroid (80%), ciliary bodies (12%) and iris (8%) (Lee, 2002; Lee et al., 2016).

The most frequent benign human ocular melanocytic neoplasms are melanocytic nevi, small pigmented lesions which may arise anywhere in the anterior or posterior uvea. Histologically, nevi can be classified as polyhedral-cell, spindle-cell, dendritic-cell and balloon-cell type (Lee, 2002; Spencer, 1996). Affected patients average 53 years of age; white and male patients are overrepresented (Spencer, 1996).

The most common human malignant melanocytic ocular neoplasia is choroidal melanoma. The histological classification of choroidal melanoma was originally proposed by Callender in 1931 and later modified by McLean, with the identification of four morphological types: spindle cells type A, spindle cells type B, epithelioid cells and mixed cells (Callender, 1931; McLean et al., 1983). Tumors of large size and epithelioid-type have a higher tendency to metastasize. Frequent sizes of metastases of choroidal melanoma are liver, lung and lymph nodes (Spencer, 1996), and micrometastases usually occurs before the diagnosis. The abundance of blood vessels in the uvea, opposed to the lack of lymphatics, leads to a preferential hematogenous route of metastases (Demirci et al., 2013).

Iris melanoma, although representing only 2−5% of all uveal melanoma (Batioğlu and Günalp, 1998), is the most common malignant neoplasm of the **human** iris, representing 49−72% of all iris lesions (Ashton, 1964; Starr et al., 2004). Elderly whites patient with a light iris color are predisposed (Khan et al., 2012). Human iris melanoma can be classified, according to two different growth patterns, as circumscribed or diffuse iris melanoma (Demirci et al., 2002; Henderson and Margo, 2008). Circumscribed iris melanoma has distinct margins, whereas diffuse iris melanoma have an infiltrative, flat, ill-defined growth pattern with confluent or multifocal iris involvement (Demirci et al., 2002). Iris melanoma may arise from pre-existing iris nevi (Shields et al., 2013).

Jakobiec and Silbert revised the Calleder's original histological classification thus identifying nine morphological categories for iris melanocytic lesions, which include benign types, that are i) melanocytosis; (ii) melanocytoma; (iii) epithelioid cell naevus; (iv) intrastromal spindle-cell naevus; (v) spindle-cell naevus with surface plaque; and (vi) borderline spindle-cell naevus. Malignant types are vii) spindle-cell melanoma; (viii) spindle and epithelioid melanoma (so called 'mixed cellularity'); and (ix) epithelioid melanoma (Jakobiec and Silbert, 1981; Starr et al., 2004). Diffuse iris melanoma represents about 10% of iris melanoma. It presents most often with unilateral hyperchromic heterochromia and secondary glaucoma, due to neoplastic seeding in anterior chamber and direct invasion of the angle (Demirci et al., 2002). Diffuse iris melanoma have a higher incidence of epithelioid-cell type morphology compared to most iris melanoma, therefore have a higher tendency to exfoliate (Demirci et al., 2002).

Iris melanoma is considered less aggressive than melanoma of the ciliary body and choroid (Henderson and Margo, 2008). However, the prognosis of diffuse iris melanoma is generally poor compared to other iris melanoma, with a metastasizing rate of 2.6%, 10.5%, and 6.9% for spindle, mixed, and epithelioid cell types, respectively (Geisse and Robertson, 1985). Associated findings include also secondary glaucoma and iritis (Khan et al., 2012). The therapeutic management of diffuse iris melanoma range from observing the tumor and treating medically the associated glaucoma to enucleation of the eye globe and custom-designed radiotherapy (Demirci et al., 2002; Khan et al., 2012; Starr et al., 2004).

Molecular analyses in human uveal melanomas identified different types of alterations in the pathogenesis of these tumors. Onken and colleagues distinguished two different molecular classes associated with metastatic risk of primary uveal melanomas (low and high risk of metastases) using gene expression profiling. They identified top 26 genes, especially those implied either in cell communication or development of the neural crest, for example *KIT*, or in cell growth, cell motility, cell death (Onken et al., 2004). In a subsequent study, therefore, they identified a diagnostic test based on the differential regulation of 12 discriminating genes: *HTR2B, ECM1, RAB31, CDH1, FXR1, LTA4H, EIF1B, ID2, ROBO1, LMCD1, SATB1, MTUS1* (Onken et al., 2010). Moreover, a screening of these same genes revealed an upregulation of 4 of them, i.e. *FXR1, LTA4H, CDH1, HTR2B*, also in

dogs with uveal melanoma with a metastasizing behavior (Malho et al., 2013). Van Raamsdonk also identified that the oncogenes *GNAQ* and *GNA11* are mutated in 83% of human uveal melanomas (Van Raamsdonk et al., 2010), whereas the presence of *BRAF* mutations had conflicting results (Henriquez et al., 2007; Rimoldi et al., 2003).

Incidence of melanomas in **cats** peak between 8-12 years of age (Smedley et al., 2011). Tumors of melanocytic origin are the most common primary neoplasm of the globe in cats (Dubielzig, 2017). Affected animals average 11,5 years and are equally distributed among sexes and breeds (Patnaik and Mooney, 1988). The most common melanocytic ocular tumor of cats is located in the iris and is known as **feline diffuse iris melanoma** (Dubielzig, 2017).

Feline diffuse iris melanoma often begins as a focal abnormal pigmentation of the iris, which may persist for years, and later expand, becoming nodular or distorting the profile of the iris or pupil (Dubielzig, 2017). Feline diffuse iris melanoma is usually malignant, even if slowly progressive. Enucleation in early stages is usually curative; otherwise, advanced stages bear increasing risk of life-threatening systemic metastasis to the liver, lung, and kidneys (Dubielzig, 2017). Affected eyes may also develop secondary glaucoma.

On histology, neoplastic cells are usually pleomorphic, mostly spindle-shaped, or, less commonly, balloon-type (Dubielzig, 2017). Feline diffuse iris melanomas can be graded histologically according to the system proposed by Kalishman and colleagues (Kalishman et al., 1998) based on tumor extension:

- Grade I: accumulation of small pigmented cells locally confined to the anterior iris surface.
- Grade II: neoplastic cells confined to the iris stroma and trabecular meshwork.
- Grade III: neoplastic cells extending into the ciliary body stroma but not disrupting the posterior iris epithelium.
- Grade IV: neoplastic cells extending throughout the ciliary body stroma and scleral venous plexus but not disrupting the posterior iris epithelium.

- Grade V: neoplastic cells confined to the iris and trabecular meshwork but also disrupting the posterior iris epithelium.
- Grade VI: neoplastic cells extending throughout the ciliary body stroma and scleral venous plexus and also disrupting the posterior iris epithelium.

Based on this classification, the authors further defined a simplified grading system:

- Early: tumor only in the iris and trabecular meshwork
- Moderate: tumor in the iris and rostral ciliary body but not in the sclera
- Advanced: tumor throughout the ciliary body and extending into the sclera

Higher grades are significantly associated with lower survival (Kalishman et al., 1998). Moreover, results from this study suggested that when enucleation is done in the early stages of tumor progression, with the tumor confined to the iris stroma, the survival time of affected cats was not influenced, whereas when enucleation is done after invasion of the ciliary body stroma, or later, there is a progressively poorer prognosis. Cats with glaucoma due to tumor infiltration of the ciliary body were also likely to die earlier (Kalishman et al., 1998). Currently the therapy of election for feline diffuse iris melanoma is the surgical enucleation of the affected eye.

More recently, other authors focused on the research of possible prognostic morphologic criteria. Among these, there were mitotic index, nucleus/cytoplasm ratio, number of nucleoli, presence of glaucoma, and cellular morphology, even if with mild prognostic significance (Duncan and Peiffer, 1991; Kalishman et al., 1998). Wiggans and colleagues highlighted extrascleral extension, necrosis within the neoplasm, a mitotic index of >7 mitoses in 10 high-power (400x) fields, choroidal invasion, and increased E-cadherin and Melan-A label intensity as associated with increased rate of metastasis (Wiggans et al., 2016).

The few molecular studies on ocular melanomas in cats revealed a significant upregulation of *KIT* and *LTA4H*, as well as a downregulation of *GNAQ, GNA11, BRAF and RASSF1* (Rushton et al., 2017). The same study from Rushton and colleagues did not identified mutation in *GNAQ, GNA11, BRAF* or any other tested genes, as opposed to human melanomas (Henriquez et al., 2007; Rushton et al., 2017; Van Raamsdonk et al., 2010).

Here it follows a brief dissertation on the main molecules investigated in the present PhD project, namely Leukotriene A4 Hydrolase (LTA4H), Fragile X mental retardation-related protein 1 (FXR1) and Matrix Metalloproteinases (MMPs).

LTA4H, Leukotriene A4 Hydrolase

LTA4H is a cytosolic hydrolytic enzyme, which catalyze the passage of conversion of leukotriene A4 into leukotriene B4 inside the arachidonic acid cascade. Prostaglandins and leukotrienes are lipid mediators derived from arachidonic acid (AA) which stimulate vascular and cellular reactions in acute inflammation. AA-derived mediators, also called eicosanoids, are synthesized by the classes of enzyme either cyclooxygenases (COX), producing prostaglandins and thromboxanes, or lipoxygenases (LO), producing leukotrienes and lipoxins. In leukocytes and mast cells, 5-lipoxygenases converts AA into hydroperoxyeicosatetraenoic acid (HPETE) which is then converted to the intermediate complex LTA4. LTA4 is subsequently converted either to LTB4 through the hydrolysis by LTA4 hydrolase or to LTC4 through the conjugation with glutathione by LTC4 synthetase. LTA4 and LTB4 are produced on either side of the nuclear envelope by nuclear or cytosolic pools of 5-lipoxygenase and LTA4H (Dubois, 2003). Leukotrienes increase vascular permeability, act for leukocytes chemotaxis and cause vasoconstriction. LTB4 is mainly a neutrophilic product and acts as a chemotactic mediator that activates neutrophils and macrophages with aggregation and adhesion to the endothelium, generation of ROS and release of lysosomal enzymes (Kumar et al., 2014; Zachary, 2017).

LTA4H expression is widely distributed and virtually detected in all tissue (Ohishi et al., 1990).

LTA4H has been extensively studied for its known role in inflammation, but, since many tumors arise from sites of chronic inflammation, its possible implication in carcinogenesis has also been in investigated. For example, LTA4H is overexpressed in esophageal adenocarcinoma in human and rats (Chen et al., 2003). It has been therefore hypothesized that LTA4H increases the inflammation and stimulate paracrine and autocrine growth of preinvasive and cancer cells (Chen et al., 2003). The amplification or overexpression of LTA4H is reported also in case of human esophageal

liposarcoma (Myung et al., 2011), primary effusion lymphoma (Arguello et al., 2006) and chronic lymphocytic leukemia (Guriec et al., 2014). Aberrant arachidonic acid metabolism is suspected to have a role in carcinogenesis due to the imbalance shifted towards the pro-carcinogenic lipoxygenase pathways (5-, 8- and 12- LO) instead that anti-carcinogenic (15-LO) (Shureiqi and Lippman, 2001). Aberrant arachidonic acid metabolism is activated during chemically-induced oral carcinogenesis in mice (Guo et al., 2011) and hamsters, with the 5-LO/LTA4H pathway responsible for the stimulation of inflammation of the epithelium and induction of hyperproliferation of chemically-initiated cells (Sun et al., 2006). In human neuroblastoma, LTA4H is widely expressed in the cytoplasm and nucleus of tumor cells and adjacent stromal cells, and presumably a leukotriene-driven autocrine survival loop exists inside the tumor (Sveinbjörnsson et al., 2008).

Moreover the role of LTA4H in carcinogenesis is further confirmed indirectly by the efficacy of anti-neoplastic molecules directed to inhibit this enzyme, as provedin some of the abovementioned studies (Chen et al., 2003; Sun et al., 2006; Sveinbjörnsson et al., 2008) or reported in cases of experimental pancreatic cancer (Oi et al., 2010) or colon cancer (Jeong et al., 2009).

In a study on human melanoma cells, LTA4 hydrolase activity was detected in cultured melanoma cells (MeWo) and malignant neoplastic melanocytes, although it seems reasonable that MeWo cells do not have any appreciable 5-lipoxygenase activity for the generation of LTA4 (Okano-Mitani et al., 1997). It was therefore hypothesized that cells lacking 5-lipoxygenase activity, such as keratinocytes, possess LTA4 hydrolase activity but have to receive the substrate LTA4 by transfer from other cells such as neutrophils and macrophages (Breton et al., 1996; Jakobsson et al., 1991; Okano-Mitani et al., 1997).

FXR1, Fragile X mental retardation-related protein 1

FXR1 is an autosomal gene encoding the cytoplasmic RNA binding protein FXR1 (Fragile X mental retardation-related protein 1). Highly conserved among vertebrates and expressed in different tissues, it belongs to a family of RNA binding protein consisting of FMR1 (Fragile X mental

retardation 1), responsible for the human fragile X mental retardation syndrome, and FXR2 (Fragile X-related 2) (Siomi et al., 1995; Zhang et al., 1995).

In inflammatory process, FXR1 controls the expression of tumor necrosis factor-α (TNF-α) repressing it at a post transcriptional level by RNA-binding proteins that interact with the TNF-α AU-rich element. Depending on FXR1, particularly following its overexpression, the anti-inflammatory cytokine transforming growth factor-β1 (TGF-β1) suppresses the production of lipopolysaccharide (LPS)-induced TNF-α protein production (Garnon et al., 2005; Khera et al., 2010a).

Besides, FXR1 has a role in muscular cells development: its absence causing the upregulation of p21 mRNA, a regulator of cell cycle progression, inducing a premature cell-cycle exit with a block at G0 (Davidovic et al., 2013).

In human oncology, FXR1 expression has been investigated in different tumors proving its potential role as a key regulator of tumor progression. FXR1 is overexpressed in lung squamous cell carcinoma and non-small cell lung cancer cell both in vitro and in vivo, with a critical role in proliferation, survival and invasion of neoplastic cells (Comtesse et al., 2007; Qian et al., 2015). FXR1 was investigated as a tumor promoter also in colorectal cancer and it was over-expressed both as mRNA and protein level in patients with tumor when compared with healthy controls (Jin et al., 2016). Qian and colleagues studied the mechanism of the FXR1-dependent regulation of lung tumorigenesis, showing that FMR members regulate mRNA translation through mRNA protein or microRNA–protein complexes. In lung cancer cells, FXR1 regulates ERK signaling (extracellular-signal-regulated kinases) pathway through interaction with PRKCI (protein kinase C, iota) and ECT2 (epithelial cell transforming 2), two known oncogenes within same 3q26-29 amplicon (with PRKCI being activated in turn by PI3 Kinase, PDK1, RAS and SRC either alone or in association with the PAR complex and ECT2 being phosphorylated by PRKCI and associated with PAR complex in order to activate ERK signaling cascade) (Qian et al., 2015). Moreover, FXR1 cooperates with other driver genes in the 3q amplicon supporting that multiple oncogenes work together to drive the cancer as drivers or as passenger genes (Qian et al., 2015).

FXR1 affects DNA stability (Ma et al., 2014) either using the miRNA pathway to regulate target mRNA expression (Edbauer et al., 2010) or playing a role in post-transcriptional regulation by interacting with mRNA directly and affecting the stability of mRNA (Davidovic et al., 2013).

Metalloproteinases and tumor-matrix interactions

Complex interactions between neoplastic cells and the extracellular matrix, the so-called tumor microenvironment, are considered critical in carcinogenesis, tumor invasion and metastasis. Metalloproteinases (MMPs), with their role in the digestion of the extracellular matrix, may be involved in tumoral invasion, since the phenomenon pave the route toward the vascular compartment, and, therefore, to the metastases.

MMPs belong to a family of calcium and zinc dependent endopeptidases which play a proteolytic activity on many constituents of the extracellular matrix (ECM). Proteolytic effects of MMPs play a role in the processing of matrix proteins, molecular adhesions and cellular migration (Raffetto and Khalil, 2008). Therefore, MMPs are implied in a variety of physiological processes, for example reproduction, fetal development, wound healing, such as in different pathological processes, for example tumor invasion and metastasis, inflammation and vascular diseases (Lepetit et al., 2005; Panek and Bader, 2006; Raffetto and Khalil, 2008; Sorensen et al., 2004). MMPs may be detected extracellularly or intracellularly, as reported in a review by Nagase and co-authors (Nagase et al., 2006). MMPs are either secreted from the cell or anchored to the plasma membrane (Raffetto et al., 2008). The structure of a typical MMP consists of a pro-peptide of about 80 amino acids, a catalytic metalloproteinase domain of about 170 amino acids, a linker peptide of variable lengths and a hemopexin (Hpx) domain of about 200 amino acids (Nagase et al., 2006). The activities of MMPs are low in normal tissues, but can be transcriptionally controlled by inflammatory cytokines, growth factors, hormones, cell-cell and cell-matrix interaction, as well as inhibited by tissue inhibitors of metalloproteinases (TIMPs). Activation implies activation of zymogens, since MMPs are synthesized as pro-proenzymes (Nagase et al., 2006).

In vertebrates, there are 28 described MMPs, 23 of which have been detected in human beings. Based on biochemical structure and biological functions, they are classified in 6 classes (Nagase et al., 2006; Raffetto and Khalil, 2008).

I. Collagenases. Collagenases-1, -2 and -3 (MMPs-1, -8 and -13) are enzymes able to degrade fibrillary collagen of types I, II, III, VII, VIII and X. Some of them are either expressed in specific tissues or are widespread and may act bot in physiological and pathological conditions.

II. Gelatinases. Gelatinases A and B (MMPs-2 and -9) are able to degrade elastin and on denatured collagen of types IV, V, VII and X. Gelatinase A is present, among various types of cells, in fibroblasts, keratinocytes, chondrocytes, endothelial cells and monocytes; gelatinase B is mainly produced by keratinocytes, monocytes, alveolar macrophages, polymorphonuclear leukocytes and tumoral cells, but not by fibroblasts.

III. Stromelysins. Stromelysins-1 and -2 (MMPs-3 and -10) are enzymes able to degrade gelatin, fibronectin, collagen of type IV and V, and are able to activate other MMPs (-1, -7, -8, and -13). Stromelysin-1 is expressed by different types of cells, including fibroblasts, keratinocytes, chondrocytes, endothelial cells and macrophages; stromelysin-2 is present in normal and neoplastic of epithelial origin.

IV. Matrilysins. This group includes matrilysins-1 and -2 (MMPs-7 and -26). Matrilysin-1 is expressed in glandular epithelial cells and in different neoplastic cells. Matrilysin-1 is able to degrade proteoglycans, laminin, gelatin, fibronectin, elastin, and collagen of types IV and X; it can also activate pro-collagenases.

V. Membrane-type metalloproteinases (MT-MMPs). MT-MMPs include transmembrane type proteins (MT1-, MT2-, MT3- and MT5-MMP, also known as MMPs-14, -15, -16 and -24) and glycosylphosphatidylinositol (GPI)-anchor proteins (MT4- and MT6-MMP, also known as MMPs-17 and -25). They are localized on plasma membrane and have a role in the degradation of extracellular matrix and activation of other MMPs.

VI. Other matrix metalloproteinases. This groups includes unclassified MMPs:

- Stromelysin-3 (MMP-11),

- Macrophage elastase (MMP-12, -19),
- Enamelysin (MMP-20, -21),
- Cysteine array CA-MMP (MMP-23, -27),
- Epilisin (MMP-28).

MMPs production is not constitutive in tissues, but is induced by different stimuli, including phorbol esters, integrin-driven signals, ECM components, growth factors, cytokines and pathogen-associated or danger-associated molecular patterns (Khokha et al., 2013). Cells of the immune system, such as neutrophils and lymphocytes, however can express low levels of MMPs even in resting state. Neutrophils store MMP-9 in tertiary granules (gelatinase granules): the release is stimulated by IL-8 and TNF and repressed by transcriptional and TIMP-mediated inhibition (Khokha et al., 2013).

MMPs activities are regulated by α2-macroglobulin and TIMPs (Nagase et al., 2006). A2-macroglobulin entraps proteinases within the macroglobulin and the resulting complex is cleared by receptor-mediate endocytosis. TIMPs (TIMP-1, -2, -3 and -4) are inhibitors of MMPs. TIMPs act by protein-protein interaction creating TIMP-MMP complexes with their N-terminal domain. They inhibit all MMPs tested, with TIMP-3 acting as a major regulator of metalloproteinase activities in vivo (Nagase et al., 2006; Raffetto et al., 2008).

Matrix metalloproteinases in melanocytic neoplasms

In human melanomas, tumor cells and tumor-associated stromal cells showed increased expression of several MMPs and TIMPs (Moro et al., 2014), and in certain cases MMPs seemed to be associated with the invasiveness, metastatic risk and unfavorable prognosis of human melanomas (Nikkola et al., 2005; Shellman et al., 2006). MMPs-9 is among the most extensively investigated MMPs as far as their role in the digestion of basal membranes and thus in the tumor potential for invasiveness.

For instance, MMP-9 is more expressed in malignant human cutaneous melanoma than pre-cancerous nevi, and is also intensely expressed in lymph node with metastasis (Candrea et al., 2014; Chen et al., 2012), thus exhibiting an association with high risk of invasion and metastatic behavior.

Scarce studies exist about MMPs expression in human oral melanoma. A study by Kondratiev and co-authors on sinonasal and oral malignant melanoma, reported that MMP-9 expression is correlated with epithelioid morphology and with the presence of metastatic disease, even if it is not significantly correlated with the survival of patients with oral melanoma (Kondratiev et al., 2008).

Ocular melanomas have been more extensively investigated for their expression of MMPs. In particular, highly aggressive choroidal human uveal melanomas express high levels of MMP-2, MMP-9, MMP-1 and MT1-MMP (Schnaeker et al., 2004). El-Shabrawi and co-authors showed that MMP-9 in human uveal melanoma is expressed in neoplastic cells in about half of the tested tumors, with a prevalence of epithelioid morphology and a presence of peri-vascular distribution. Moreover, MMP-9 expression was positively correlated with metastasizing behavior, whereas TIMP-1 and TIMP-2 expression was correlated with a better survival rate (El-Shabrawi et al., 2001).

TIMP-3 mRNA expression was shown to be downregulated in human uveal melanomas with poor prognosis (Singh et al., 2007) and the decrease of its genetic expression has been identified as a progression marker of metastasis, even if not yet associated with the protein expression (van der Velden et al., 2003).

A study from Lai and colleagues described the topographical expression of MMPs and TIMPs in human uveal melanoma. Specifically, most tumors (80%) in this study had a moderate to strong MMP-9 immunolabelling, which included also tumor vessels and intravascular leukocytes, and 40% had weak cytoplasmic TIMP-2 immunolabelling, including tumor vasculature. MMPs (MMP-1, -2, -19, MT-MMP) and TIMPs (TIMP-2 and -3) had a reduced immunoreactivity at the tumor-scleral junction compared to the neoplastic mass, except for the heterogeneous expression of MMP-9 (Lai et al., 2008). Low concentrations of TIMP-2 may promote activation of latent MMP-2. MMPs and TIMPs play a role in melanoma tumorigenesis being involved in degradation of the vascular basement membranes, in activation of angiogenic factors and in tumoral angiogenesis and vasculogenic mimicry (Lai et al., 2008).

Experimental selective silencing or downregulation of MMP-9 results in the inhibition of the invasion and migration of murine melanoma cell lines (Shi et al., 2015; Tang et al., 2013). Therefore, the application of MMP-9 inhibitors is currently ongoing in human research for perspective melanoma therapy (Aksenenko and Ruksha, 2013).

In veterinary literature, few studies analyzed the expression of MMPs and TIMPs in canine melanocytic tumors. A study conducted on various types of canine melanomas revealed an overexpression of MMP-9 in malignant melanomas, compared with melanocytomas, even if in this case the comparison was carried out among oral and cutaneous tumors (Docampo et al., 2011). In the same study, MMP-9 was the only significantly differentially expressed matrix metalloproteinase, despite the further investigation of MMP-2 and MT1-MMP (Docampo et al., 2011). Nakaichi compared the expression of MMP-2 in different types of canine oronasal tumors, revealing a higher MMP-2 activity in melanoma and squamous cell carcinoma than in acanthomatous epulis and nasal adenocarcinoma (Nakaichi et al., 2007). To the best of the authors' knowledge, there are no data on the role of MMPs in feline melanomas.

AIMS

The present PhD project investigates selected markers related to the pathogenesis and prognosis of two spontaneous non-UV induced melanomas in dogs and cats, that are canine oral melanoma and feline diffuse iris melanoma. In particular, specific aims of the project are the following.

I. The investigation of the expression of LTA4H and FXR1 genes and proteins in canine oral melanoma: to quantify and describe if and how these molecules, previously related to metastasizing behavior in other types of melanoma in humans and dogs, are expressed in canine oral melanomas, in order to identify possible correlations with prognostic parameters, specifically. Ki-67 index and mitotic index, and with clinical outcome.

   I-a. The technical validation of anti-FXR1 antibodies for the use in the canine species: in order to pursue the investigation of FXR1, to validate the use of anti-FXR1 antibodies in dogs and define technical protocols, for the description of the expression of FXR1 protein in normal canine tissue and, preliminary, in different types of canine melanocytic tumors.

II. The study of the expression of matrix metalloproteinases (MMPs) in oral melanocytic tumors, to assess:

   II-a. if the expressions of FXR1 and MMP are correlated, and

   II-b. if MMPs activity is associated with the clinical outcome.

III. The study of matrix metalloproteinases and tumor-matrix interaction in feline diffuse iris melanoma: to describe the immunohistochemical expression of MMP-9 and its inhibitor TIMP-2 and correlate these data with known histological criteria of malignancy, i.e. histological grade and mitotic index.

I. VALIDATION OF ANTI-FXR1 ANTIBODIES IN CANINE NORMAL TISSUES AND MELANOCYTIC NEOPLASMS

Abstract

Fragile X mental retardation-related protein 1 (FXR1) is a cytoplasmic RNA-binding protein highly conserved among vertebrates. It has been studied for its role in muscle development, inflammation, and tumorigenesis, being related, for example, to metastasizing behavior in human and canine uveal melanoma. Anti-FXR1 antibodies have never been validated in the canine species. To investigate FXR1 expression in canine melanocytic tumors, the present study tested two commercially available polyclonal anti-human FXR1 antibodies, raised in goat and rabbit, respectively.

The cross-reactivity of the anti-FXR1 antibodies was assessed by Western blot analysis, and the protein was localized by IHC in a set of normal canine tissues and in canine melanocytic tumors (10 uveal and 10 oral). Western blot results demonstrated that the antibody raised in rabbit specifically recognized the canine FXR1, while the antibody raised in goat did not cross-react with this canine protein. FXR1 protein was immunodetected using rabbit anti-FXR1 antibody, in canine normal tissues with different levels of intensity and distribution. It was also detected in 10/10 uveal and 9/10 oral melanocytic tumors. The present study validated for the first time the use of anti-FXR1 antibody in dogs and highlighted different FXR1 protein expression in canine melanocytic tumors, the significance of which is undergoing further investigations.

Introduction

FXR1 is an autosomal gene encoding for the cytoplasmic RNA binding protein FXR1 (Fragile X mental retardation-related protein 1). FXR1 is a homologue of the Fragile X mental retardation syndrome protein FMR1, and both belong to the family of Fragile X mental retardation-related RNA-binding proteins together with FXR2 (Fragile X mental retardation-related protein 2) (Coy et al., 1995; Siomi et al., 1995; Zhang et al., 1995). These proteins are involved in nuclear export, cytoplasmic transport and translation control of target mRNAs (Bardoni et al., 2001). FMR1, FXR1

and FXR2 are more than 70% homologous in their N-terminal half and have the same functional domains (Bardoni et al., 2001). The human *FXR1* and *FXR2* genes are autosomally encoded and are located, respectively, in 3q28 and 17p13.2 (Bardoni et al., 2001).

FMR1 spans about 40 kb encoding a mRNA of 3.9 kb. The N-terminal region has a functional nuclear localization signal (NLS), followed by two KH domains, a nuclear export signal (NES) and an RGG box in the C-terminal region (Bardoni et al., 2001). Its homologues FXR1 and FXR2 have two KH domains, like FMR1, and a RGG box. FXR1, FMR1 and FXR2 share 63% of amino acid identity in the first half of the protein (Kirkpatrick et al., 1999). Expression of the protein is similar but not overlapping, for example, FXR1 is highly expressed in muscle and heart, where FMR1 is almost absent (Bardoni et al., 2001), while FXR2 is more expressed than FXR1 in the brain (Kirkpatrick et al., 1999). FXR1 and FXR2 are predominantly cytoplasmic, even if FXR2 and one FXR1 isoform have also nucleolar targeting signal (Kirkpatrick et al., 1999; Bardoni et al., 2001).

FXR1 is highly conserved among vertebrates (Bardoni et al., 2001). The *FXR1* gene is conserved in chimpanzee, Rhesus monkey, dog, cow, mouse, rat, chicken, zebrafish, and frog (NCBI, 2017). FXR1 is a protein of 621 amino acids with a molecular mass of 69721 Da. Post translational modifications includes dimethylation of Arg-445. BLAST alignment analyses between human and dog FXR1 proteins reveal 99% identity (619/621 amino acids) (BLAST, 2017). In human, mouse and laboratory models (e.g. frog *Xenopus laevis*), FXR1 is normally expressed in a wide variety of tissues, with the highest level in muscle, heart, and testis (Siomi et al., 1995; Kirkpatrick et al., 1999; Bardoni et al., 2001), and it is considered to play a role in muscular cell development (Davidovic et al., 2013), and in inflammatory process by controlling the expression of tumor necrosis factor-α (TNF-α) (Garnon et al., 2005; Khera et al., 2010a, 2010b) and regulating monocytes migration(Le Tonqueze et al., 2016). Moreover, *FXR1* has been investigated in oncology for its potential role as a key regulator of tumor progression, resulting over-expressed at genetic level, for example, in human lung squamous cell carcinoma, non-small cell lung cancer (Comtesse et al., 2007; Qian et al., 2015), and colorectal cancer (Jin et al., 2016). It has been supposed that *FXR1* affects DNA stability (Ma et al., 2014), either regulating target mRNA expression by miRNA pathways (Edbauer et al., 2010) or regulating post-transcription by direct interaction with mRNA (Davidovic et al., 2013). *FXR1* was also

demonstrated to be over-expressed in human and canine uveal malignant melanoma with a positive correlation with the metastatic potential of the tumor (Malho et al., 2013; Onken et al., 2010).

Currently, the expression of FXR1 protein in normal canine tissues has not been investigated and, despite a few molecular studies on gene regulation, there are no data concerning the expression of FXR1 protein in canine melanocytic tumors. To the best of authors' knowledge, anti-FXR1 antibodies were not previously validated in the canine species. Therefore, in the present study, the authors tested the immunoreactivity of FXR1 protein in normal canine tissues and melanocytic tumors.

Materials and methods

Cell culture

Primary cultures of fibroblasts were established from abdominal full-thickness skin excised from the margins of a specimen obtained during therapeutic surgical procedure, as previously described with slight modifications (Dieci et al., 2013). Immediately after collection, skin fragments were placed in PBS on ice; all the fat tissue was removed from the skin with scissors, skin tissues were trimmed to 0.5 cm × 0.5 cm fragments and finely minced into small pieces evenly distributed onto the bottom of a tissue culture 25-cm^2 flask in D-MEM Medium with GlutaMax™ (Gibco Thermo-Fisher, Cat. no. 10569-010) supplemented with 10% of Fetal Bovine Serum. After 24 h of culture, when the pieces have adhered, the medium volume was gradually increased to 5 ml. After a week, when a substantial outgrowth of cells was observed, the explants were removed from the centre of the outgrowth with a scalpel and the medium was replaced. Fibroblasts were cultured until the outgrowth has spread to cover at least 70% of the growth surface.

All the chemicals and reagents used in this part of study were purchased from Sigma-Aldrich - Merck KGaA, Darmstadt (Germany) except for those specifically mentioned.

Cells at passage 0 were harvested by incubation for 5 minutes on ice with 0.25% trypsin in 0.01% EDTA and collected by centrifugation. Protein extraction was carried out on ice or at 4 °C. Fibroblasts were homogenized in 5 µl/mg TES buffer (10 mM Tris–HCl, pH 7.6; 1 mM EDTA, 0.25 M sucrose) and centrifuged at 10,000 ×g, for 30 min, at 4 °C. Protein concentration values were determined by the

Pierce BCA Protein Kit (VWR), using BSA as a protein standard, according to the manufacturer's manual.

Western blot

Human and canine serum and canine fibroblasts were separated on a 12% sodium dodecyl sulphate polyacrylamide gel electrophoresis (SDS–PAGE) and blotted onto nitrocellulose membrane. Before gel separation, 1 µl ß-mercaptoethanol (Sigma Aldrich, Saint Louise, MO, USA) was added to each sample. Immunolabelling was performed using a goat polyclonal anti-FXR1 antibody (ab51970 Abcam, Cambdrige, UK) and a rabbit polyclonal anti-FXR1 (ab50841 Abcam, Cambdrige, UK) as primary antibodies (0.25 µg/ml for 1 h min at room temperature, RT, for each), while an anti-goat IgG labelled with peroxidase (Sigma-Aldrich, Saint Louise, MO, USA) and an anti-rabbit IgG labelled with peroxidase (Vector Laboratories, Burlingame, CA, USA), respectively, were used as secondary antibodies (1:5000 dilution for 45 min at RT). Antibodies were diluted using Roti®-Block (Carl Roth, Karlsruhe, Germany). Immunoreactive bands were visualized by enhanced chemiluminescence (ECL) using Immobilon Western Chemiluminescent HRP Substrate (Millipore, Billerica, MA, USA). In order to further assess the specificity of the secondary antibodies for FRX1 protein, western blotting experiments were repeated replacing the primary antibodies with PBS and using only the respectively secondary antibodies labelled with peroxidase (1:5000 dilution for 45 min at RT), to perform a negative control and to detect any possible non-specific bands. Human serum was used as positive control. Fibroblasts were used as negative controls, since these cells do not express FXR1 protein (Human protein atlas, 2017).

Immunohistochemistry

Immunohistochemical expression of FXR1 protein was tested in canine normal tissues and melanocytic tumors. A pool of canine tissues was examined, using microarrays of normal tissue created by assembling multiple formalin-fixed samples (5 x 5 x 3 mm each) in the same paraffin block. Tissues examined included stomach, intestine, pancreas, liver, thyroid, adipose tissue, lung, kidney, testis, brain, heart, adult and fetal skeletal muscle. Immunohistochemistry was also

performed on conventional tissue sections of canine oral (n = 10) and uveal (n = 10) melanocytic tumors.

Serial sections were cut 4 µm thick and mounted on poly-lysine coated slides (Menzel-Gläser, Braunschweig, Germany). Immunohistochemical staining with the standard avidin-biotin-peroxidase complex (ABC) method was performed.

Preliminary set up of the immunohistochemical protocol compared different heat-induced antigen retrieval methods (microwave oven, pressure cooker, water bath) and serial concentration of the primary antibody. The chosen protocol applied to the sections was the following: sections were deparaffinized in xylene and rehydrated through a descending series of ethanol concentrations. The endogenous peroxidase activity was blocked with 0.3% H2O2 in methanol for 30 min. Antigen retrieval was performed by heating the slides in citrate buffer solution (pH 6.5) in a water bath at 95°C for 30 minutes, followed by cool down in buffer at RT for 30 minutes. Sections were therefore incubated for 20 min at RT with normal goat serum (1:70) to block any nonspecific protein binding. Serial sections were incubated at 4°C overnight in a humidified chamber with the primary antibody: rabbit polyclonal anti-FXR1 (ab50841 Abcam, Cambridge, UK), 1:100 dilution.

Sections were then rinsed in Tris buffer solution, and incubated with the secondary anti-rabbit biotinylated antibody (1:200, 30 minutes RT) (Vector Laboratories, Burlingame, CA, USA), followed by rinsing in Tris buffer and therefore incubation with the ABC reagent (30 minutes RT) (Vector Laboratories, Burlingame, USA). The chromogen 3-amino-9-ethylcarbazole (AEC) (Vector Laboratories, Burlingame, CA, USA) was applied for 15 minutes and, after rinsing in tap water, slides were counterstained with Mayer's hematoxylin (Diapath srl, Martinengo, Italy) for 2 minutes. Slides were therefore dried and mounted in aqueous mounting agent (Aquatex, Merck, Darmstadt, Germany).

Negative controls for the technique were carried out by replacing the primary antibodies with rabbit IgG (Santa Cruz, Dallas, TX, USA).

Fibroblasts were used as negative controls. Canine fetal muscle was used as positive control. Immunolabeling was semi-quantitatively scored with postexamination masking method by two pathologists (LN, CG) simultaneously. At the time of samples evaluation, a prior extensive revision

of human literature was intentionally not performed to avoid bias in the scoring of tissues. In normal canine tissue and melanomas, the percentage of positive cells was recorded (<10%, 10-30%, 30-50%, 50-80%, >80%), and the intensity of single cell staining was scored from 1+ (mild) to 3+ (marked). A 3+ signal equated to an intensity easily seen on low magnification, whereas a 1+ signal was seen on high magnification, and 2+ bordered between a strong and a weak staining signal.

In tissue labelled with the rabbit anti-FXR1 antibody, the immunoreactive score of Remmele and Stegner (IRS score) was calculated combining the intensity and ratio of positivity as follows (Remmele and Stegner, 1987): IRS score (0 - 12) = percentage of positive cells (with: no positive cells= 1, <10% positive cells= 1, 10-50 % of positive cells= 2, 50-80% of positive cells= 3, >80% of positive cells= 4) * intensity of staining (with: no positive cells= 0, 1+/mild = 1, 2+/moderate= 2, 3+/marked= 3).

Results

Western blot

Western blotting experiments were carried out to determine whether the antibodies cross-reacted with the respective canine protein. The rabbit anti-FXR1 antibody cross-reacted with a band of 60-70 kDa, corresponding to the predicted molecular weight (predicted molecular weight: 68 kDa, band detected by the producer: 65 kDa) (Figure 2).

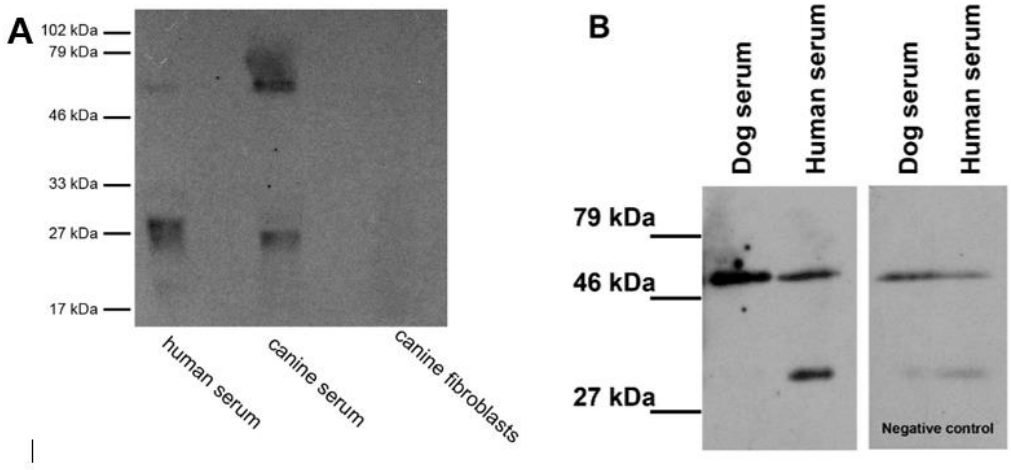

Figure 2 - Western blot analyses. A: Rabbit polyclonal anti-FXR1 ab50841, detected band around 65 kDa in human and canine sera; canine fibroblasts did not show any cross-reactivity. B: Goat polyclonal anti-FXR1 antibody ab51970 (left), and negative control (right).

Canine fibroblasts did not show any cross-reactivity. In the negative control for the secondary antibody, the incubation with the lone anti-rabbit secondary antibody did not show reactive bands (Figure 2). Conversely, goat anti-FXR1 antibody showed bands lower than expected MW (predicted molecular weight: 68 kDa, band detected by the producer: 80 kDa). These results indicated that rabbit anti-FXR1 polyclonal antibody specifically recognized the canine FXR1 protein and did not react with other canine serum proteins, while goat anti-FXR1 appeared non-specific.

Immunohistochemical expression of FXR1 in normal canine tissues

Both anti-FXR1 antibodies tested stained positive in a variety of normal canine tissues as detailed in Table 2. Positive staining was always intra-cytoplasmic and its intensity ranged from mild (1+) to marked (3+). A nuclear staining, e.g. in renal pelvis urothelium or in chondrocytes of bronchial cartilage, was occasionally obtained with goat anti-FXR1 and was interpreted as not specific staining. In general, goat anti-FXR1 antibody was more prone than rabbit anti-FXR1 to give a slight diffuse background staining (Figure 4).

In details, in the gastrointestinal tract, the mucosal epithelium exhibited strong immunoreactivity in the stomach (parietal/chief cells) and intestine (enterocytes), whereas the connective tissue of the lamina propria and the muscular layers were not stained. In the liver, hepatocytes were strongly positive and ductal epithelium stained mildly for FXR1 expression. Pancreatic acini stained moderately. In the lung, pneumocytes stained mildly and bronchial epithelium intensely; in the kidney, tubular epithelial cells and the pelvis urothelium were diffusely and moderately positive, whereas glomeruli did not stain. Thyroid follicular epithelial cells were diffusely and strongly positive. Neurons in the brain stained intensely for FXR1. Adult striated skeletal muscles was diffusely, moderately FXR1 positive, striated cardiac muscles was mildly positive. Canine fetal skeletal muscle was intensely immunoreactive (Figure 3). In blood vessels, the endothelium

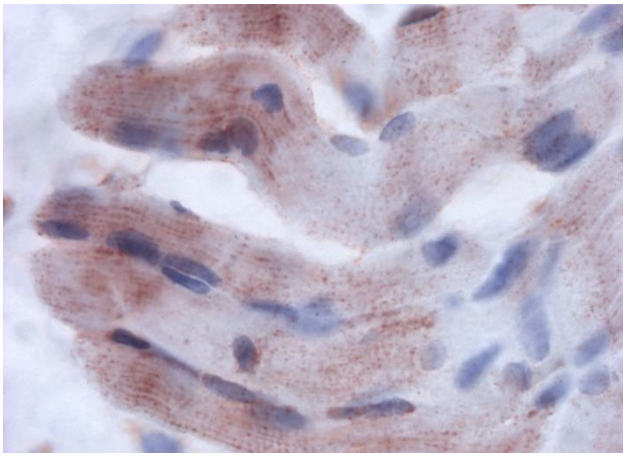

Figure 3 - Canine fetal skeletal muscle, IHC, rabbit anti-FXR1 antibody, 40x

multifocally stained moderately positive for FXR1, while the smooth muscle of the tunica media was mostly negative, and only occasionally mildly positive. An intense signal was detected in Leydig cell of the testis, whereas Sertoli and seminal cells were always negative. Stromal connective tissue were consistently and diffusely negative for FXR1.

Table 2 - Immunohistochemical expression of FXR1 in a series of normal canine tissues.

Tissue		**Goat anti-FXR1 clone ab51970**	**Rabbit anti-FXR1 clone ab50841**		
		Intensity	**Intensity**	**% positive cells**	**IRS score**
Thyroid	Follicular epithelial cells	2+	3+	50-80	9
Pancreas	Acinar cells	2+	2+	30-50	4
Liver	Hepatocytes	3+	3+	50-80	9
	Ductal epithelium	3+	1+	>80	12
Intestine	Enterocyte	2+	3+	50-80	3
	Lamina propria	-	-	>80	12
	Muscular layer	1+	-	0	0
	Serosal layer	1+	1+	0	0
Stomach	Parietal/chief cell	2+	3+	30-50	2
	Mucus cell	1+	-	>80	12
	Connective tissue	1+	-	0	0
	Muscular layer	1+	-	0	0
Adipose tissue	Adipocytes	1+	-	0	0
Lung	Bronchial epithelium	2+	3+	0	0
	Pneumocytes	2+	1+	>80	12
	Cartilage	3+	1+	30-50	2
Kidney	Glomeruli	-	-	30-50	2
	Tubular epithelium	1+	2+	0	0
	Interstitium	-	-	50-80	6
	Urothelium	3+	2+	0	0
Brain	Neuron	3+	3+	>80	8
	Axons	2+	1+	>80	12
Heart	Striated cardiac myocytes	2+	1+	50-80	3
Testis	Interstitial cells	2+	3+	>80	12
	Spermatic line	2+	-	0	0
Muscle	Striated skeletal myocytes	2+	2+	>80	8

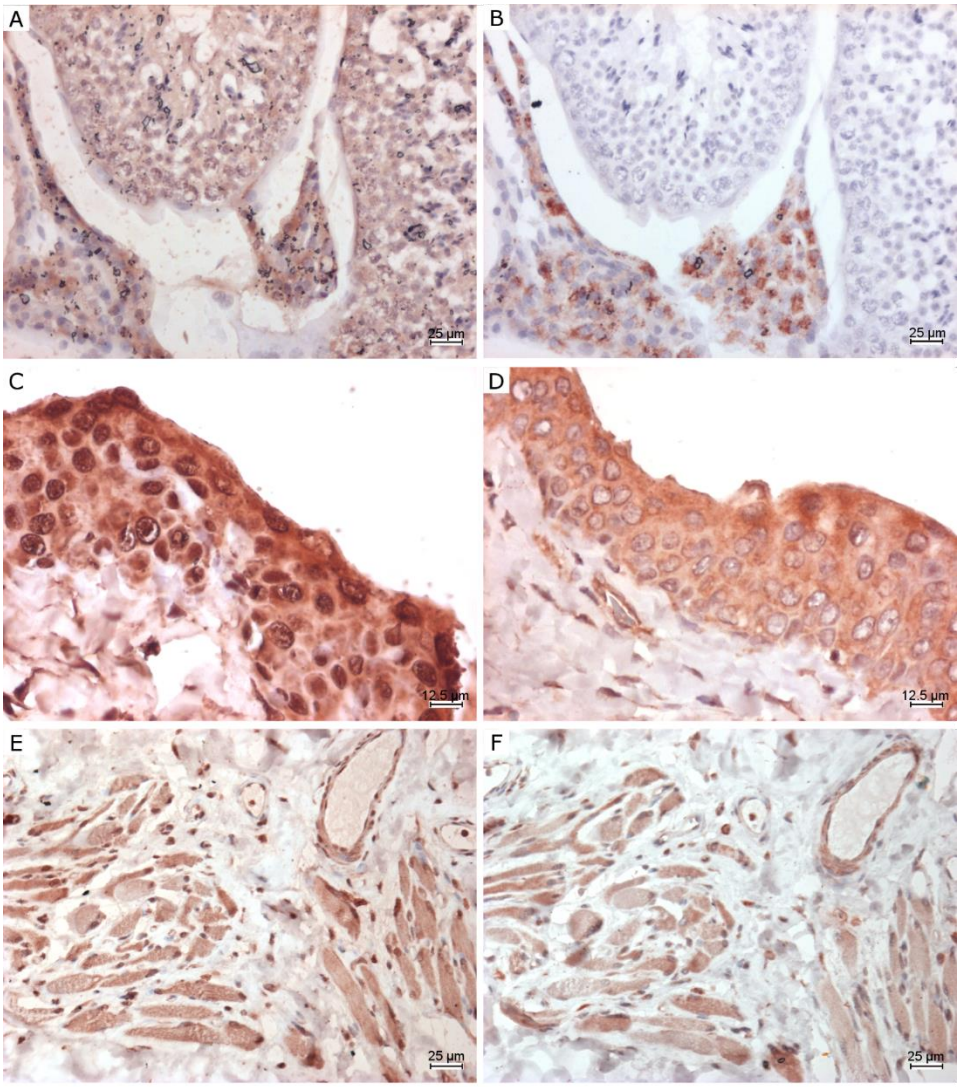

Figure 4 - Immunohistochemical staining anti-FXR1 in normal canine tissues, ABC method, AEC chromogen. A-C-E: Goat polyclonal anti-FXR1 antibody ab51970; B-D-F: Rabbit polyclonal anti-FXR1 ab50841. A-B: testis; C-D: kidney, renal pelvis; E-F: skeletal muscle.

Immunohistochemical expression of FXR1 in canine oral and uveal melanoma

All but one oral melanomas were positive with both tested antibodies. The immunostaining was always intra-cytoplasmic. Among oral melanomas, one case stained positive with goat and negative to rabbit anti-FXR1 antibody (Table 3, Figure 5). In 4 cases, there was agreement in immunolabelling between the two different tested clones of antibody both as percentage of positive cells and intensity of staining. In 6 cases, immunostaining with goat anti-FXR1 antibody exceeded rabbit anti-FXR1 antibody, either in percentage of positive cells (n = 3) or both in percentage and intensity (n = 3). 10/10 tested uveal melanocytic tumors were positive to FXR1 immunostaining (Table 4, Figure 5): in one case the two antibodies obtained equal results, whereas the rabbit antibody gave a slightly more intense staining in 3 cases, a higher percentage of positive cells in 1 case, and both more

abundant and more intense positivity in 2 cases. Two cases had a higher percentage of positive cells using goat-antibody. One case was more intense with goat-antibody, but had a higher number of positive cells with rabbit-antibody.

Depicting a detailed evaluation of FXR1 immunolabelling in melanoma using the rabbit anti-FXR1 antibody, nine (9/10) oral melanomas were FXR1 positive: four cases had a IRS score of 12 (corresponding to >80% intensely labelled cells), one had IRS 6, two 4, two 2 and one case was negative.

Still with rabbit antibody, ten (10/10) uveal melanocytic tumors were positive to FXR1 immunostaining. The cases were homogeneously and variably distributed among the semi-quantitative classes of evaluation. Three cases were above 80% of positive neoplastic cells, four varied between 30-50% and three had less than 10% of positive neoplastic cell. Three cases were intensely positive, six moderately, and one case was mildly positive.

In tissue circumscribing tumors, scattered melanocytes with dendritic appearance were recognizable and they did not stain. No immunolabeling was observed in negative controls.

Table 3 - Immunohistochemical expression of FXR1 in ten canine oral melanomas.

			Goat anti-FXR1 clone ab51980			**Rabbit anti-FXR1 clone ab50841**		
#	**Morphology**	**Pigmentation**	**% positivity**	**intensity**	**IRS score**	**% positivity**	**intensity**	**IRS score**
1	spindle	+++	>80	3+	12	Negative	Negative	0
2	spindle	+	>80	3+	12	>80	3+	12
3	epithelioid	+	>80	3+	12	30-50	2+	4
4	spindle	++	50-80	2+	6	30-50	2+	4
5	epithelioid	+++	>80	3+	12	10-30	1+	2
6	mixed	+	>80	3+	12	>80	3+	12
7	epithelioid	++	50-80	2+	6	<10	2+	2
8	epithelioid	++	>80	3+	12	>80	3+	12
9	mixed	+	>80	2+	8	50-80	2+	6
10	mixed	+	>80	3+	12	>80	3+	12

Table 4 - Immunohistochemical expression of FXR1 in ten canine uveal melanocytic tumors.

	Goat anti-FXR1 clone ab51970			Rabbit anti-FXR1 clone ab50841		
#	% positivity	intensity	IRS score	% positivity	intensity	IRS score
1	>80	2+	8	>80	3+	12
2	50-80	2+	6	30-50	2+	4
3	<10	1+	1	<10	1+	1
4	<10	1+	1	<10	2+	2
5	50-80	2+	6	30-50	2+	4
6	50-80	1+	3	30-50	2+	4
7	<10	1+	1	30-50	3+	6
8	10-30	1+	2	>80	3+	12
9	<10	1+	1	<10	2+	2
10	50-80	2+	6	>80	2+	8

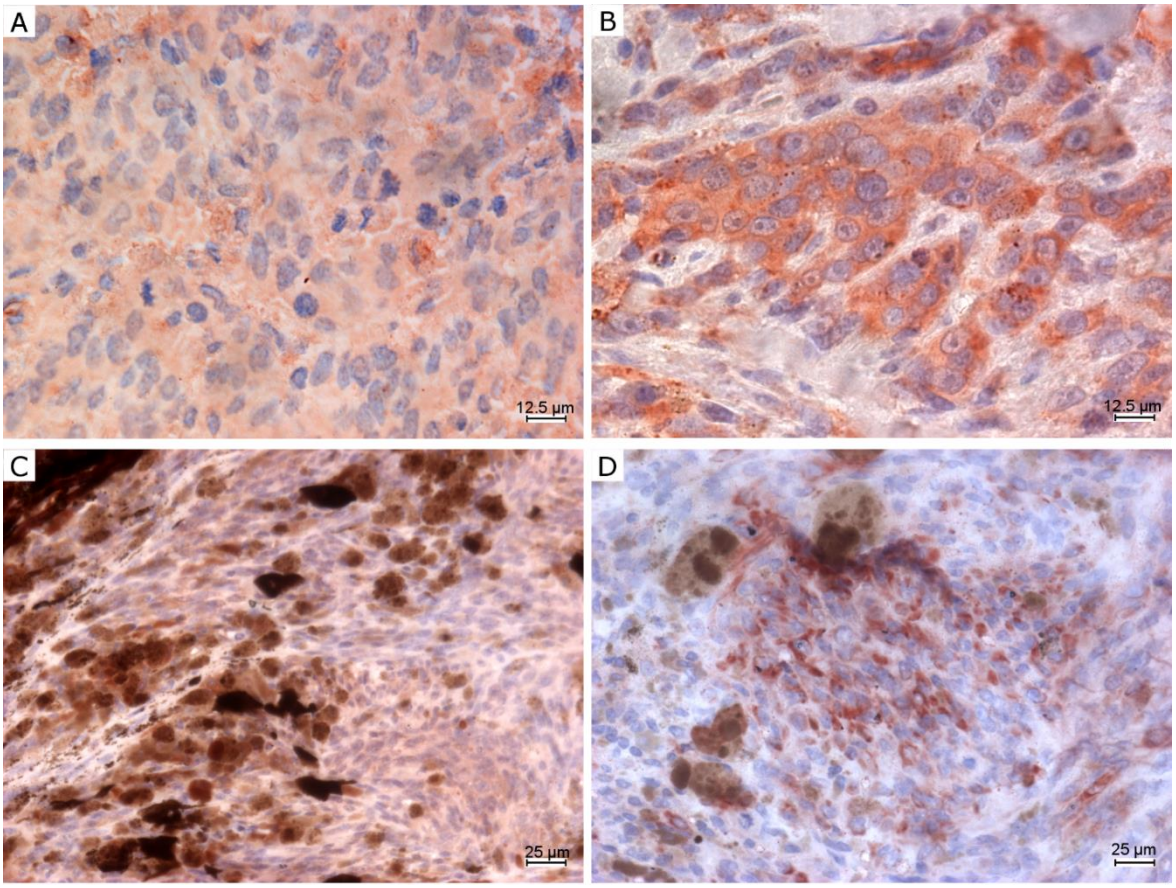

Figure 5- Immunohistochemical staining anti-FXR1 in canine melanoma, ABC method, AEC chromogen. A-C: Goat polyclonal anti-FXR1 antibody ab51970, B-D: Rabbit polyclonal anti-FXR1 ab50841. A-B: oral melanoma (same case) (A moderate staining in >70% of neoplastic cells, B intense staining in 50-70% of neoplastic cells); C-D: uveal melanocytoma (same case) (C mild staining in 50-70% of neoplastic cells, D intense staining in 30-50% of neoplastic cells).

Discussion

FXR1 is a cytoplasmic RNA binding protein whose codifying gene's expression has been related to metastasizing behavior in human and canine uveal melanoma (Comtesse et al., 2007; Jin et al., 2016; Malho et al., 2013; Onken et al., 2004; Qian et al., 2015). In the current literature, few studies investigated FXR1 protein localization in normal human tissue (Agulhon et al., 1999; Qian et al., 2015) and in different tumors (Comtesse et al., 2007; Jin et al., 2016; Onken et al., 2004; Qian et al., 2015). Detailed tissue expression of FXR1 has been described in the Human Protein Atlas (Human Protein Atlas, 2017). To the best of authors' knowledge, no data are available concerning the tissue immunolocalization of FXR1 protein in the canine species. Moreover, commercially available anti-human antibodies were not previously validated in dogs.

The commercially available anti-human polyclonal anti-FXR1 antibodies tested in the present study were predicted to react with the canine species. On western blotting, a rabbit anti-FXR1 antibody showed a band with a molecular weight consistent with what expected as per manufacturer's indications (predicted molecular weight: 68 kDa, band detected by the producer: 65 kDa) and therefore it was considered to react specifically with human and canine serum. Moreover, the polyclonal antibody rabbit anti-FXR1 is raised against an immunogen sequence within amino acids 338-513, a sequence that is not present in the FXR2 sequence, which is characterized by a homology of 70% with FXR1 (Agulhon et al., 1999; Bardoni et al., 2001), further endorsing the specific binding of this antibody to FXR1 protein. The goat anti-FXR1 antibody recognized a band with a MW lower than expected and it was therefore considered not specific. Therefore, in-depth evaluations of the immunohistochemical scores were performed only on the results obtained with the rabbit antibody.

In the present study, the specific tissue immunolocalization of FXR1 protein was investigated for the first time in the canine species. On immunohistochemical examination, FXR1 protein was detected in normal canine tissues with different degrees of intensity and resulted to be present in at least one tissue or cell population in all organ tested. These results in canine tissues were consistent with the immunohistochemical expression of FXR1 in human tissues as described in the

Protein Atlas. Connective tissue in the dog was not immunoreactive: this finding was consistent with the predicted results according to western blot results and human data (Human Protein Atlas, 2017).

An intense FXR1 expression was particularly observed in canine fetal skeletal muscle, testicular interstitial cells of Leydig and neurons. These results were consistent with the human literature, where FXR1 is reported to be expressed in different tissues (Agulhon et al., 1999; NCBI, 2017), even if studies on FXR1 expression in normal tissue mostly relied on investigations of gene or mRNA expression (Siomi et al., 1995; NCBI, 2017). Anyway, canine and human tissues exhibited also slight differences in FXR1 expression, for example in the testis, where the spermatic line resulted negative, while it is reported to be strongly positive in humans. It may be reasonable to hypothesize that tissue-specific isoforms of FXR1 exists and that they probably have a different distribution and expression in different species. Since 1995, RT-PCR analyses on human tissues revealed that different isoforms of FXR1 exist in brain and testis, presumably suggesting a tissue-specific alternative splicing (Siomi et al., 1995). Isoforms share extensive regions of identity and vary only in specific domains (Siomi et al., 1995). This fact probably account for tissue-specific function of the protein (Kirkpatrick et al., 1999; Siomi et al., 1995), thus explaining subtle differences in the expression between humans and dogs.

Even though both rabbit and goat antibodies stained the tested tissues with a similar distribution, the quality of the signal was different: unspecific and background staining was more frequently observed when goat anti-FRX1 antibody was used. For example, goat anti-FRX1 antibody gave multifocal positivity of the nuclei (e.g. in renal urothelium), contrary to what expected from the cytoplasmic localization of this protein, and, in general, the staining was more prone to a stromal background positivity. This confirmed that, as already seen on western blot experiments, the cross-reaction with goat anti-FXR1 antibody was not specific.

FXR1 gene has been previously shown to be over-expressed in those human and canine uveal melanomas with higher tendency toward a metastasizing behavior (Onken et al., 2010; Malho et al., 2013), however at the present day there is no knowledge about the expression of this protein in canine melanocytic neoplasms. Interestingly, in the present study FXR1 immunostaining was obtained in all but one (with rabbit anti-FRX1 antibody) tested oral melanomas, with different levels

of staining intensity and percentage of positive cells (results ranged from a negative case up to over 80%). Even though a higher percentage of positive cells was obtained with goat anti-FXR1 antibody than with rabbit, the latter gave more specific staining, without signal in stromal cells or nuclei. Moreover, the cases stained with the rabbit anti-FRX1 antibody were more distributed between the classes of semi-quantitative score, as far as both the intensity of the staining and the percentage of positive cells (results ranged from a negative case up to over 70%). These data indicated that FXR1 protein is actually expressed in canine oral melanomas and the results may suggest to further investigate the possible relation between the immunohistochemical expression and the biological behavior.

In the cohort of uveal melanocytic neoplasms examined, all cases were positive for FXR1, and the positivity among different classes of semi-quantitative score seemed to be more variably distributed than oral melanomas. This could reflect a different biological behavior of these two different types of tumor, i.e it could be related to a different expression of the protein and its codifying gene, a finding that, in previous studies (Onken et al., 2010; Malho et al., 2013), has been related to metastasizing behavior, and would be worth clarifying further in regard to the single cases.

Conclusions

In the present study, between the two tested antibodies, the rabbit polyclonal anti-FRX1 had a more specific binding to FXR1 protein on both western blot and immunohistochemistry, whereas goat polyclonal anti-FRX1 antibody appeared much less specific. Moreover, the distribution of positive immunohistochemical signal obtained with rabbit anti-FXR1 antibody may indicate a potential ability of this marker in discriminating among different classes of protein expression possibly related to the tumor behavior. Further studies are ongoing to correlate FXR1 immunostaining with a possible prognostic significance in canine melanomas.

Results of the present work have been presented as follows:

- *Nordio L., Marques A. T., Lecchi C., Stefanello D., Giudice C. (2018). "Immunohistochemical expression of FXR1 in canine normal tissues and melanomas". Journal of Histochemistry and Cytochemistry, 66:585-593.*

- *Nordio L., Marques A. T. (2017). "Validation of anti-FXR1 antibodies in the canine species and application to an immunohistochemical study of canine oral melanomas". Proceeding of Veterinary and Animal Science Days 2017, 6th-8th June 2017, Milano (oral presentation). International Journal of Health, Animal Science and Food safety, 4.*

II. MOLECULAR AND IMMUNOHISTOCHEMICAL EXPRESSION OF LTA4H AND FXR1 IN CANINE ORAL MELANOMAS

Abstract

Oral melanoma is a common tumor in dogs. Although generally considered malignant, there is still poor consensus about histological criteria able to predict the likely progression of the disease in individual dogs. In the present study, Leukotriene A4 hydrolase (LTA4H) and Fragile X mental retardation-related protein 1 (FXR1) gene and protein expression were investigated in canine oral melanomas. LTA4H (an enzyme of the arachidonic acid cascade) and FXR1 (a cytoplasmic RNA binding protein) have been previously studied in carcinogenesis in different tumors, including human and canine uveal melanomas in which they have been related with metastatic potential of the tumor.

Formalin fixed paraffin-embedded (FFPE) canine oral melanomas (n=36) were collected. Complete histological evaluation was performed and Ki-67 proliferation index was immunohistochemically assessed. Immunohistochemistry was performed with a mouse monoclonal antibody anti-LTA4H (n=32) and a rabbit polyclonal anti-FXR1 (n=34) and semi-quantitatively scored as IRS score. RT-PCR was performed to quantify LTA4H and FXR1 gene expression.

In the present cases, mitotic index ranged 1-106 (median 15), Ki-67 index ranged 4.5-52.3 (median 13,7). 32/32 melanomas were positive for LTA4H staining, 33/34 for FXR1, with variable levels of distribution and intensity. RT-PCR values, expressed as ΔCt, ranged 0.76-5.11 for LTA4H and 0.22-6.24 for FXR1 (in 3 cases FXR1 was not detected).

Genetic expression showed marked differences among cases but was not statistically correlated with Ki-67 index, mitotic index or IRS score. There was no apparent relation between the favorable/unfavorable outcome and the level of expression of LTA4H/FXR1 in our cohort of cases. Even though a significant correlation between LTA4H-FXR1 and known indicators of malignancy has not been detected, the expression of LTA4H-FXR1 has been verified at both gene and protein levels. These data encourage further investigation on a possible role of FXR1 and LTA4H in the pathogenesis of canine oral melanoma.

Introduction

Melanoma is an aggressive neoplasia, common in dogs, which often represents a diagnostic and prognostic challenge. Melanoma represents about 3% of all canine tumors and 7% of all canine

malignant tumors. It affects the oral cavity (62%), the skin (27%), the digit (6%), and other sites, including the eye (5%) (Smith et al., 2002; Gillard et al., 2013). Melanoma is the most common malignant tumor of the oral cavity in dogs (Uzal et al., 2016).

Oral melanomas are traditionally considered malignant. They grow rapidly, are invasive, often recur after surgical resection and frequently metastasize, via lymphatic or blood vessels, to regional lymph nodes, lungs and viscera (Bergman, 2007; Smith et al., 2002). In dogs, the reported average survival time after diagnosis of oral melanoma spans 5-7 months (Gillard et al., 2014; Ramos-Vara et al., 2000; Spangler and Kass, 2006). However, a subset of oral melanocytic tumors with more favorable clinical course and prolonged survival exists, as expected mainly in dogs with histologically well-differentiated melanocytic neoplasms (Bergin et al., 2011; Esplin, 2008; Poorman et al., 2015; Spangler and Kass, 2006).

Classical histological malignancy criteria however have demonstrated poor indicators of metastatic behavior: several studies evaluated histological and immunohistochemical prognostic markers and possible threshold values to define morphological standards (Bergin et al., 2011; Spangler and Kass, 2006), but obtained different or even conflicting results. At this time, there is no good way to predict the likely progression of disease in individual dogs.

Recent studies both in human and in veterinary medicine have focused on the research of genetic markers that can have a good predictive value, with specific emphasis to markers of potential development of metastatic disease (Onken et al., 2010; Malho et al., 2013; Poorman et al., 2015). The studies of Onken and colleagues and Malho and colleagues investigated genetic biomarkers of uveal melanoma in human and veterinary medicine, respectively (Malho et al., 2013; Onken et al., 2010, 2004). These studies highlighted the existence of different molecular classes of expected survival based on the differential expression of a set of genes. Among them, an increased expression in Leukotriene A4 hydrolase (*LTA4H*) and Fragile X mental retardation-related protein 1 (*FXR1*) genes was related to metastasizing behavior in human and canine uveal melanoma.

LTA4H is a cytosolic hydrolytic enzyme, which catalyze the conversion of leukotriene A4 into leukotriene B4 inside the arachidonic acid cascade. LTA4H expression is widely distributed in several different tissues (Ohishi et al., 1990). Beside its known role in inflammation, LTA4H has also possible

implications in carcinogenesis, since many tumors arise from sites of chronic inflammation. LTA4H over-expression has been described in esophageal adenocarcinoma in human and rats (Chen et al., 2003), human esophageal liposarcoma (Myung et al., 2011), primary effusion lymphoma (Arguello et al., 2006), chronic lymphocytic leukemia (Guriec et al., 2014), and in chemically-induced oral carcinogenesis in mice and hamsters (Guo et al., 2011; Sun et al., 2006), human neuroblastoma (Sveinbjörnsson et al., 2008), pancreatic (Oi et al., 2010) and colon cancer (Jeong et al., 2009). *LTA4H* was also overexpressed in ocular canine (Malho et al., 2013) and feline melanomas (Rushton et al. 2017).

FXR1 is a cytoplasmic RNA binding protein, highly conserved among vertebrates and expressed in different tissues. FXR1 belongs to a family of RNA binding protein consisting of FMRP (fragile X mental retardation protein), responsible for the human fragile X mental retardation syndrome, and FXR2 (Fragile X mental retardation syndrome-related protein 2) (Siomi et al., 1995; Zhang et al., 1995). FXR1 acts in inflammatory process controlling the expression of tumor necrosis factor-α (TNF-α) at a post transcriptional level (Garnon et al., 2005; Khera et al., 2010a) and has a role in muscular cells development (Davidovic et al., 2013). Moreover, it has been shown to be over-expressed, in pulmonary squamous cell carcinoma, non-small cell lung cancer (Comtesse et al., 2007; Qian et al., 2015) and colorectal cancer (Jin et al., 2016).

The aims of the study were:

- to investigate the expression of LTA4H and FXR1 in canine oral melanoma, at both genetic and protein level (RT-PCR was used to analyze and quantify the expression of the codifying genes, standard ABC immunohistochemistry was adopted to localize and semi-quantitatively score the expression of proteins);
- to identify possible correlations among LTA4H and FXR1 expression and commonly adopted histological prognostic parameters, i.e. Ki-67 index and mitotic index;
- to compare laboratory results with clinical outcome data, when available, in order to establish if LTA4H and FXR1 can be proposed as prognostic markers.

The present study assessed the expression of LTA4H and FXR1 in formalin fixed and paraffin embedded (FFPE) samples of canine oral melanomas. The approach was intentionally directed to

FFPE samples because this is the type of material commonly available in the routine diagnostic activity of veterinary diagnostic laboratories: this study was conceived in the perspective of carrying out feasible and repeatable analyses for a diagnostic laboratory, in case that LTA4H/FXR1 expression would result significant for a further characterization of the tumor.

Materials and methods

Case selection and histology

Samples of FFPE oral melanomas were analyzed. Samples were collected from the diagnostic service of histopathology of the University of Milan (2011-2017) and from Clinica Veterinaria San Marco in Padova, for a total of 36 cases. Samples were routinely formalin fixed and paraffin embedded and 4 µm-thick sections were stained with hematoxylin and eosin (H&E).

H&E stained sections were evaluated on light microscope. For each sample, a histopathological description was provided, including traditional criteria of malignancy such as cellular atypia and number of mitoses. Mitotic index was calculated as the number of mitoses on 10 consecutive fields, starting in the area with the highest mitotic activity (Bergin et al., 2011).

Pigmentation of melanomas was semi-quantitatively evaluated, as "-" with complete absence of detectable pigment, ''mild/+'' when pigment represented approximately 1 to 10% cells with pigment, ''moderate/++'' when represented approximately 10 to 50% pigmented cells, and ''high/+++'' when greater than 50% pigmented cells (adapted from Smedley et al., 2011). In samples with no detectable pigment, the diagnosis of melanoma was confirmed through anti-PNL2 immunohistochemistry (see following section) (Ramos-Vara et al., 2000; Giudice et al., 2010).

Four fresh samples collected at Ospedale Veterinario Universitario of the University of Milan during the study (2015-2017) were also frozen in RNA-later to set up the amplification protocol. Referring veterinarians responsible for the clinical cases included in the study were asked, by email and/or phone call, to provide clinical follow up data.

Immunohistochemical detection of LTA4H, FXR1, Ki-67 and PNL2

Immunohistochemistry (IHC) for LTA4H, FXR1 and Ki-67 was performed in all samples to analyze their expression. IHC for PNL2 was performed in 5 non-pigmented samples to confirm the diagnosis of melanoma.

Serial paraffin sections were cut 4 µm thick and mounted on poly-lysine coated slides (Menzel-Gläser, Braunschweig, Germany). Immunohistochemical staining with the standard avidin-biotin-peroxidase complex (ABC) method was performed (Table 5).

Briefly, sections were deparaffinized in xylene and rehydrated through a descending series of ethanol concentrations. Incubation with H_2O_2 10% in Tris buffer saline (TBS; pH 7.4) for two hours at 55°C in a laboratory stove was used to bleach heavily pigmented sections and to block endogenous peroxidase activity (Momose et al., 2011). In the set up phase of the protocol, five sections of oral melanomas were treated with and without bleaching to assess if immunoreactivity was maintained.

Antigen retrieval was then performed by heating the slides in citrate buffer solution (pH 6.5) in a water bath at 95°C for 30 minutes (for LTA4H and FXR1) or in citrate buffer solution in pressure cooker for 18 minutes (for Ki-67) or in microwave oven in EDTA buffer solution (pH 8.5) for 10 minutes at 500W (for PNL2), followed by cooling down in buffer at room temperature (RT) for 30 minutes. Sections were therefore incubated for 20 min at RT with normal horse (LTA4H, Ki-67, PNL2) or goat (FXR1) serum (dilution 1:70) to block any nonspecific protein binding. Sections were then incubated at 4°C overnight in a humidified chamber with primary antibodies:

- mouse monoclonal leukotriene A4 hydrolase/LTA4H antibody (1E9 clone) (Novus Biologicals, Littleton, Co, USA), 1:100 dilution in TBS buffer;
- rabbit polyclonal anti-FXR1 antibody ab50841 (Abcam, Cambdrige, UK), 1:100 dilution (Nordio et al., 2018);
- mouse monoclonal anti-human Ki-67, clone MIB-1 (Dako, Glostrup, Denmark), 1:600 dilution;
- mouse monoclonal anti Melanoma-Associated Antigen, clone PNL2 (Monosan, Uden, Netherlands), 1:50 dilution.

Sections were then rinsed in TBS for three minutes for three times and incubated with the secondary anti-mouse (LTA4H; Ki-67; PNL2) or anti-rabbit (FXR1) biotinylated antibody (1:200, 30 minutes RT) (Vector Laboratories, Burlingame, CA, USA) followed by rinsing in TBS and therefore incubation with the ABC reagent (30 minutes RT) (Vector Laboratories, Burlingame, USA). After rinsing in TBS, the 3-amino-9-ethylcarbazole (AEC) chromogen (Vector Laboratories, Burlingame, CA, USA) was applied for 15 minutes and, after rinsing in tap water, slides were counterstained with Mayer's haematoxylin (Diapath srl, Martinengo, Italy) for 2 minutes. Slides were therefore dried and mounted in aqueous mounting agent (Aquatex, Merck, Darmstadt, Germany).

Canine skeletal myocytes adjacent to the neoplasm, when present, and neutrophils were adopted as internal positive controls for FXR1 and LTA4H immunolabelling, respectively (Chen et al., 2004; Nordio et al., 2018). Epithelium of intestinal crypts from a section of normal canine intestine was adopted as positive control for Ki-67, while a section of partially pigmented canine melanoma was adopted as positive control for PNL2. Negative controls were carried out by replacing the primary antibodies with mouse or rabbit IgG (Santa Cruz; Dallas, TX).

Table 5 - Immunohistochemical examination: details of antibodies used, dilutions, retrieval methods and positive controls.

IHC marker	Antigen retrieval	Primary antibody	Positive control
LTA4H	Water bath, citrate buffer pH 6.0 (30', 95°)	Mouse monoclonal leukotriene A4 hydrolase/LTA4H antibody (1E9 clone) (Novus Biologicals, Littleton, Co, USA), 1:100	Neutrohils
FXR1	Water bath, citrate buffer pH 6.0 (30', 95°)	Rabbit polyclonal anti-FXR1 antibody ab50841 (Abcam, Cambdrige, UK), 1:100	Skeletal myocytes
Ki-67	Pressure cooker, citrate bugger pH 6.0 (18')	Mouse monoclonal anti-human Ki-67, clone MIB-1 (Dako, Glostrup, Denmark), 1:600	Intestinal crypts epithelium
PNL2	Microwave oven, EDTA buffer pH 8.5 (10', 500W)	Mouse monoclonal anti Melanoma-Associated Antigen, clone PNL2 (Monosan, Uden, Netherlands), 1:50	Melanoma

Immunolabelled sections were evaluated at optic microscope. LTA4H and FXR1 labelled sections were semi-quantitatively scored, considering the percentage of positive cells (<10%, 10-30%, 30-50%, 50-70%, >70%), cellular localization of the signal (nuclear/cytoplasmic), intensity of staining

(mild, moderate, intense). The immunoreactive score adapted from Remmele and Stegner (IRS score) was calculated combining the intensity and ratio of positivity as follows: IRS score (0 - 12) = percentage of positive cells (with: no positive cells= 0, <10% positive cells= 1, 10-50 % of positive cells= 2, 50-70% of positive cells= 3, >70% of positive cells= 4) * intensity of staining (with: no positive cells= 0, 1+/mild = 1, 2+/moderate= 2, 3+/marked= 3) (Remmele and Stegner, 1987). To analyze if immunohistochemical scores were related with survival, IRS scores were therefore categorized in cumulative classes of expression, as summarized in Table 6.

Table 6 - IHC IRS scores categorization

IRS values	Class	Expression
0-3	1	mild
4-8	2	intermediate
9-12	3	marked

Ki-67 index was calculated as the mean number of labeled neoplastic cells in the 5 grid fields at 400x (Bergin et al., 2011). The number of positive nuclei was counted using a digital automatic counter (QCapture Pro 6.0). PNL2 positivity was evaluated as presence or absence of the signal.

Relative expression of LTA4H and FXR1

1) The **set up** of the amplification condition was assessed on frozen sample of oral cavity with melanoma and tested on frozen sample of healthy oral cavity, and FFPE samples of both healthy oral cavity and oral melanoma. Once ascertained the good efficiency obtained from FFPE material, the effective screening on melanoma samples started.

2) **RNA extraction** from FFPE tissue was performed using the RecoverAll Total Nucleic Acid Isolation Kit (Life Technologies). Eight section 10 µm thick were cut from FFPE tissue blocks and the extracted RNA was eluted in a final volume of 60 µl using the Elution Solution of the kit after an on-column DNasi treatment. RNA was quantified using NanoDrop ND-100 Spectrophotometer and stored at -80°C until molecular analyses. RNA extraction from frozen fresh samples was performed using RNeasy Minikit (Qiagen).

3) **Reverse transcription** transcribed RNA to cDNA (of at least 200 ng of RNA for every reaction) through QuantiTect Reverse Transcription kit, preparing two mixes: RT+ (containing reverse transcriptase) for subsequent qPCR analyses and RT- (not containing reverse transcriptase) as a control of a complete removal of contaminating DNA.

4) **Targets and primers**. Preliminarily, two housekeeping genes (*B2M*, Beta-2 microglobulin, and *ACTB*, actin beta) were tested to screen their expression stability in a subset of 10 samples. Sequences of primers for the housekeeping (*B2M, ACTB*) and the target (*LTA4H, FXR1*) genes and the amplification fragment size are detailed in Table 7.

Table 7 - Primers sequences and amplification fragment size

Name	Sequence	Amplification fragment size
LTA4H F	5' GTCACTCTCCAATGTTATTG 3'	73 base pairs
LTA4H R	5' CCAAGTTTTGTTGGTCAC 3'	
FXR1 F	5' TGGCAATTGGAACACATG 3'	115 base pairs
FXR1 R	5' TCAGCACTCTCTCCATAG 3'	
B2M F	5' TCCTCATCCTCCTCGCT 3'	85 base pairs
B2M R	5' TTCTCTGCTGGGTGTCG 3'	
ACT F	5' ATCGCTGACAGGATGCAGAA 3'	141 base pairs
ACT R	5' ACATTTGCTGGAAGGTGGACA 3'	

5) **Qualitative PCR and quantitative PCR (qPCR)**. Preliminary qualitative PCRs were performed to set up the amplification condition and verify the efficacy of the reverse transcription. qPCR mixes were subsequently prepared using SsoAdvanced Universal SYBR Green Supermix, BIO-RAD. Primers concentration and thermal profiles are described in Table 8 and Table 9.

Table 8 - Details of the reaction mixes

	Final condition for B2M, FXR1 and ACTB	Final condition for LTA4H
Sybr Green (2X)	1 X	10 µl
Forward primer	250 nM	400 nM
Reverse primer	250 nM	400 nM

A melting curve was assessed for each gene in order to verify the specificity of the amplification fragment and the absence of contaminating fragments. Data were normalized versus the reference gene and expressed as ΔCt.

Table 9 - Details of the amplification cycles thermal protocols

ACTB	***B2M***	***FXR1***	***LTA4H***
95°C for 0:15 58°C for 0:30 40 more times Melt Curve: 55 to 95°C, increment 0.5°C. 0:05	98.0 C for 0:10 58.0 C for 0:30 72.0 C for 0:15 39 more times Melt Curve 65.0 to 95.0 C, increment 0.5 C. 0:05	98.0 C for 0:10 50.0 C for 0:15 72.0 C for 0:15 39 more times Melt Curve 65.0 to 95.0 C, increment 0.5 C. 0:05	98.0 C for 0:10 55.0 C for 0:15 72.0 C for 0:15 39 more times Melt Curve 65.0 to 95.0 C, increment 0.5 C. 0:05

Statistical analyses

Molecular and immunohistochemical levels of LTA4H and FXR1 were compared between tumors with low (<19.5) and high Ki-67 index (≥19.5) and tumors with low (<4) and high (≥4) mitotic index, according to the prognostic thresholds proposed by Bergin and colleagues (Bergin et al., 2011). Adopted statistical tests were Mann Whitney U test and Kruskal-Wallis test ($p < 0.05$). Correlation between immunohistochemical IRS scores and molecular ΔCt was assessed by Spearman Rho test ($p < 0.05$). Survival analysis was performed in a subset of cases evaluating the overall survival by Kaplan–Meier estimator and Log-rank test, and the overall difference among cases with favorable and unfavorable clinical outcome was compared by Wilcoxon rank sum test.

Results

Case selection and histology

Thirty-six cases of oral melanomas belonging to thirty-two dogs were enrolled in the study (two animals had biopsy and later recurrence, one had a surgical biopsy and then the necropsy sample, and one animal had two samples in different sites of the oral cavity). Dogs belonged to different breeds and ranged 5-18 years of age (mean 11.8, median 12). Fifteen animals were male, fifteen were female, and for two animals sex was not reported. When data were provided, specific site of the tumor was recorded, specifically oral melanomas were located in the gum (n=10, 27.8%), labial mucosa (n=5, 13.9%), palate (n=2, 5.6%) and tonsillary region (n=1, 2.8%). All data are summarized in Table 10.

Histologically, melanomas exhibited different morphological types (epithelioid, spindle or mixed) and various degree of pigmentation. Nineteen tumors (52.8%) were morphologically classified as epithelioid, nine (25%) as spindle and eight (22.2%) as mixed. Seventeen tumors (47.2%) were amelanotic or mildly pigmented, thirteen (36.1%) had moderately pigmentation and six (16.7%) were highly pigmented. Mitotic index ranged 1-106 (mean 23.8, median 15). Five tumors had a mitotic index < 4, whereas 31 had mitotic index ≥ 4.

Immunohistochemical expression of LTA4H, FXR1 and Ki67

Of the originally selected 36 cases, 2 cases were excluded from the immunohistochemical results because they were poorly reactive, and 2 cases were excluded from the anti-LTA4H staining because no further material was available in the paraffin block. Immunoreactivity was of equal intensity in the preliminary subset of 5 samples treated with and without bleaching, thus confirming the maintenance of immunoreactivity after the bleaching protocol. Five non-pigmented samples were preliminarily confirmed as melanomas by positive immunolabeling with PNL2.

LTA4H had positive expression in all evaluated melanoma sections, FXR1 had positive expression in all but one case (Figure 6) (detailed results are provided in Table 10).

Briefly, LTA4H staining was evaluated on 32 cases. Sections were LTA4H-positive in 32/32 cases, with a percentage of positive neoplastic cells of 30-50% in 2 cases, 50-70% in five and above 70% in 25 cases. The intensity of staining was from mild to intense. The localization of the positivity was cytoplasmic (n = 19), nuclear (n = 3), or both nuclear and cytoplasmic (n = 10). IRS score varied from 3 to 12, being between 4 and 8 in 18/32 cases (56.3%) and between 9 and 12 in 14/32 cases (43.8%) (Graph 1).

FXR1 immunolabelling was evaluated in 34 oral melanomas and stained positive in 33/34. Eight cases had more than 70% of positive neoplastic cells, nine between 50-70%, five 30-50%, five 10-30%, six under 10% and one case was negative. Fourteen cases were intensely stained, thirteen moderately and six mildly. The immunostaining was always cytoplasmic. IRS score varied from 0 to 12, being between 0 and 3 in 6/34 cases (17.6%), between 4 and 8 in 13/34 cases (38.2%) and between 9 and 12 in 11/34 cases (32.4%) (Graph 1).

Ki-67 index was assessed in 28 cases. The average number of positive neoplastic nuclei ranged 4.5-52.3, with a mean of 16.9 and a median of 13.7. Ki-67 index was beneath 19.5 in 19 cases and above 19.5 in 9 cases.

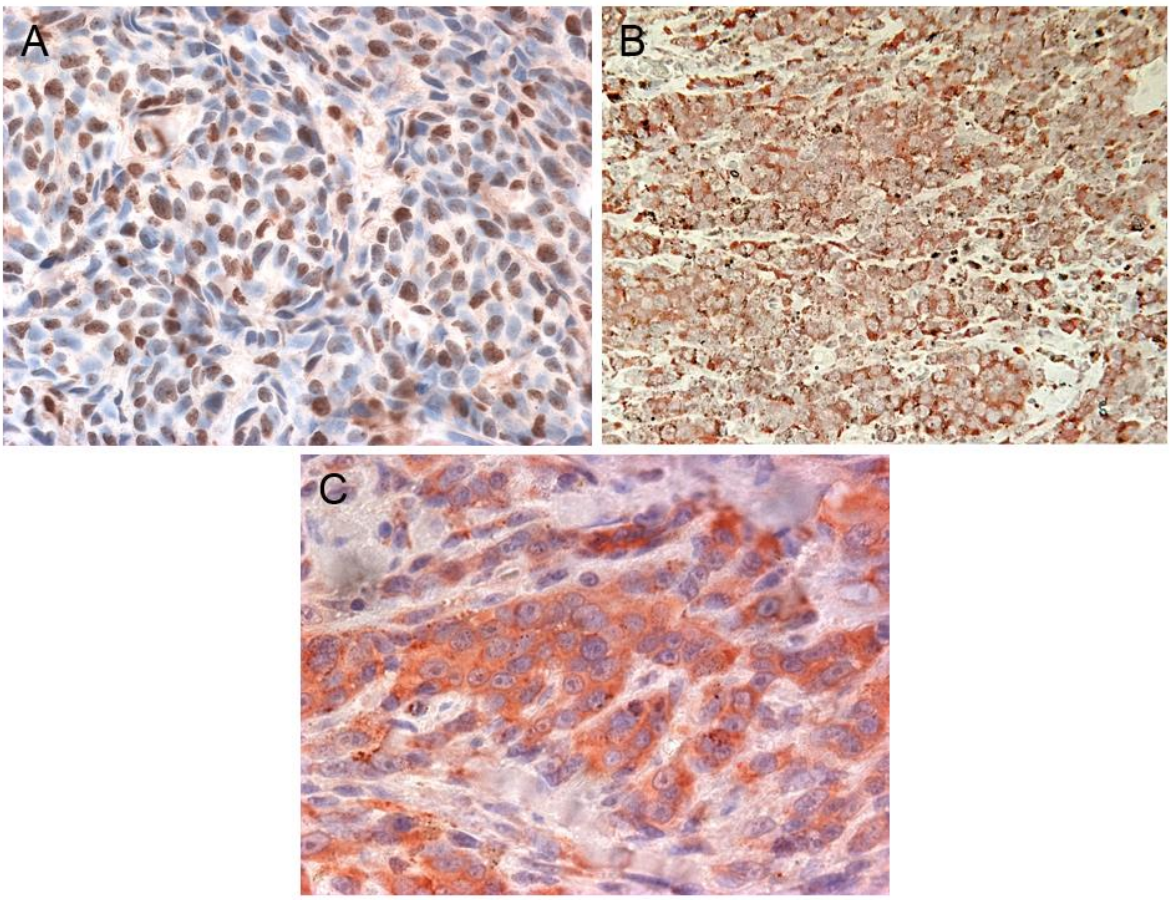

Figure 6 - Canine oral melanoma, immunohistochemistry. A) Anti-LTA4H staining, diffuse nuclear signal. AEC chromogen, 40x. B) Anti-LTA4H staining, diffuse cytoplasmic signal. AEC chromogen, 20x. C) Anti-FXR1 multifocal intense signal. AEC chromogen, 40x.

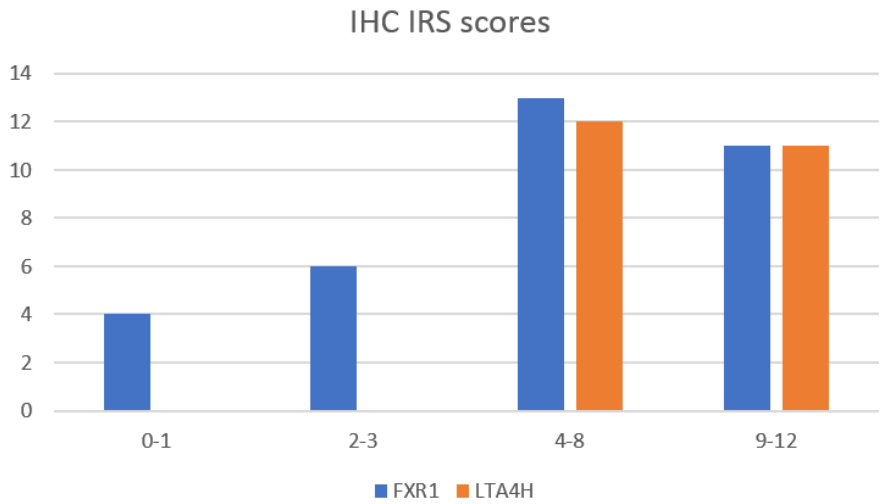

Graph 1 - Immunohistochemical IRS scores of LTA4H and FXR1 expression in canine oral melanomas.

The comparison of groups with low and high Ki-67 index (<19.5 and ≥19.5) with the levels of immunohistochemical scores of LTA4H and FXR1 revealed no statistically significant differences (p=0.212 and 0.138, respectively) (Graph 2). Groups with low and high mitotic index (<4 and ≥4) had no significantly different levels of immunohistochemical FXR1 (p=0.153) but had significantly different IRS scores of LTA4H (p=0.017) (Graph 3). The intracellular localization of LTA4H immunohistochemical signal (nuclear, cytoplasmic, or nuclear and cytoplasmic) showed no statistical correlation with LTA4H IRS score (p=0.532).

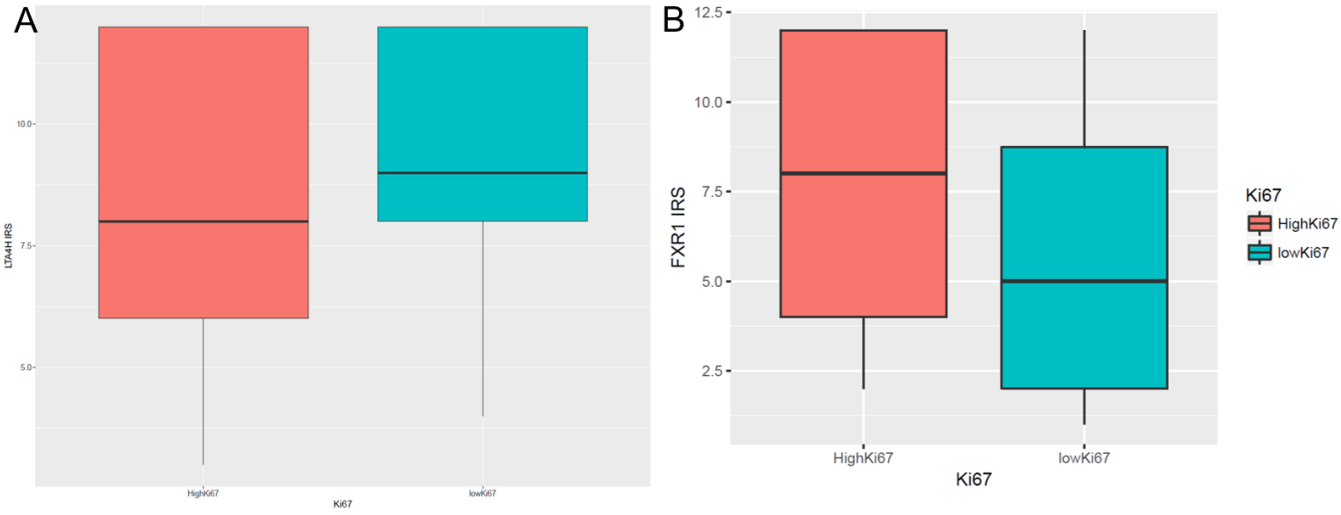

Graph 2 - LTA4H (A) and FXR1 (B) IRS scores: comparison among groups with low and high Ki-67 index. (A) p=0.212, (B) p=0.138.

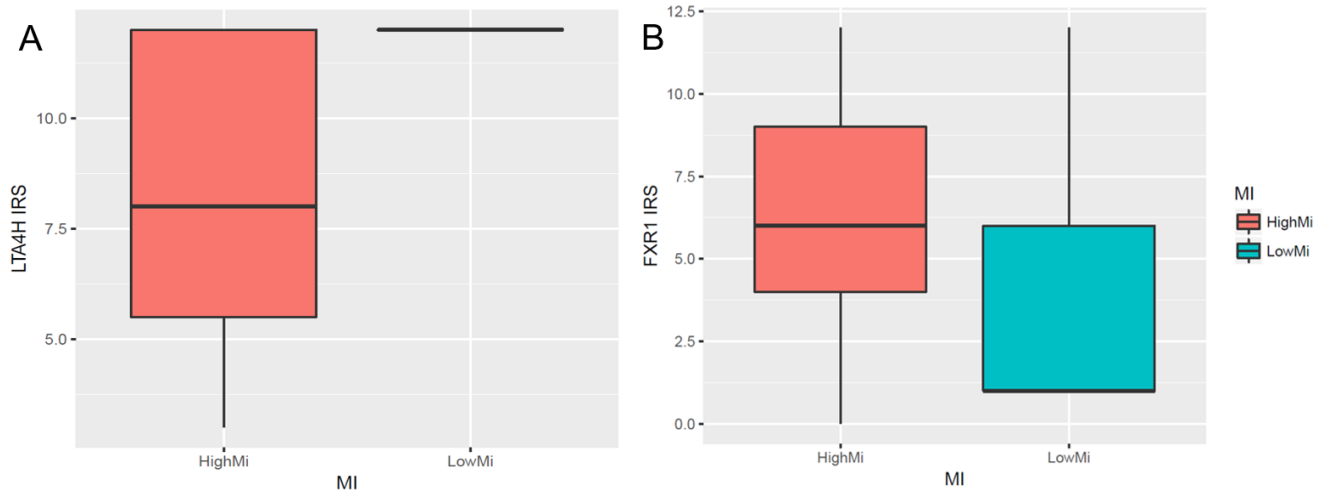

Graph 3 - LTA4H (A) and FXR1 (B) IRS scores: comparison among groups with low and high mitotic index (MI). (A) p=0.017, (B) p=0.153.

LTA4H and FXR1 gene expression

36 FFPE cases of canine oral melanoma were analyzed with RT-PCR to quantify the expression of the target genes *LTA4H* and *FXR1*.

B2M and *ACTB* were preliminary tested as housekeeping genes in a subset of 10 samples, to asses if the expression trend was stable. Despite the presence of a difference in the threshold cycles (Ct) of *B2M* and *ACTB* (paired t test: t9=8.48; p<0.0001), the relation between the two genes expression was linear (p<0.0001), thus indicating that the ratio of expression between *B2M* and *ACTB* was constant. The Ct of these two housekeeping genes were related by the equation: Ct B2M = 7.3 + 0.82*Ct ACTB (R^2 = 0.92) (Figure 7).

Therefore, due to the paucity of available cDNA material, *B2M* was chosen as housekeeping gene to complete the analyses of the samples in order to quantify the expression of the investigated target genes.

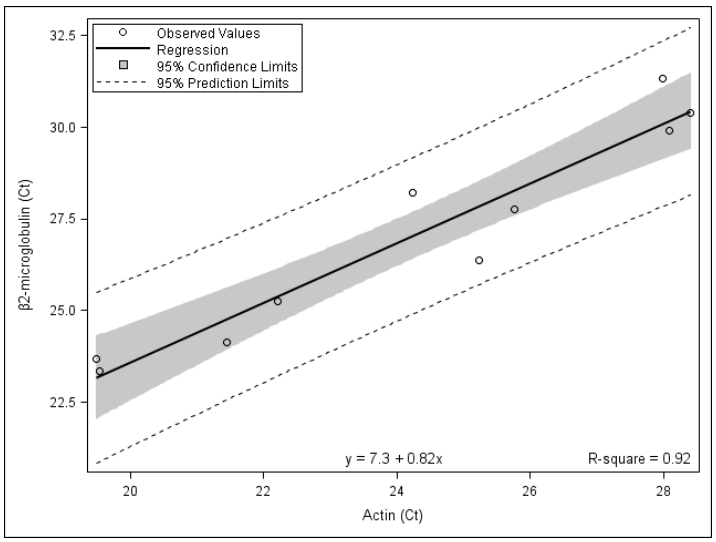

Figure 7 – Regression line between ACT Ct – B2M Ct. R^2 = 0.92

Among the analyzed samples, an extraction of RNA suitable for PCR was obtained in 23 cases and in these samples *LTA4H* and *FXR1* were successfully amplified. Final results of expression, expressed as ΔCt, comparing the Ct of the target gene with the Ct of the housekeeping gene, were obtained in these samples, which ranged 0.76-5.11 for *LTA4H* and 0.22-6.24 for *FXR1*. The amplification of *FXR1* gene for three samples was not quantified due to the Ct value out of the dynamic range of the reaction.

Molecular expression of both *LTA4H* and *FXR1* genes did not differ among groups with low and high Ki-67 index (<19.5 and ≥19.5) (LTA4H p=0.502, FXR1 p= 0.635), nor among groups with low and high mitotic index (<4 and ≥4) (LTA4H p=0.5005, FXR1 p= 0.140). LTA4H molecular and immunohistochemical values were correlated (p=0.014), but FXR1 were not (p=0.122) (Graph 4).

All the results of the experiments are summarized in Table 10.

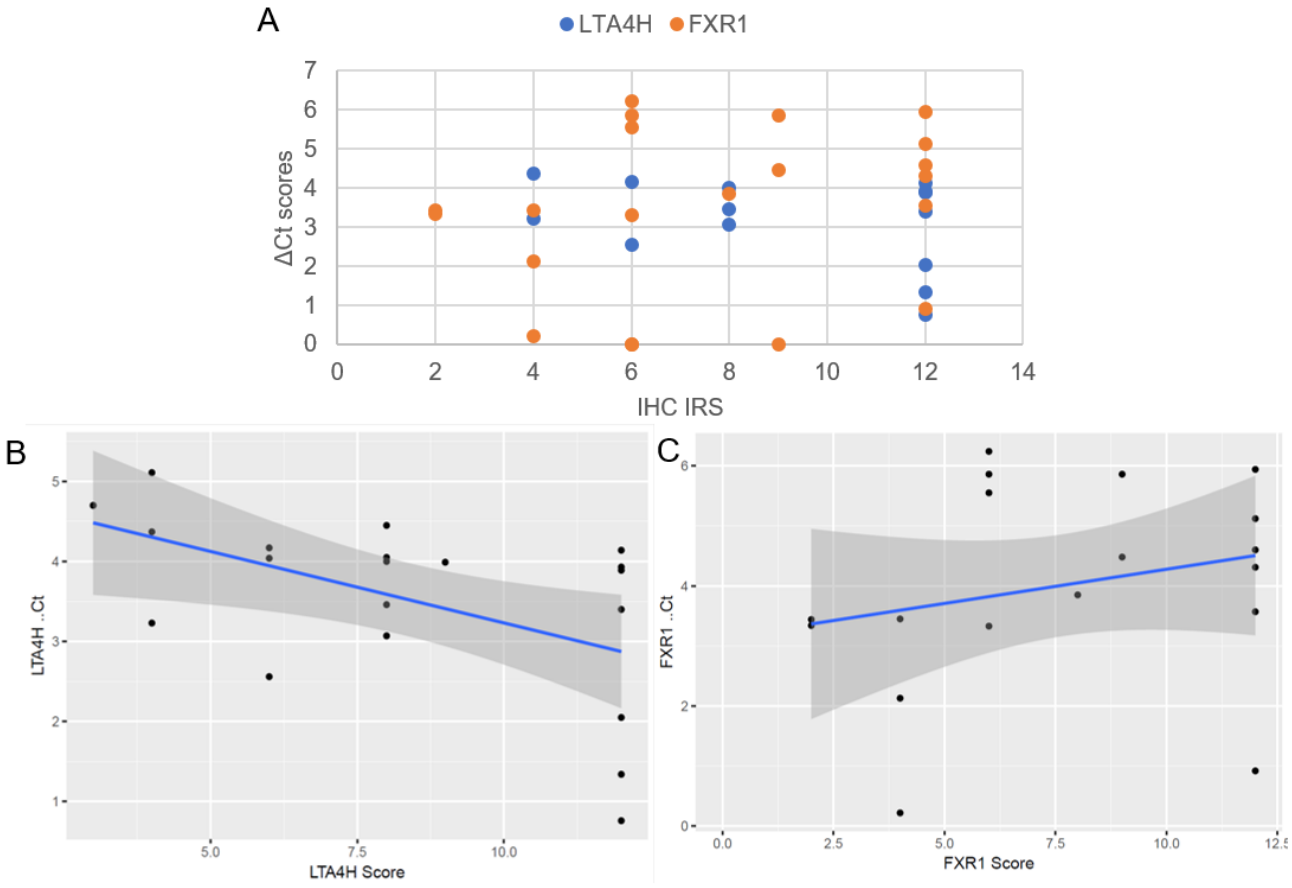

Graph 4 – (A) Comparison among the IHC IRS scores (x axis) and the molecular ΔCt (y axis) of LTA4H and FXR1 in canine oral melanomas. Every dot represents a single case. (B) LTA4H and (C) FXR1: correlation among IHC IRS score (x axis) and ΔCt (y axis). LTA4H p=0.014, FXR1 p=0.122.

Clinical outcome

Data about the clinical outcome were retrieved in a subset of 14 dogs. Among these cases, 11 dogs were dead at the time of writing, and death happened in a period that ranged from 1 day to 7 months after the first diagnosis. In 7 cases, euthanasia was performed, while in 4 cases spontaneous death occurred. Local recurrences were reported in 4 of these cases, distant metastases were proven in 3 cases (two by full necropsy and one by X-rays). Finally, 3 dogs were still alive at the time

of writing, 2 (1 case) and 3 years (2 cases) after the diagnosis. In 7 of these 14 cases, molecular quantification of the target genes was obtained.

The IRS scores of LTA4H and FXR1, categorized in the classes of expression 1/mild, 2/intermediate, and 3/marked, did not show any significant relationship with the overall survival data (LTA4H p=0.996, FXR1 p=0.684) (Graph 5).

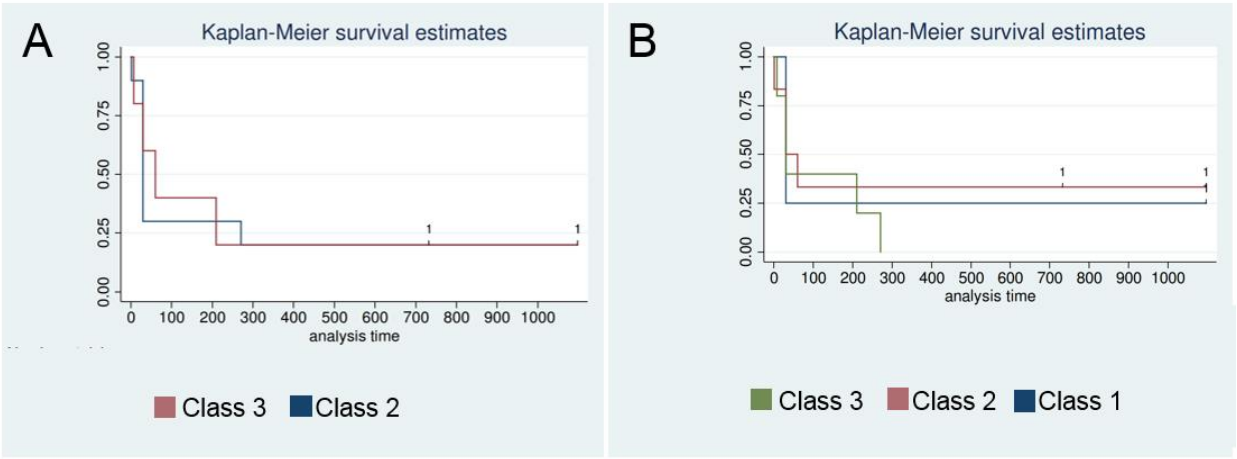

Graph 5 - Kaplan-Meier survival analysis. The analyzed parameters is the immunohistochemical expression of LTA4H (A)(p=0.996) and FXR1 (B)(p=0.684) summarized as follows: IRS scores 0-3 = class 1, IRS scores 4-8 = class 2, IRS scores 9-12 = class 3.

There was no overall significant difference in IRS scores of both LTA4H (p=0.448) and FXR1 (p=0.395) in dead versus alive dogs by Wilcoxon rank sum test (Graph 6).

Further analyses on the relationship of survival with the molecular results were not carried out because the cohort of cases for which both molecular and survival data were obtained was too small.

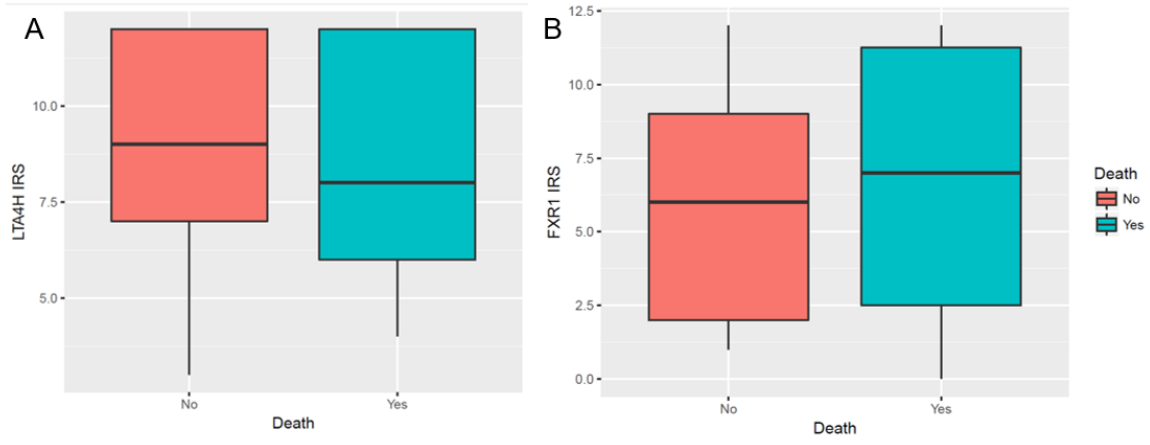

Graph 6 – No significant differences are evident in the comparison of dead versus alive dogs for their LTA4H (A) (p=0.448) and FXR1 (B) (p=0.395) IRS scores by Wilcoxon rank sum test.

Discussion

In the present study, a caseload of canine oral melanomas was investigated for the expression of two targets, i.e. LTA4H and FXR1, at both gene and protein level.

Anamnestic and histological data of dogs included in the study were mostly consistent with previous literature reports. Dogs were equally distributed among sexes and variably distributed among breeds, with a prevalence of mixed breed. The onset was in adult-old age with a mean of 11,7 years of age, consistent with previous reports in literature (Bergin et al., 2011; Bolon et al., 1990). As in previous reports, the most represented site of onset was the gum (Smith et al, 2002). Histologically, a high variability of neoplastic cells was observed, with a prevalence of epithelioid morphology followed by the spindle and mixed types. The pigmentation of neoplastic cells was also highly variable, although, in almost half of the samples, scant or absent. Smedley and co-authors referred that different studies tried to evaluate the prognostic significance of the degree of tumor pigmentation, but, most likely due to the subjectivity in the quantification of the pigment, the authors were not able to identify threshold levels of pigmentation that define malignancy (Smedley et al., 2011).

In the cohort of cases investigated in the present study the presence of LTA4H and FXR1 was detected at both gene and protein levels. LTA4H and FXR1 are two genes/molecules that have been previously correlated with metastasizing behavior in other types of non-UV induced melanomas.

LTA4H has been previously described to be over-expressed in different types of tumor in human, mice, dogs and cats (Arguello et al., 2006; Chen et al., 2003; Guo et al., 2011; Guriec et al., 2014; Myung et al., 2011; Oi et al., 2010; Rushton et al., 2017; Sun et al., 2006; Sveinbjörnsson et al., 2008). Eicosanoids such as leukotrienes are mediators of inflammation and chronic tissue inflammation has been linked to increased risk for the development of cancer (Dubois, 2003). Aberrant arachidonic acid metabolism is suspected to have a role in carcinogenesis due to the imbalance shifted towards the pro-carcinogenic lipoxygenase pathways (5-, 8- and 12- LO) instead that anti-carcinogenic (15-LO) (Dubois, 2003; Shureiqi and Lippman, 2001).

FXR1 has also been investigated in tumorigenesis (Comtesse et al., 2007; Jin et al., 2016; Qian et al., 2015). FXR1 is supposed to affect DNA stability with two pathways (Ma et al., 2014), either using

miRNA pathway to regulate target mRNA expression (Edbauer et al., 2010), or playing a role in post-transcriptional regulation directly interacting with mRNA and affecting its stability (Davidovic et al., 2013). In lung tumorigenesis, for example, FXR1-dependent regulation of mRNA may specifically regulate ERK (extracellular-signal-regulated kinases) signaling pathway (Qian et al., 2015). Moreover, FXR1 recruits transcription factor STAT1 or STAT3 to gene promoters and, through the regulation of transcription, mediates cell proliferation in human cancers harboring TP53 homozygous deletion (Fan et al., 2017). In addition, as already mentioned for LTA4H, FXR1 also play a role also in inflammation, as it represses the expression of tumor necrosis factor-α (TNF-α) (Garnon et al., 2005; Khera et al., 2010a).

LTA4H and *FXR1* have been specifically found to be over-expressed in human and canine uveal melanomas (Demirci et al., 2013; Malho et al., 2013; Onken et al., 2010). *LTA4H* has also been reported to be upregulated in ocular melanomas in cats (Rushton et al., 2017). The immunohistochemical expression of FXR1 protein has also been previously demonstrated in a small caseload of canine uveal and oral melanocytic tumors (Nordio et al., 2018).

In the present study, RT-PCR was used to quantify the expression of the investigated genes *LTA4H* and *FXR1*. *LTA4H* was detected and quantified in all cases (23), *FXR1* was detected in 20 out of 23 cases. Both genes displayed a high variability of expression (0.76-5.11 for *LTA4H* and 0.22-6.24 for *FXR1*).

Immunohistochemistry was applied to identify and localize LTA4H and FXR1 proteins in histological sections of melanomas. LTA4H was immunohistochemically detected in neoplastic cells in all samples, in most cases with high levels of expression (IRS mean 8.5), whereas FXR1 was expressed in all but one melanomas, with a broader distribution among the semi-quantitative classes of IHC staining (IRS mean 6.1).

In general, for both antigens tested, immunohistochemical positivity showed negligible expression differences among cases. Conversely, the RT-PCR relative expression of *LTA4H* and *FXR1* genes exhibited marked differences among cases. Comparing immunohistochemical results, expressed as IRS score, with RT-PCR results, expressed as ΔCt, a correlation among protein and gene expression was significant only for LTA4H. This discrepancy between immunohistochemical and RT-

PCR results can have different explanations. Firstly, immunohistochemistry, although extremely useful in providing information concerning the localization of antigens, is not a quantitative technique, as opposite to RT-PCR. Moreover, protein tissue expression does not instantly reflect possible alterations during the synthesis process, which can take place from transcription to post-translational modifications, i.e. protein expression not necessarily mirrors gene expression. Finally, molecular analyses may be influenced by residual constitutive expression of genes in normal adjacent tissues or extracellular matrix.

The second aim of the present study, once assessed the presence of target genes and proteins, was to evaluate their possible association with accepted indicator of malignancy (i.e. mitotic index and Ki-67 index) in order to test if their presence/expression could be related with biological behavior of the tumor.

Mitotic index and Ki-67 index are widely accepted diagnostic criteria of malignancy in canine oral melanoma (Smedley et al., 2011). The threshold currently adopted for mitotic index is 4 mitotic figures in 10 high power field. In the present work, most of the tumors (31) were above this threshold. Analyzing data of expression of the investigated targets, no difference between groups with different mitotic index emerged on both gene and protein levels for both LTA4H and FXR1.

Bergin and co-authors also identified a Ki-67 index value of 19.5 as discriminating prognostic factor in canine oral melanoma (Bergin et al., 2011), with tumors characterized by Ki-67 index higher than 19.5 being more prone to death or euthanasia due to melanoma by 1 year postdiagnosis. In the present study, PCR and immunohistochemical data obtained on LTA4H and FXR1 were compared with Ki-67 index of melanomas. No statistically significant association between Ki-67 index and molecular expression of either LTA4H or FXR1 was present.

Finally, in a smaller subset of samples, the immunohistochemical expression of LTA4H and FXR1 could be compared with the clinical outcome. We decided to evaluate the overall survival time due to the wide variability of medical treatments adopted by clinicians. No significant association was evident between the immunohistochemical expression of LTA4H/FXR1 and the overall survival of the dogs.

The present study demonstrated that LTA4H and FXR1 gene and protein are actually expressed in canine oral melanoma. Unfortunately, both LTA4H and FXR1 were not related with validated criteria of malignancy for canine oral melanoma, i.e. mitotic index and Ki-67 index. These results suggest that LTA4H and FXR1 expression is unrelated to tumor behavior in oral melanoma, conversely to what has been demonstrated in uveal melanoma. However, their extensive expression in the present cohort of cases could indicated that they nevertheless play a role, although different and still undefined, in canine oral melanomas too.

On the other hand, in previous studies the overexpression of *LTA4H* and *FXR1* genes has been specifically associated with increased metastatic risk of uveal melanoma, while in the present study LTA4H and FXR1 were compared with indicators of tumor malignancy, but not specifically with the presence of metastases. In this regard, it is worth considering that canine uveal and oral melanocytic tumors are characterized by different biological behavior. Indeed, while uveal melanomas are generally slowly progressive and slowly metastasizing tumors, oral melanomas are aggressive tumors with rapid progression and frequently already metastasized at the time of diagnosis (Smith et al., 2002; Bergman, 2007), (Wilcock and Peiffer 1986; Dubielzig, 2017). Therefore, while in uveal melanomas tumor-related death is mostly due to distant metastases, patient affected by oral melanoma are frequently euthanatized due to severe deterioration of life quality and general health conditions. In these latter conditions, metastases, if they occurred, remain undetected and a full necropsy is most often declined by the owners.

Therefore, the more homogeneous, rapidly aggressive, behavior of canine oral melanomas may affect the lack of discriminating value of the markers that we investigated. Moreover, considerations on the clinical outcome should be taken carefully, considering the small number of cases investigated, and the factors influencing negatively the homogeneity of the population (age of the affected animals, different therapeutic choices).

Conclusions

LTA4H and FXR1 genes and proteins are expressed in canine oral melanoma, even if their differential expression seemed not associated with known histological criteria of malignancy or with the clinical outcome.

Even though a significant correlation bewteen LTA4H and FXR1 and known indicators of tumor malignant behavior has not been detected, the expression of this two molecules has been verified at both gene and protein levels. This data encourage further investigation on a possible role of FXR1 and LTA4H in the pathogenesis of canine oral melanoma, possibly on a larger cohort of cases.

Results of the present work have been presented as follows:

- *Nordio L., Bazzocchi C., Genova F., Serra V., Longeri M.L., Rondena M., Stefanello D., Giudice C. "Molecular and immunohistochemical expression of LTA4H and FXR1 in canine oral melanomas". Manuscript in preparation.*

- *Nordio L., Genova F., Serra V., Bazzocchi C., Longeri M.L., Stefanello D., Rondena M., Giudice C. (2017). "LTA4H and FXR1 gene and protein expression in canine oral melanoma". 3rd Joint European Congress of the ESVP, ESTP and ECVP, Lyon, 30th August-2nd September 2017 (poster presentation).*

- *Nordio L., Genova F., Serra V., Bazzocchi C., Longeri M.L., Stefanello D., Giudice C. (2016). "LTA4H expression in canine oral melanomas: preliminary results". 34th ESVP – 27th ECVP Annual Meeting, Bologna, 7th-10th September 2016 (poster presentation), Journal of Comparative Pathology 2017, Vol. 156, 54-141, ESVP and ECVP Proceedings 2016.*

- *Nordio L., Genova F., Serra V., Giudice C. (2016). "LTA4H expression in canine oral melanomas: methodological set up and preliminary results". Proceeding of Veterinary and Animal Science Days 2016, 8th - 10th June 2016, Milan, Italy (oral presentation). International Journal of Health, Animal Science and Food safety, 3.*

									IHC LTA4H				IHC FXR1						
	Breed	**sex**	**Age**	**Oral cavity: location**	**Morphology**	**Pigmen-tation**	**Mitotic index**	**Ki67 index**	**localization**	**% positivity**	**intensity**	**IRS score**	**localization**	**% positivity**	**intensity**	**IRS score**	**LTA4H ΔCt**	**FXR1 ΔCt**	**Clinical outcome**
1	Bernese mountain dog	SF	11	labial mucosa	spindle	+++	5	na	na	na	na	na	negative	0	0	0	na	na	dead (unknown interval)
2	English setter	M	15	na	epithelioid	+	71	13,33	c + n	>70	3	12	c	>70	3	12	1.34	3,57	local recurrence after 3 months and death after 7 months
3	Dachshund	M	na	gum, upper maxillary arch	spindle	+	28	10,00	c	>70	2	8	c	30-50	2	4	3,46	2,13	na
4	Mixed breed	M	10	na	spindle	+	39	7,08	n	>70	3	12	na	na	na	na	4,14	5,42	na
5	Pit bull	F	13	upper labial mucosa	epithelioid	++	8	12,63	c	>70	3	12	c	30-50	2	4	3,4	3,45	na
6	Shar pei	SF	7	palate	spindle	+	18	4.50	c	>70	1	4	c	50-70	3	9	3,23	5,86	na
7	Mixed breed	SF	12	na	epithelioid	++	17	22,33	c + n	30-50	1	3	c	30-50	3	6	4,7	5,86	na
8	Mixed breed	SF	18	na	epithelioid	+++	37	27,21	c + n	>70	3	12	c	10-30	1	2	na	na	na
9	Dachshund	M	14	gum	epithelioid	+	11	11,67	c	>70	2	8	c	30-50	3	6	3,07	5,55	na
10	Mixed breed	SF	12	gum/ labial mucosa	spindle	+	54	12,08	c	>70	3	12	c	50-70	3	9	3,89	4,48	na
11	Rottweiler	SF	7	na	mixed	-	43	33,33	c + n	>70	3	12	c	>70	3	12	0.76	0,92	euthanized after 1 week
12	Golden retriever	F	14	na	mixed	+++	2	5,71	c	>70	3	12	c	<10	1	1	na	na	na
13	Nd	nd	nd	labial mucosa	epithelioid	++	7	15,00	c	>70	1	4	c	50-70	2	6	4,37	6.24	alive after 2 years
14	Mixed breed	SF	13	gum	spindle	+++	1	5,33	c + n	>70	3	12	c	50-70	2	6	3,93	out of range (>35)	euthanized after 1 month for posterio paraparesis
15	Mixed breed	NM	14	na	epithelioid	++	11	5,54	c	>70	2	8	c	50-70	3	9	na	na	local recurrence after 5 months and euthanasia after 9 months
16	English setter	SF	10	soft palate	epithelioid	+++	3	18,17	c	>70	3	12	c	<10	1	1	na	na	alive after 3 years
17	Mixed breed	M	14	na	mixed	-	11	39,42	c	50-70	2	6	c	>70	3	12	4,17	5,12	na
18	Nd	M	14	na	epithelioid	++	5	7,79	c	>70	2	8	c	<10	2	2	na	na	euthanized after 1 month
19	Mixed breed	M	11	na	spindle	++	9	na	na	na	na	na	c	50-70	2	6	4,09	out of range (>35)	na

20	German sheperd	M	11	gum	epithelioid	++	17	24,42	c	>70	2	8	c	10-30	2	4	na	na	na
21	West highland white terrier	SF	7	gum	mixed	++	26	19,67	c + n	50-70	2	6	c	>70	3	12	2,56	4,6	two local recurrences, euthanized after 1 month
22	German sheperd	M	16	na	mixed	++	7	17,67	c	>70	3	12	c	10-30	1	2	2,05	3,44	na
23	Dachshund	M	11	gum	epithelioid	+++	2	11,67	c + n	>70	3	12	c	<10	1	1	na	na	na
24	Mixed breed	nd	nd	na	epithelioid	++	8	na	c	>70	1	4	c	<10	2	2	na	na	na
25	Mixed breed	SF	12	oral vestibule	epithelioid	++	92	52,25	c	>70	1	4	c	<10	2	2	na	na	dead after 1 month
26	Mixed breed	F	11	tonsillar region	epithelioid	+	27	14	c	>70	2	8	c	10-30	2	4	4	0.22	dead after 1 month
27	Hungarian spitz	M	13	maxillary region	epithelioid	+	28	na	n	30-50	2	4	c	30-50	3	6	na	na	dead with metastases after 1 day
28	Labrador retriever	NM	13	gum	epithelioid	+	6	na	na	na	na	na	na	na	na	na	3,66	5,38	alive after 3 years
29	Mixed breed	F	10	gum, maxillary area	spindle	+	6	na	c	>70	1	4	c	50-70	3	9	5.11	out of range (>35)	recurrence of case #4
30	Pekingese	M	12	gum, molar area	epithelioid	++	44	10,33	c	>70	2	8	c	10-30	1	2	4,05	3,34	na
31	Golden retriever	F	5	gum	epithelioid	++	1	na	na	na	na	na	c	>70	3	12	4,41	5,94	na
32	German sheperd	M	11	oral cavity mandible region	mixed	+	22	na	c + n	50-70	3	9	c	50-70	2	6	3,99	3,33	na
33	German sheperd	M	11	oral cavity mandible region	mixed	+	13	10,42	c + n	50-70	3	9	c	50-70	3	9	na	na	recurrence of case #32
34	Mixed breed	M	12	lower lip mucosa	epithelioid	-	49	23,08	c	>70	3	12	c	>70	2	8	na	na	local recurrence after 2 months, euthanized after 2 months with lymphnodal metastasis
35	Beagle	M	14	upper gum	mixed	-	22	22,25	c + n	>70	2	8	c	>70	3	12	4,45	4,31	euthanized after 1 months, visceral metastases proved by autopsy
36	Beagle	M	14	upper gum (necropsy of #36)	mixed	-	106	15,92	n	50-70	2	6	c	>70	2	8	4,04	3,85	necropsy sample of case #36

Table 10 - Summary of caseload of analyzed canine oral melanomas, with signalment, histology, IHC, RT-PCR.
Legend: c= cytoplasmic, n= nuclear, na = not assessed; 1 = mild, 2 = moderate, 3 = intense

III. PRELIMINARY OBSERVATIONS ON MATRIX METALLOPROTEINASES IN CANINE ORAL MELANOMA: ASSOCIATION OF MMP-9 AND TIMP-2 WITH FXR1 IMMUNOHISTOCHEMICAL EXPRESSION AND CLINICAL OUTCOME

Abstract

Canine oral melanoma is an aggressive tumor that arise and metastasize spontaneously, similarly to human mucosal melanoma. Among previously studied gene with a role in the prognosis of melanomas, there is FXR1. FXR1 belongs to a family of RNA binding protein able to modulate mRNA of selected molecules, such as the proteolytic enzyme matrix metalloproteinase-9 (MMP-9).

The present study investigates the association of MMP-9 expression with FXR1 expression and with clinical outcome data in a cohort of canine oral melanomas. FXR1 gene and protein have been evaluated through RT-PCR and immunohistochemistry (IHC), respectively. MMP-9 and its inhibitor TIMP-2 have been investigated through IHC. IHC was evaluated combining the intensity and percentage of positive neoplastic cells as IRS score. Comparisons were carried out among the IHC IRS score of MMP-9 and TIMP-2 in groups with high and low expression of gene/protein FXR1 (group A n=5 and group B n=7, respectively), and in groups with overall survival (OS) above/below one year after diagnosis (group C n=3 and group D n=7, respectively).

The mean IRS scores of MMP-9 and TIMP-2 were 7.6 and 9.2 with high FXR1, respectively, and 5.3 and 5.4 with low FXR1. The mean MMP-9-TIMP-2 IRS scores were 6-9 with OS < 1 year, respectively, and 3-4.3 with OS > 1 year.

MMP-9 expression seemed not associated with FXR1 differential expression. A trend for higher expression of MMP-9/TIMP-2, even if not significant, was observed in cases with high expression of FXR1 and unfavorable clinical outcome, suggesting that these proteins could be associated independently with the aggressiveness of the tumor.

Introduction

Spontaneous occurring oral melanomas are frequent in dogs and can be considered spontaneous animal model of human mucosal melanoma. Canine oral melanomas represent about 7% of all

malignant neoplasia in dogs (Smith et al., 2002), are highly heterogeneous and aggressive, and arise and metastasize spontaneously, thus more closely reflecting the process of spontaneous tumorigenesis. In human medicine, oral melanomas represent about 25-40% of mucosal melanomas that are, in turn, considered a rare but aggressive variant of melanoma (Mihajlovic et al., 2012). Canine oral melanoma shares biological and molecular features with human mucosal melanoma: both exhibit a malignant behavior, that includes biological aggressiveness, metastasizing tendency and poor prognosis, and specific mutations, such as those affecting *NRAS* and *PTEN* genes (van der Weyden et al., 2016). More recently, altered expression of specific genes, such as *FXR1*, has been demonstrated in a subset of human and canine melanomas, possibly correlating with the biological behavior of the neoplasms (Onken et al., 2010; Malho et al., 2013).

FXR1 (Fragile X mental retardation-related protein 1) is a cytoplasmic RNA binding protein, which belongs to a family of RNA binding protein consisting of FMRP (fragile X mental retardation protein), responsible for the human fragile X mental retardation syndrome, and FXR2 (Fragile X mental retardation syndrome-related protein 2) (Siomi et al., 1995; Zhang et al., 1995). This family of mRNA binding protein, particularly FMRP, can target, among the others, the mRNA coding for MMP-9 (matrix metalloproteinase-9) (Castagnola et al., 2017). MMP-9, in turn, is an endopeptidase with proteolytic activity (Nagase et al., 2006), whose ability to digest the extracellular matrix has been involved in the process of tumor invasion, in the wider scenario of the interaction between neoplastic cells and the so-called tumor microenvironment.

Complex interactions between neoplastic cells and the extracellular matrix are considered critical in carcinogenesis, tumor invasion and metastasis. MMPs belong to a family of calcium and zinc dependent endopeptidases, which play a proteolytic activity on many constituents of the extracellular matrix (ECM). MMPs are implied in a variety of physiological processes, for example reproduction, fetal development, wound healing, as well as in different pathological processes, for example tumor invasion and metastasis, inflammation and vascular diseases (Lepetit et al., 2005; Panek and Bader, 2006; Raffetto and Khalil, 2008; Sorensen et al., 2004). TIMPs (tissue inhibitors of matrix metalloproteinases) act as inhibitors of MMPs. MMPs and TIMPs are usually balanced in healthy tissues, whereas, on one hand, an excess of TIMPs may lead toward an excess of matrix

deposition, and, on the other hand, an excess of MMPs leads to degeneration of the ECM (Khokha et al., 2013; Moro et al., 2014; Nagase et al., 2006; Roeb, 2018). The balance among the MMPs and TIMPs, rather than the single results, gives an overall effect on the ECM remodeling.

Among MMPs, MMP-9 (gelatinase B) has been reported to be implied in tumorigenesis (El-Shabrawi et al., 2001; Yadav et al., 2014). MMP-9 is able to degrade elastin and denatured collagen of types IV, V, VII and X. It is produced as inactive zymogen, which requires activation, mainly by keratinocytes, monocytes, alveolar macrophages, polymorphonuclear leukocytes and tumoral cells (Nagase et al., 2006; Raffetto and Khalil, 2008; Ramos-DeSimone et al., 1999; Visse and Nagase, 2003).

The aims of the present study are to investigate the expression of MMP-9 and its inhibitor TIMP-2 in a caseload of canine oral melanomas that have been already tested for their level of FXR1 gene/protein expression in order to assess, firstly, if there is an association between MMP-9 and FXR1 expression, and, secondly, if there are possible associations of MMP-9/TIMP-2 expression with the clinical outcome.

Materials and methods

Case selection

Samples of formalin fixed and paraffin embedded (FFPE) oral melanocytic tumors collected from the archive of the diagnostic service of Veterinary Histopathology of Università degli Studi di Milano (2011-2017) and from Veterinary Laboratory San Marco in Padova were analyzed, as already detailed in the section “LTA4H AND FXR1 GENE AND PROTEIN EXPRESSION IN CANINE ORAL MELANOMA” of the present thesis. Data about the clinical outcome were collected from referring veterinarians.

For the present study, we selected 15 cases of canine oral melanocytic tumors for which the semi-quantitative expression of the protein FXR1 (evaluated by immunohistochemistry and expressed as IRS score) was available. A subset of 4 cases had also the quantitative expression of the gene *FXR1* (quantified by RT-PCR and expressed as ΔCt) available (see section “LTA4H AND FXR1

GENE AND PROTEIN EXPRESSION IN CANINE ORAL MELANOMA" of the present thesis for detailed methods).

Comparisons were carried out among groups independently identified.

Firstly, in order to assess the association between MMP-9 and FXR1 expression, two groups were compared:

- group A ("high" FXR1) (n=5): samples included were characterized by immunohistochemical IRS value >6 (median on the IRS scale 0-12) and ΔCt *FXR1* ≤ 4.31 (median of the previously screened group) (subset of 2 cases). The reported values are considered as high molecular and immunohistochemical values of FXR1 expression;
- group B ("low" FXR1) (n=7): samples included were characterized by immunohistochemical IRS value ≤ 6 and ΔCt *FXR1* > 4.31 (subset of 2 cases). The reported values are considered as low molecular and immunohistochemical values of FXR1 expression.

Secondly, in order to assess the association of MMP-9 with the clinical outcome, two different groups were created:

- group C (n=3): cases with overall survival (OS) above 1 year (subjects alive 1 year after the diagnosis);
- group D (n=7): cases with OS below 1 year (subjects dead within 1 year after the diagnosis).

Immunohistochemistry

Immunohistochemical labelling for matrix metalloproteinases MMP-9 and its tissue inhibitor TIMP-2 was performed. Serial sections were cut 4 µm thick and mounted on poly-lysine coated slides (Menzel-Gläser, Braunschweig, Germany). Immunohistochemical staining with the standard avidin-biotin-peroxidase complex (ABC) method was performed.

Sections were deparaffinized in xylene and rehydrated through a descending series of ethanol concentrations. Blocking of endogenous peroxidase was performed by incubation in 3% H_2O_2 for 20 minutes. Antigen retrieval was then performed by heating the slides in citrate buffer solution (pH 6.5) in a water bath at 95°C for 30 minutes, followed by decooling for 30 minutes at room temperature (RT). Sections were therefore incubated for 20 min at RT with normal horse serum

(1:70) to block any nonspecific protein binding. Serial sections were incubated at 4°C overnight in a humidified chamber with primary antibodies:

- Mouse monoclonal antibody anti MMP-9 (Clone IIA5), 1:400 dilution (ThermoFisher, Waltham, MA, USA);
- Mouse monoclonal antibody anti TIMP2 (clone 3A4), 1:200 dilution (ThermoFisher, Waltham, MA, USA);

Sections were then rinsed in Tris buffer solution (TBS) (pH 7.4) and incubated with the secondary biotinylated antibody anti-mouse (1:200, 30 minutes RT) (Vector Laboratories, Burlingame, CA, USA) followed by incubation with the ABC reagent (30 minutes RT) (Vector Laboratories, Burlingame, USA). After rinsing in TBS for three times for three minutes, the chromogen 3-amino-9-ethylcarbazole (AEC) (Vector Laboratories, Burlingame, CA, USA) was applied for 15 minutes and, after rinsing in tap water, slides were counterstained with Mayer's haematoxylin (Diapath srl, Martinengo, Italy) for 2 minutes. Slides were therefore dried and mounted in aqueous mounting agent (Aquatex, Merck, Darmstadt, Germany). Tunica media of blood vessels was adopted as internal positive controls (Gavin et al., 2003). Negative controls were carried out by replacing the primary antibodies with mouse IgG (Santa Cruz; Dallas, TX).

Immunolabelled sections were evaluated on optic microscope. The evaluated parameters were the percentage of positive cells (<10%, 10-30%, 30-50%, 50-70%, >70%) and the intensity of the positive stain (mild, moderate, intense). The immunoreactive score adapted from Remmele and Stegner (IRS score) was calculated combining the intensity and ratio of positivity as follows: IRS score (0 - 12) = percentage of positive cells (with: no positive cells= 0, <10% positive cells= 1, 10-50 % of positive cells= 2, 50-70% of positive cells= 3, >70% of positive cells= 4) * intensity of staining (with: no positive cells= 0, 1+/mild = 1, 2+/moderate= 2, 3+/marked= 3) (Remmele and Stegner, 1987).

Lacking suitable fresh tissue to quantify gelatinase activity through gelatin zymography, an indirect evaluation of the ratio among MMP-9 and TIMP-2 was drawn from the comparison among their respective immunohistochemical results. Specifically, expression results were further classified in classes, which were called "a" when the percentage of positive cells for MMP-9 class was equal to TIMP-2 (MMP-9 = TIMP-2), "b" with MMP-9 > TIMP-2, and "c" with MMP-9 < TIMP-2.

Groups were statistically analyzed through Mann Whitney U-test, Spearman Rho test and Fisher's Exact Test and significance level was set at 0.05.

Results

Association of FXR1- MMP-9 expression

MMP-9 was detected in the cytoplasm of 11/12 tested canine oral melanomas (Figure 8, Table 11). Specifically, in the group with high levels of molecular and/or immunohistochemical expression of FXR1, MMP-9 was detected in all samples, with a percentage of positive cells ranging from 30-50% to more than 70%, and an overall IRS score ranging from 4 to 9 (IRS mean: 7.6). In the group with low levels of molecular and/or immunohistochemical expression of FXR1, MMP-9 was immunodetected in 6/7 cases, with a percentage of positive cells ranging from less than 10% to more than 70%, and an overall IRS score ranging from 0 to 12 (IRS mean: 5.3).

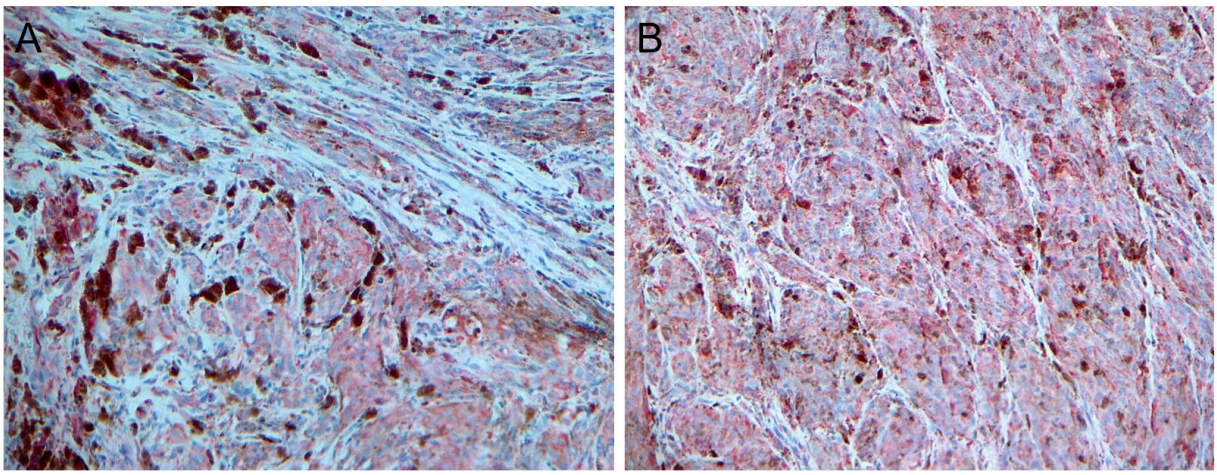

Figure 8 - Canine oral melanoma, immunohistochemistry anti-MMP-9 (A) and anti-TIMP-2 (B). AEC chromogen, 20x

TIMP-2 was detected in the cytoplasm of all tested canine oral melanomas (Figure 8, Table 11). In particular, in the group with “high” FXR1, TIMP-2 was detected in all samples, with a percentage of positive cells ranging from 30-50% to more than 70%, and an overall IRS score ranging from 4 to 12 (IRS mean: 9.2). In the group with “low” FXR1, TIMP-2 was expressed in all cases, with a percentage of positive cells ranging from less than 10% to more than 70%, and an overall IRS score ranging from 1 to 9 (IRS mean: 5.4).

Table 11 - MMP-9 and TIMP-2 expression compared among groups with high and low expression of FXR1

	FXR1 IRS	FXR1 ΔCt	MMP-9 %	MMP-9 intensity	MMP-9 IRS	TIMP-2 %	TIMP-2 intensity	TIMP-2 IRS	MMP-9/TIMP-2 group
Group A ("high" FXR1)	12	0.92	50-70	3	9	>70	3	12	c
	12	4.31	>70	2	8	>70	3	12	c
	9	na	50-70	3	9	50-70	3	9	a
	9	na	30-50	2	4	30-50	2	4	a
	8	na	>70	2	8	>70	3	12	c
Group B ("low" FXR1)	6	5.86	50-70	2	6	50-70	2	6	a
	6	6.24	50-70	3	9	50-70	2	6	b
	6	>35	50-70	2	6	50-70	3	9	c
	6	>35	>70	3	12	>70	2	8	b
	1	na	<10	1	1	10-30	2	4	c
	1	na	<10	3	3	10-30	2	4	c
	1	na	0	0	0	<10	1	1	c

MMP-9 immunohistochemical expression did not differ significantly among groups (p=0.286), while TIMP-2 did (p=0.047) (Graph 7). The IRS score of FXR1 correlated significantly with both MMP-9 (p=0.044, R=0.587) and TIMP-2 (p=0.004, R=0.707) immunohistochemical IRS score.

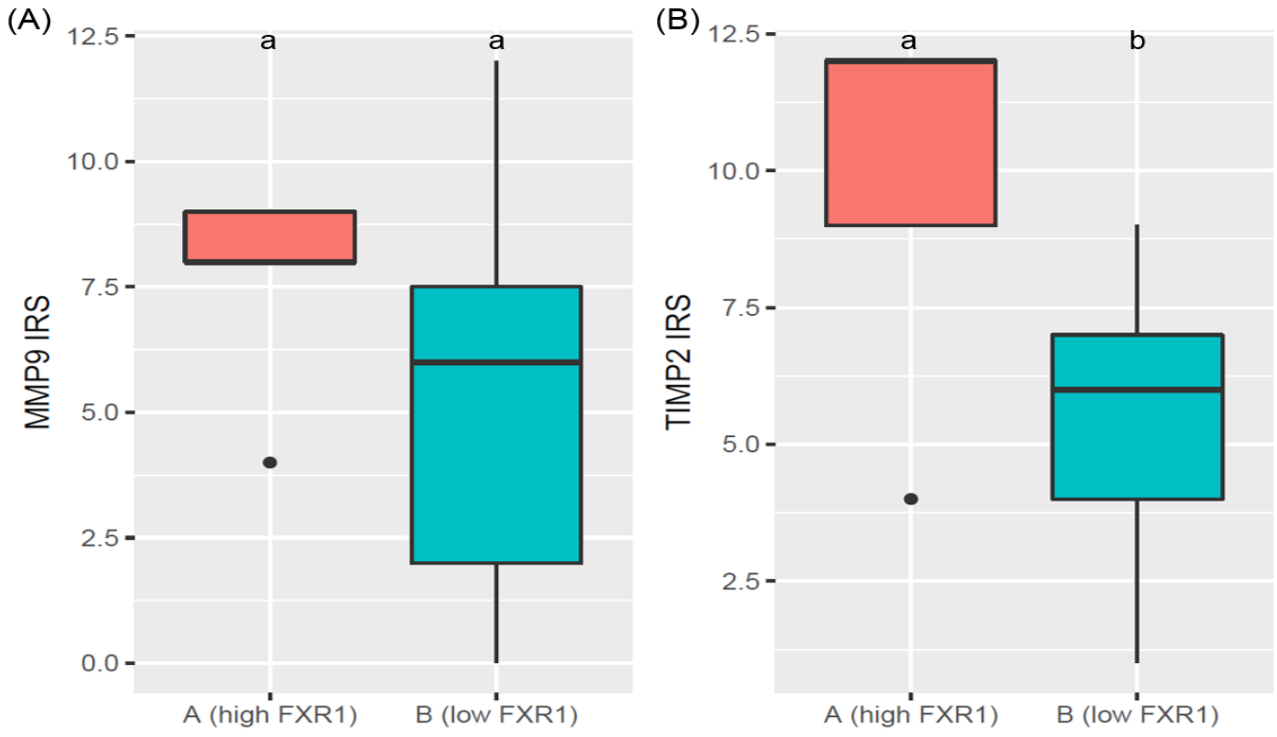

Graph 7 - MMP-9 (A) and TIMP-2 (B) IHC IRS scores compared in groups with high and low FXR1 (groups A vs B). Mann Whitney U-test, significance <0.05.

On the other hand, the molecular expression of *FXR1*, quantified as ΔCt, was not correlated with MMP-9 or TIMP-2 (p=0.105 and 0.894, respectively). Analyzing the distribution of a-b-c classes, representing the ratio among MMP-9/TIMP-2, between groups with low and high FXR1, no significance was detected (p = 0.575). TIMP-2 expression was statistically correlated with the expression of MMP-9 in the low FXR1 group (p = 0.025, R = 0.816), but not in the high FXR1 group (p = 0.559, R = 0.353).

Association of MMP-9 and TIMP-2 expression with clinical outcome

MMP-9 was immunodetected in the cytoplasm of 8/10 tested canine oral melanomas. Specifically, in the group of dogs with OS > 1 year after the diagnosis of oral melanoma, MMP-9 was detected in 1/3 cases. In the positive case, 50-70% of the neoplastic cell were intensively positive (average IRS score of the groups: 3). In the group of dogs dead with OS < 1 year, MMP-9 was expressed in 7/7 cases, with a range of IRS score of 1-9 (IRS mean: 6) (Table 12).

TIMP-2 was present in the cytoplasm of all tested melanomas in group C. IRS scores of oral melanomas in group C had a mean of 4.3 (range 1-6). All melanomas in group D expressed TIMP-2, with a mean IRS of 9 (range 1-12) (Table 12).

MMP-9 expression did not differ significantly among groups with different OS (C vs D) (p=0.295), whereas TIMP2- expression seemed to be different among groups and approached significance, even not being statistically relevant (p= 0.062) (Graph 8). The correlation among MMP-9 and TIMP-2 could be estimated only in the group “D”, due to the paucity of cases of group “C”, and was not significant (R= 0.721, p=0.067). The distribution of a-b-c classes showed no significant differences among different groups (p=0.358). MMP-9/TIMP-2 expression were not mutually correlated in group C (p= 0.666) and D (p= 0.067).

Table 12 - MMP-9 and TIMP-2 expression compared among groups win cases with overall survival above 1 year (favorable outcome) or below 1 year (unfavorable outcome)

	Clinical outcome	MMP-9 %	MMP-9 intensity	MMP-9 IRS	TIMP-2 %	TIMP-2 intensity	TIMP-2 IRS	MMP-9/TIMP-2 group
Group C (OS > 1 year)	Alive after 2 years	50-70	3	9	50-70	2	6	b
	Alive after 3 years	0	0	0	<10	1	1	c
	Alive after 1 year	0	0	0	10-30	3	6	c
Group D (OS < 1 year)	Euthanized after 1 week	50-70	3	9	>70	3	12	c
	Euthanized after 1 month	50-70	2	6	50-70	3	9	c
	Local recurrence after 5 months and euthanasia after 9 months	50-70	3	9	50-70	3	9	a
	Euthanized after 1 month	<10	1	1	>70	2	8	c
	Two local recurrences in a month, euthanized after 1 month	<10	1	1	<10	1	1	a
	Local recurrence after 2 months, euthanized after 2 months with lymphnodal metastasis	>70	2	8	>70	3	12	c
	Euthanized after 1 month, visceral metastases proved by autopsy	>70	2	8	>70	3	12	c

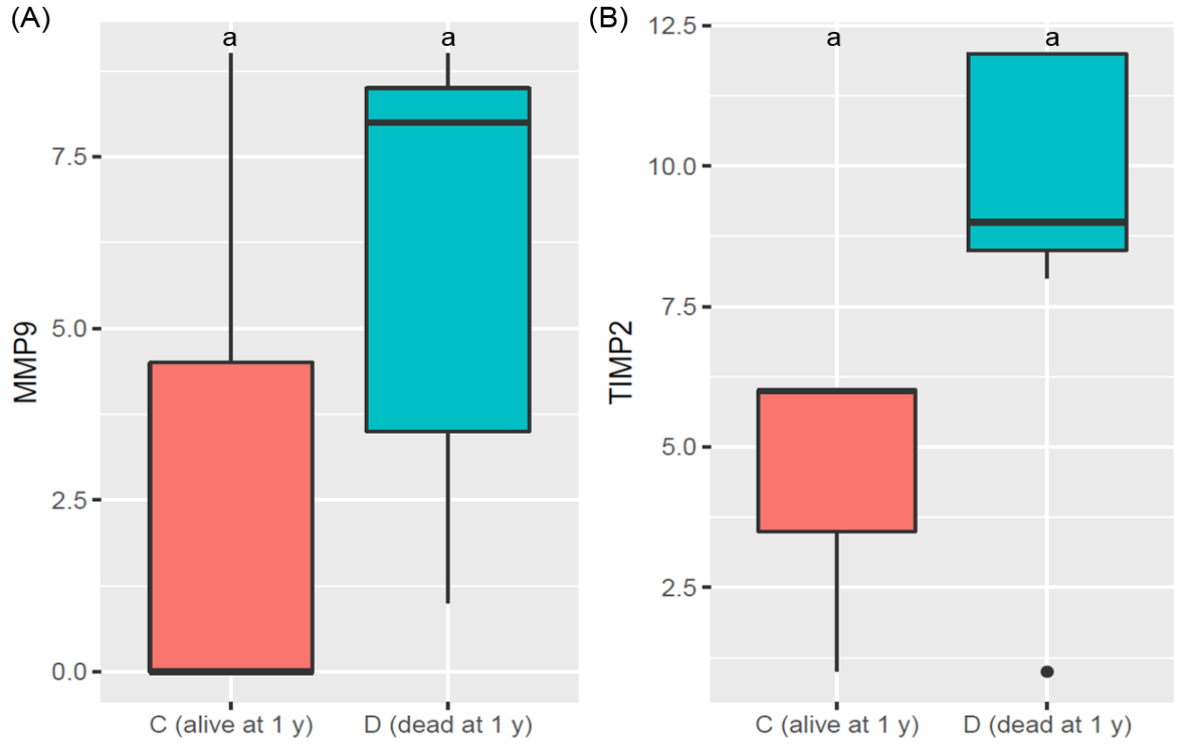

Graph 8 - MMP-9 (A) and TIMP-2 (B) IHC IRS scores compared in groups with OS > 1 year and OS < y year (groups C vs D). Mann Whitney U-test, significance <0.05.

Discussion

The present study investigated the immunohistochemical expression of MMP-9 and its inhibitor TIMP-2 in a cohort of canine oral melanomas. Immunohistochemical expression of the investigated proteins was semi-quantitatively scored and summarized as IRS score, in order to compare results among different groups.

Specifically, groups of canine oral melanomas with high and low expression of FXR1, quantified either as gene and/or protein, were compared for their expression of matrix metalloproteinases. Although not statistically significant, a trend for a higher mean level of expression of both MMP-9 and TIMP-2 was observed in the group with high FXR1. Moreover, the immunohistochemical IRS score of FXR1 protein, but not the molecular expression of *FXR1* gene, was positively correlated with the immunohistochemical expression of both MMP-9 and TIMP-2.

These findings were slightly in conflict with the expected results. In fact, the mRNA coding MMP-9 is a target of FMRP, a protein very close to FXR1 which belongs to the same family, which is able to down-regulate the expression of MMP-9. In the absence of FMRP the expression levels of MMP-9 increase (Castagnola et al., 2017). To cite an inherent example in human pathology, there are increasing evidence that the FMRP-induced suppression of the translation of MMP-9 plays a role in the human Fragile X Syndrome(Castagnola et al., 2017; Reinhard et al., 2015).

FXR1 is a homologue of the Fragile X mental retardation syndrome protein FMRP (Coy et al., 1995; Siomi et al., 1995; Zhang et al., 1995). Although FMRP, FXR1, and FXR2 share 63% of amino acid identity in the first half of the protein (Kirkpatrick et al., 1999), their expression is not overlapping, since, for example, FXR1 is strongly expressed in the muscle and moderately in the brain, whereas FMRP is absent in the muscle and FXR2 is strongly expressed in the brain (Kirkpatrick et al., 1999; Bardoni et al., 2001). Therefore, we hypothesize that: firstly, the FMRP-induced modulation of MMP-9 may be a prerogative of this specific protein, rather than of the entire family of mRNA binding proteins, or, secondly, that this thorough modulation may be linked to the organ (nervous system) and the specific pathway involved in the process of brain development. Finally, we considered that the semi-quantitative immunohistochemical evaluation of MMP-9/TIMP-2

examined the expression of the proteins, but the evaluation of effectively translated proteins do not necessarily instantly reflect mRNA synthesis.

In addition, overexpression of FXR1 have been associated with malignant and metastasizing behavior in different types of tumors, such as human pulmonary squamous cell carcinoma, non-small cell lung cancer (Comtesse et al., 2007; Qian et al., 2015), colorectal cancer (Jin et al., 2016), and human and canine uveal melanoma (Onken at al., 2010; Malho et al., 2013). Similarly, intense expression of MMPs and TIMPs is implicated in tumoral aggressiveness, invasion and metastasizing ability, due to the proteolytic effect on ECM (Liotta and Stetler-Stevenson, 1991; Mignatti and Rifkin, 1993; Nagase et al., 2006). Therefore, we also hypothesize that intense expression of the proteins FXR1 and MMP-9 may be devoid of strong mutual interconnection and rather be associated in an independent manner with the aggressiveness of the investigated melanomas.

In order to associate the expression of MMPs with the biological aggressiveness of the tumors, we also analyzed our data with regard to the clinical outcome of canine oral melanomas. Interestingly, the average MMP-9 and TIMP-2 expression in the group of dogs with OS below 1 year was about twice the group of dogs still alive one year after the diagnosis, even if results just approached significance due to the narrow subgroups.

In human melanomas, both tumor cells and tumor-associated stromal cells showed increased expression of several MMPs and TIMPs (Moro et al., 2014). MMP-9 is correlated with malignancy in human cutaneous melanoma (Candrea et al., 2014; Chen et al., 2012) and associated with high risk of invasion and metastatic behavior (Nikkola et al., 2005; Shellman et al., 2006). Specifically in human sinonasal and oral malignant melanoma, MMP-9 expression is correlated with epithelioid morphology and with the presence of metastatic disease, even if, in oral melanoma, not significantly correlated with survival (Kondratiev et al., 2008). The association of MMP-9 with metastatic disease is also reported in human uveal melanoma (El-Shabrawi et al., 2001; Schnaeker et al., 2004). In a study performed on canine melanocytic tumors, yet comparing oral melanocytic tumors with cutaneous ones, an overexpression of MMP-9 was detected in malignant melanomas over benign melanocytomas (Docampo et al., 2011).

In the present study, a trend for an intense expression of MMP-9 and TIMP-2, even if not statistically significant, seemed to be associated with an unfavorable clinical outcome in canine oral melanoma.

Finally, we compared the expression of TIMP-2 with MMP-9. In the present study, the categories “a”, “b”, and “c”, which identified the ratio among the two considered enzymes, did not seem to be significantly distributed in the considered groups. The MMP/TIMP correlation was poor in the group with high FXR1, with average TIMP-2 being greater than average MMP-9, presumably as an inhibitory attempt to lower MMP-9.

Conclusions

MMP-9 seemed not to be associated with FXR1 expression in canine oral melanomas. Anyway, intense levels of expression of MMP-9/TIMP-2 were observed in cases with high expression of FXR1, suggesting that these proteins could be associated independently with the aggressiveness of the tumor. Moreover, a trend for an average more intense expression of MMP-9/TIMP-2 seemed to be associated with an unfavorable clinical outcome in canine oral melanoma. These preliminary results warrant more investigations on the role of matrix metalloproteinases in the progression of canine oral melanoma.

Future works will analyze the expression of MMP-9 and TIMP-2 in a larger cohort of cases in order to enlarge the caseload of canine oral melanomas and complete the present study.

IV. EXPRESSION OF MMP-9 AND TIMP-2 IN FELINE DIFFUSE IRIS MELANOMA AND CORRELATION WITH HISTOLOGICAL PARAMETERS OF MALIGNANCY

Abstract

Feline diffuse iris melanoma (FDIM) is a malignant slowly progressive tumor and the most common primary intraocular neoplasm in cats. MMP-9 (matrix metalloproteinase-9) is an endopeptidase able to digest the extracellular matrix, with involvement in tumor invasion. TIMP-2 (tissue inhibitor of metalloproteinases-2) is one of its inhibitors. This study investigates the immunohistochemical expression of MMP-9 and TIMP-2 in a caseload of FDIMs in order to correlate data with the histological grade and mitotic index (MI).

Sixty-two samples of FFPE FDIM were selected (n=22 simplified grade I, n=20 simplified grade II, n=20 simplified grade III) and evaluated on light microscopy, where grade and MI were recorded. Immunohistochemical staining was performed with monoclonal anti-MMP-9 and anti-TIMP-2 antibodies, and results were semi-quantitatively scored in classes of positivity and statistically analyzed by Mann-Whitney U test. MI ranged 0 to 71, with MI ≤7 in 49 cases and MI > 7 in 13 cases. MMP-9 and TIMP-2 were expressed, respectively, in 71.4% and 67.3% of FDIM with MI ≤7, and 100.0% and 84.6% of FDIM with MI >7. MMP-9 and TIMP-2 expression was statistically higher with high MI. MMP-9 was expressed in 77.4% FDIM: specifically, in 59.1% grade I FDIM, 90.0% grade II and 85.0% grade III. TIMP-2 was expressed in 71.0% FDIM: in 59.1% grade I FDIM, 80.0% grade II and 75.0% grade III. MMP-9 expression differed significantly among grade I and the other two grades, TIMP-2 expression differed significantly among grade I and II. Both MMP-9 and TIMP-2 differed significantly among groups with MI ≤7 and > 7. MMP-9/TIMP-2 balanced ratio was over-represented in grade I tumors. In conclusion, intense immunohistochemical expression of MMP-9 seems to be associated with histological criteria of aggressiveness in FDIM.

Introduction

In cats, tumors of melanocytic origin are the most common primary intraocular neoplasm and mainly affect the iris (FDIM) (Dubielzig, 2017). Feline diffuse iris melanoma (FDIM) is a malignant tumor, even if slowly progressive. The growth may begin as focal abnormal pigmentation of the iris, which may persists for years, and later expands, becoming nodular or diffuse and eventually distorting the profile of the iris and the pupil and causing secondary glaucoma (Dubielzig, 2017;

Duncan and Peiffer, 1991; Kalishman et al., 1998). Enucleation in early stages is usually curative; otherwise, later stages slowly develop risk of systemic metastasis to the liver, lung, and kidneys (Dubielzig, 2017). Scleral and choroidal invasion and high mitotic index (MI>7) have been considered histological features of malignancy (Kalishman et al., 1998; Wiggans et al., 2016).

Complex interactions between neoplastic cells and the extracellular matrix, the so-called tumor microenvironment, are considered critical in carcinogenesis, tumor invasion and metastasis. Previous studies have shown that matrix metalloproteinases (MMPs) and their endogenous inhibitors (tissue inhibitors of MMPs, i.e. TIMPs) are involved in this process (Liotta and Stetler-Stevenson, 1991; Mignatti and Rifkin, 1993; Nagase et al., 2006). MMPs belong to a family of calcium and zinc dependent endopeptidases which play a proteolytic activity on many constituents of the extracellular matrix (ECM). Proteolytic effects of MMPs play a role in the processing of matrix proteins, molecular adhesions and cellular migration (Raffetto and Khalil, 2008). MMPs are implied in a variety of physiological processes, for example reproduction, fetal development, wound healing, as well as in different pathological processes, for example tumor invasion and metastasis, inflammation and vascular diseases (Lepetit et al., 2005; Panek and Bader, 2006; Raffetto and Khalil, 2008; Sorensen et al., 2004). Among MMPs, MMP-9 has been specifically implied in tumorigenesis (El-Shabrawi et al., 2001; Yadav et al., 2014). MMP-9 (gelatinase B) is able to degrade elastin and denatured collagen of types IV, V, VII and X. It is produced as inactive zymogen, which requires activation, mainly by keratinocytes, monocytes, alveolar macrophages, polymorphonuclear leukocytes and tumoral cells (Nagase et al., 2006; Raffetto and Khalil, 2008; Ramos-DeSimone et al., 1999; Visse and Nagase, 2003).

In human uveal melanoma, high levels of MMP-9 have been associated with the invasiveness of the tumor and with metastasizing behavior (El-Shabrawi et al., 2001; Schnaeker et al., 2004). To the best of the authors' knowledge, there are currently no data in veterinary literature on the role of MMPs in ocular melanomas.

While MMPs and TIMPs are usually balanced in healthy tissues, degeneration of the ECM, and thus invasive potential, arise when there is a prevalence of MMPs over TIMPS (Khokha et al., 2013; Moro et al., 2014; Nagase et al., 2006; Roeb, 2018). We hypothesize that the expression of MMP-9

may be higher in those FDIMs with marked features of malignancy (absolute expression), and, specifically, that the ratio MMP/TIMP may be unbalanced toward a prevalence of MMP-9 over TIMP-2 (relative expression). The golden standard to measure the activity of proteinase is gelatin zymography, but, due to the unavailability of fresh substrates to analyze, we will perform immunohistochemistry on FFPE tissues and deduce an expected overall ratio MMP-9/TIMP-2 through an indirect comparison among them.

The present study investigates the expression and localization of MMP-9 and one of its inhibitors, TIMP-2, in a caseload of feline diffuse iris melanomas, with the aim of correlating these data with already known histological criteria of malignancy, that are, specifically, histological grade and mitotic index.

Materials and methods

Case selection and histology

Sixty-two formalin fixed and paraffin embedded (FFPE) eyes with a diagnosis of feline iris diffuse melanoma were retrieved from the archive of the Diagnostic service of Histopathology of the Università degli Studi di Milano (2004-2017). 4 µm-thick sections were obtained from paraffin blocks and stained with hematoxylin and eosin (H&E). H&E stained sections were evaluated on light microscopy. Mitotic index, i.e. the total number of mitoses on 10 HPF, was recorded, and, according to Wiggans (Wiggans et al., 2016), 7 mitoses per 10 HPF was adopted as threshold for malignancy.

Melanomas were also graded according to simplified grading system proposed by Kalishman (Kalishman et al., 1998), briefly:

- Early / simplified grade I: tumor only in the iris and trabecular meshwork.
- Moderate / simplified grade II: tumor in the iris and rostral ciliary body but not into the sclera.
- Advanced / simplified grade III: tumor throughout the ciliary body and extending into the sclera.

Simplified grades I-II-III will be hereafter referred as grades I-II-III.

Immunohistochemistry

Immunohistochemical labelling for matrix metalloproteinases MMP-9 and the tissue inhibitor TIMP-2 was performed. Serial FFPE sections were cut 4 µm thick and mounted on poly-lysine coated slides (Menzel-Gläser, Braunschweig, Germany). Immunohistochemical staining with the standard avidin-biotin-peroxidase complex (ABC) method was performed.

Briefly: sections were deparaffinized in xylene and rehydrated through a descending series of ethanol concentrations. Blocking of endogenous peroxidase was performed by incubation in 3% H_2O_2 for 20 minutes. Antigen retrieval was then performed by heating slides in citrate buffer solution (pH 6.5) in a water bath at 95°C for 30 minutes, followed by cooling down at room temperature (RT) for 30 minutes. Sections were then incubated for 20 min at RT with normal horse serum (1:70) to block any nonspecific protein binding, and therefore incubated at 4°C overnight in a humidified chamber with primary antibodies:

- Mouse monoclonal antibody anti MMP-9 (Clone IIA5), dilution 1:400 (ThermoFisher, Waltham, MA, USA);
- Mouse monoclonal antibody anti TIMP-2 (clone 3A4), dilution 1:200 (ThermoFisher, Waltham, MA, USA).

Sections were then rinsed in Tris buffer solution (TBS) (pH 7.4), incubated with the secondary biotinylated antibody (1:200, 30 minutes RT) (Vector Laboratories, Burlingame, CA, USA), rinsed again in TBS buffer and then incubated with ABC reagent (30 minutes, RT) (Vector Laboratories, Burlingame, USA). After further TBS rinsing, the chromogen 3-amino-9-ethylcarbazole (AEC) (Vector Laboratories, Burlingame, CA, USA) was applied for 15 minutes and, after rinsing in tap water, slides were counterstained with Mayer's haematoxylin (Diapath srl, Martinengo, Italy) for 2 minutes. Slides were therefore dried and mounted in aqueous mounting agent (Aquatex, Merck, Darmstadt, Germany). Sections of feline healthy myocardium were used as a positive control for MMP-9 and TIMP-2 (Porcellato et al., 2014). Negative controls were carried out by replacing the primary antibodies with normal rabbit IgG (Santa Cruz; Dallas, TX).

Immunohistochemical scoring

Immunolabelled sections were evaluated at optic microscope. A semi-quantitative score was given, which included the intracellular localization of staining (cytoplasmic, nuclear) and the percentage of positively stained cells (0%, 1-10%, 11-30%, 31-50%, 51-70%, >70%). The groups thus identified have been renamed as follow, for simplicity: 0% = class 0, 1-10% = class 1, 11-30% = class 2, 31-50% = class 3, 51-70% = class 4, >70% = class 5. To draw a ratio among MMP-9 and TIMP-2 expression, results were further classified in classes, which were called “a” when the class of percentage of positive cells for MMP-9 class was equal to TIMP-2, “b” when MMP-9 was more expressed than TIMP-2, and “c” when MMP-9 was less expressed than TIMP-2. Moreover, Spearman's Rho test was adopted to correlate the expression of MMP-9 and TIMP-2.

Statistical analysis was performed. Kruskal-Wallis test and Mann-Whitney U test were adopted to compare protein expression in tumors with different histological grades and different mitotic index. Fisher's Exact Test and Standardized Residuals Analysis compared the distribution of “a”-“b”-“c” cases in groups with different grades and mitotic index. Significance level was set at 0.05.

Results

Case selection and histology

Sixty-two cases of FDIM were evaluated (Table 13). The age at enucleation ranged from 1.3 to 18 years, with a mean of 10.4 and a median of 10. Thirty-one affected cats were females (31/62, 50.0%) (16 entire females and 15 spayed females), and twenty-five cats were males (25/62, 40.3%) (15 neutered males and 10 entire males); for 6 cats, sex was not reported. Most cats were European Shorthaired (40/62, 64.5%), followed by Persian (11/62, 17.7%), Chartreux (2/62, 3.2%), and Norwegian Forest cats (1/62, 1.6%); for 9 cases data were not available.

Based on the simplified histological grading proposed by Kalishman (Kalishman et al., 1998), 22 tumors were graded as early/ grade I FDIM, 20 as moderate/ grade II and 20 as advanced/ grade III.

Mitotic index ranged from 0 mitoses to 71 mitoses in 10 HPF, with a mean of 5.6 and a median of 1.5. MI was lower or equal to 7 in 49 cases (49/62, 79.0%) and higher than 7 in 13 cases (13/62,

21.0%). All cases with MI > 7 were graded as grade II or III, and all cases graded as grade I had MI ≤7.

Table 13 - Feline diffuse iris melanomas: signalment and detailed immunohistochemical evaluations

#	Breed	Sex	Age	Grade	MI	MMP-9 % neoplastic cells	MMP-9 % class	TIMP-2 % neoplastic cells	TIMP-2 % class	MMP-9/TIMP-2 group
1	European Shorthair	NM	11	1	0	1-10	1	1-10	1	a
2	European Shorthair	SF	12	1	0	31-50	3	31-50	3	a
3	Norwegian Forest	SF	8	1	0	11-30	2	0	0	b
4	Chartreux	F	4	1	0	0	0	1-10	1	c
5	European Shorthair	SF	4	1	0	0	0	0	0	a
6	European Shorthair	SF	10	1	0	0	0	1-10	1	c
7	European Shorthair	SF	9	1	0	0	0	0	0	a
8	nd	nd	12	1	0	0	0	0	0	a
9	nd	F	nd	1	0	1-10	1	1-10	1	a
10	nd	SF	13	1	0	0	0	0	0	a
11	European Shorthair	NM	9	1	0	0	0	0	0	a
12	nd	NM	10	1	0	1-10	1	1-10	1	a
13	nd	nd	nd	1	0	1-10	1	0	0	b
14	European Shorthair	F	16	1	0	1-10	1	1-10	1	a
15	European Shorthair	SF	7,5	1	0	>70	5	11-30	2	b
16	European Shorthair	F	1.3	1	0	0	0	1-10	1	c
17	European Shorthair	M	7	1	0	1-10	1	0	0	b
18	European Shorthair	NM	6	1	0	0	0	1-10	1	c
19	European Shorthair	nd	nd	1	1	11-30	2	31-50	3	c
20	European Shorthair	M	14	1	2	51-70	4	51-70	4	a
21	nd	NM	7	1	0	1-10	1	1-10	1	a
22	European Shorthair	SF	10	1	0	51-70	4	0	0	b
23	Chartreux	F	4,7	2	0	0	0	0	0	a
24	European Shorthair	F	14	2	0	31-50	3	11-30	2	b
25	European Shorthair	SF	12	2	5	11-30	2	31-50	3	c
26	European Shorthair	M	9	2	12	11-30	2	31-50	3	c
27	European Shorthair	NM	12	2	11	>70	5	>70	5	a
28	European Shorthair	NM	7	2	5	51-70	4	>70	5	c
29	European Shorthair	SF	8	2	0	1-10	1	11-30	2	c
30	nd	SF	9	2	0	31-50	3	11-30	2	b
31	European Shorthair	NM	6	2	2	1-10	1	11-30	2	c
32	European Shorthair	M	14	2	11	31-50	3	31-50	3	a
33	European Shorthair	nd	11	2	0	1-10	1	0	0	b
34	European Shorthair	SF	12	2	3	31-50	3	50-70	4	c
35	European Shorthair	F	15	2	11	51-70	4	0	0	b
36	Persian	NM	13	2	0	>70	5	31-50	3	b
37	nd	nd	nd	2	8	>70	5	11-30	2	b
38	Persian	F	14	2	2	51-70	4	1-10	1	b
39	European Shorthair	F	12	2	0	0	0	0	0	a
40	European Shorthair	NM	11	2	7	11-30	2	51-70	4	c
41	Persian	M	13	2	23	51-70	4	1-10	1	b
42	European Shorthair	NM	15	2	7	>70	5	1-10	1	b
43	European Shorthair	SF	8	3	7	>70	5	51-70	4	b
44	European Shorthair	F	8	3	0	0	0	0	0	a
45	European Shorthair	SF	14	3	0	31-50	3	1-10	1	b

#	Breed	Sex	Age	Grade	MI	MMP-9 % neoplastic cells	MMP-9 % class	TIMP-2 % neoplastic cells	TIMP-2 % class	MMP-9/TIMP-2 group
46	European Shorthair	F	6	3	7	51-70	4	11-30	2	b
47	Persian	NM	18	3	71	31-50	3	11-30	2	b
48	Persian	F	14	3	2	31-50	3	1-10	1	b
49	nd	F	14	3	3	51-70	4	11-30	2	b
50	European Shorthair	NM	9	3	14	51-70	4	70	5	c
51	European Shorthair	M	8	3	0	1-10	1	0	0	b
52	Persian	F	13	3	19	11-30	2	51-70	4	c
53	European Shorthair	M	10	3	48	31-50	3	0	0	b
54	Persian	M	11	3	3	31-50	3	11-30	2	b
55	Persian	M	13	3	3	1-10	1	0	0	b
56	European Shorthair	NM	10	3	6	11-30	2	1-10	1	b
57	European Shorthair	SF	10	3	11	>70	5	51-70	4	b
58	Persian	F	13	3	10	1-10	1	11-30	2	c
59	Persian	F	13	3	5	51-70	4	1-10	1	b
60	Persian	M	10	3	5	>70	5	11-30	2	b
61	European Shorthair	NM	10	3	17	11-30	2	1-10	1	b
62	European Shorthair	nd	nd	3	7	0	0	0	0	a

Legend. MI = mitotic index; NM = neutered male; M = male; SF = spayed female; F = female; nd = not declared; a = MMP-9=TIMP-2; b = MMP-9>TIMP-2; c = MMP-9<TIMP-2.

Immunohistochemistry

Neoplastic melanocytes were evaluated for the immunohistochemical expression of MMP-9 and TIMP-2. Immunohistochemical labelling was always cytoplasmic (Figure 9). Immunohistochemical scores are detailed in Table 13.

MMP-9 protein was immunodetected in 48/62 FDIM cases (77.4%); TIMP-2 in 44/62 cases (71.0%). MMP-9 was expressed in 71.4% of FDIM with MI ≤ 7 (35/49) and in 100.0% (13/13) of FDIM with MI > 7, thus differing significantly between the two groups (p = 0.003). TIMP-2 was detected in 67.3% of cases with MI ≤ 7 (33/49) and 84.6% of cases MI > 7 (11/13), with a statistically significant difference between the two groups (p = 0.012) (Graph 9).

The correlation among the immounohistochemical expression of MMP-9 and TIMP-2 was not significant in the group with high MI (p = 0.324, R = 0.246), contrarily to the group with low MI (p < 0,000, R = 0.633).

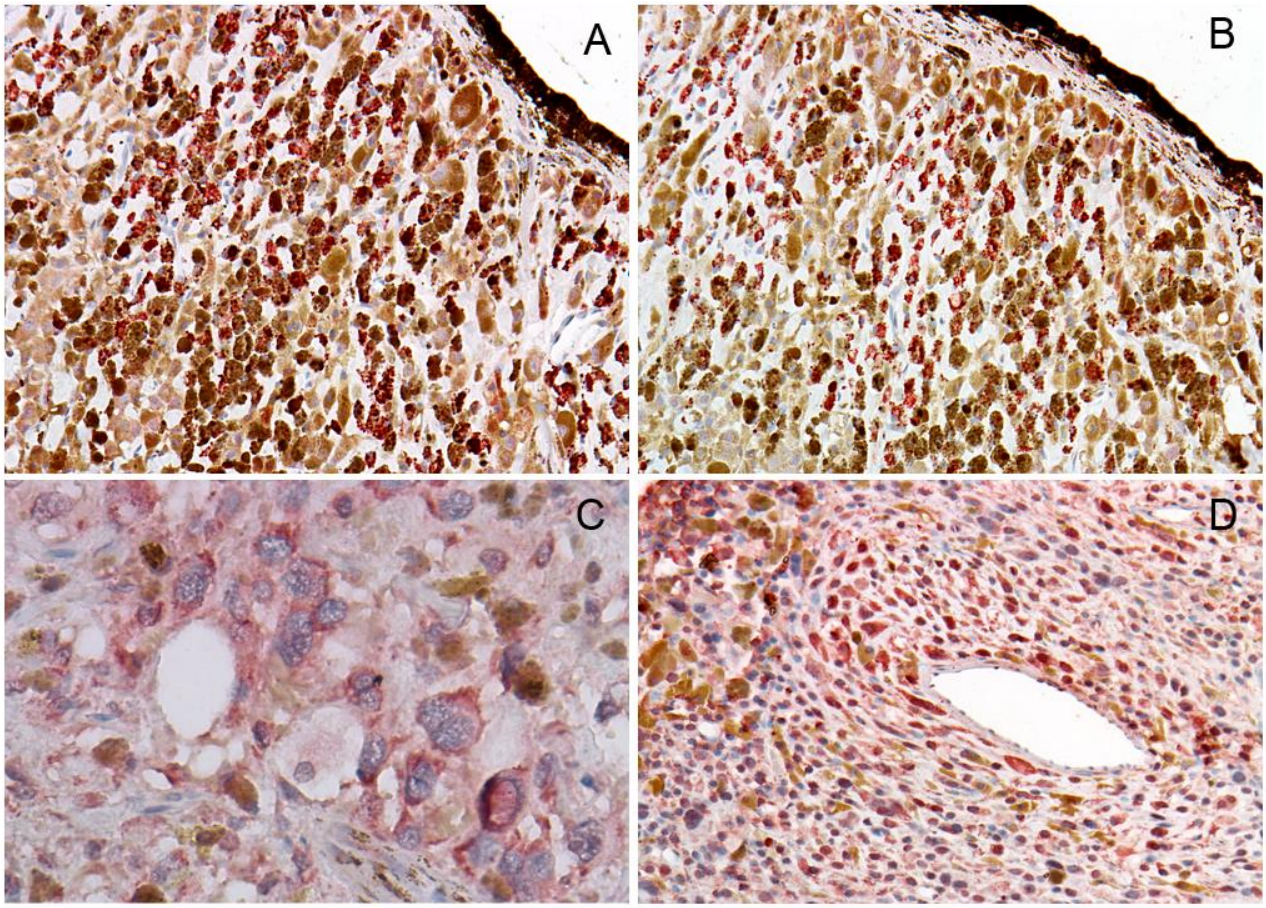

Figure 9- Feline diffuse iris melanoma, immunohistochemistry, AEC chromogen. A) Anti-MMP-9 staining, 10x. B) Anti-TIMP-2 staining, 10x. C) Anti-MMP-9 staining, positive neoplastic melanocytes with marked anisocytosis, anisokaryosis, multinucleation and nuclear pseudoinclusions, 40x. D) Anti-TIMP-2 stain, intensely positive perivascular neoplastic melanocytes, 40x.

When immunohistochemical results were compared with the histological grade, MMP-9 was expressed in 13/22 (59.1%) grade I FDIM , in 18/20 (90.0%) grade II FDIM and 17/20 (85.0%) grade III FDIM. Tumors with MMP-9 expression in more than 50% of neoplastic cells (classes 4-5) were 3/22 (13.6%) in grade I cases, 8/20 (40.0%) in grade II and 7/20 (35.0%) in grade III. MMP-9 immunohistochemical expression in grade I FDIM, in terms of percentage of positively immunostained cells, differed significantly from grade II ($p = 0.008$) and grade III ($P = 0.010$), whereas grades II did not differed significantly from grade III ($p = 1$) (Graph 9).

TIMP-2 was detected in 13/22 (59.1%) grade I FDIM, in 16/20 (80.0%) grade II and 15/20 (75.0%) grade III FDIM. Tumors with TIMP-2 expression in more than 50% of neoplastic cells (classes 4-5) were 1/22 (4.5%) grade I cases, 4/20 (20.0%) grade II and 4/20 (20.0%) grade III FDIM. TIMP-2

immunohistochemical expression differed significantly among grades I-II (p = 0.034). No statistical difference were noted among grades I-III (p = 0.999) and II-III (p = 0.999).

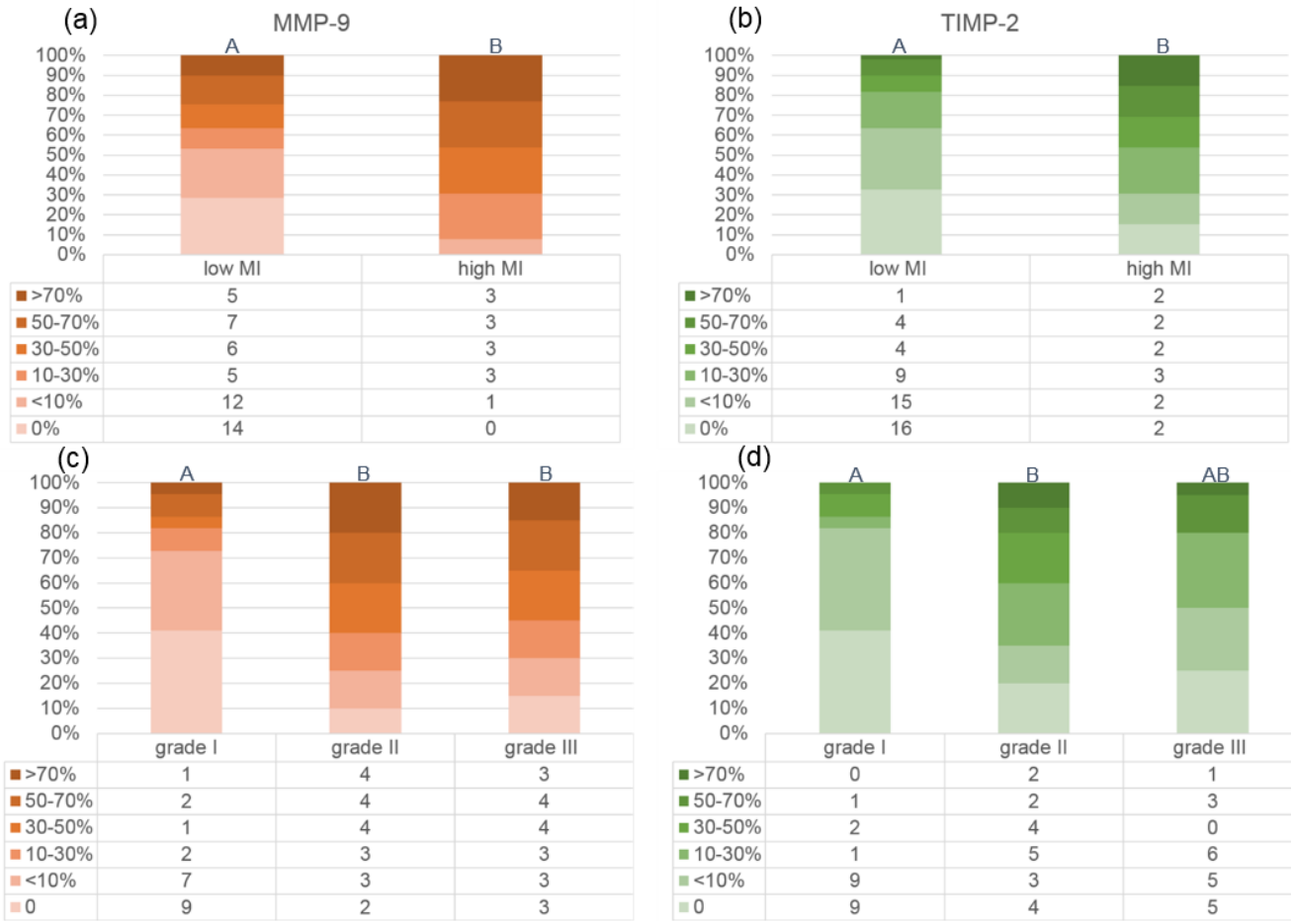

Graph 9- Immunohistochemical expression of MMP-9 and TIMP-2, based on mitotic index (a-b, respectively) and histological grade (c-d, respectively)

The ratio between MMP-9 and TIMP-2 was also examined, classifying the cases in the tree classes "a"-"b"-"c" ("a" = MMP-9=TIMP-2; "b" = MMP-9>TIMP-2; "c" = MMP-9<TIMP-2) and comparing their distribution in groups with different histological grade and mitotic index. The distribution of the three classes was significantly different when compared among histological grades (p=0.004), but not when compared among groups with different mitotic index (p=0.446). Based on standardized residuals analysis (a standardized residual greater than 2 or lower than -2 is indicative of statistical significance), a higher than expected number of subjects in class "a" displayed a histological grade I (Graph 10). TIMP-2 expression was statistically correlated with MMP-9

expression in grade I and III tumors (p = 0.040, R = 0.439 and p = 0.001, R = 0.660, respectively), but not in grade II (p = 0.227, R = 0.283).

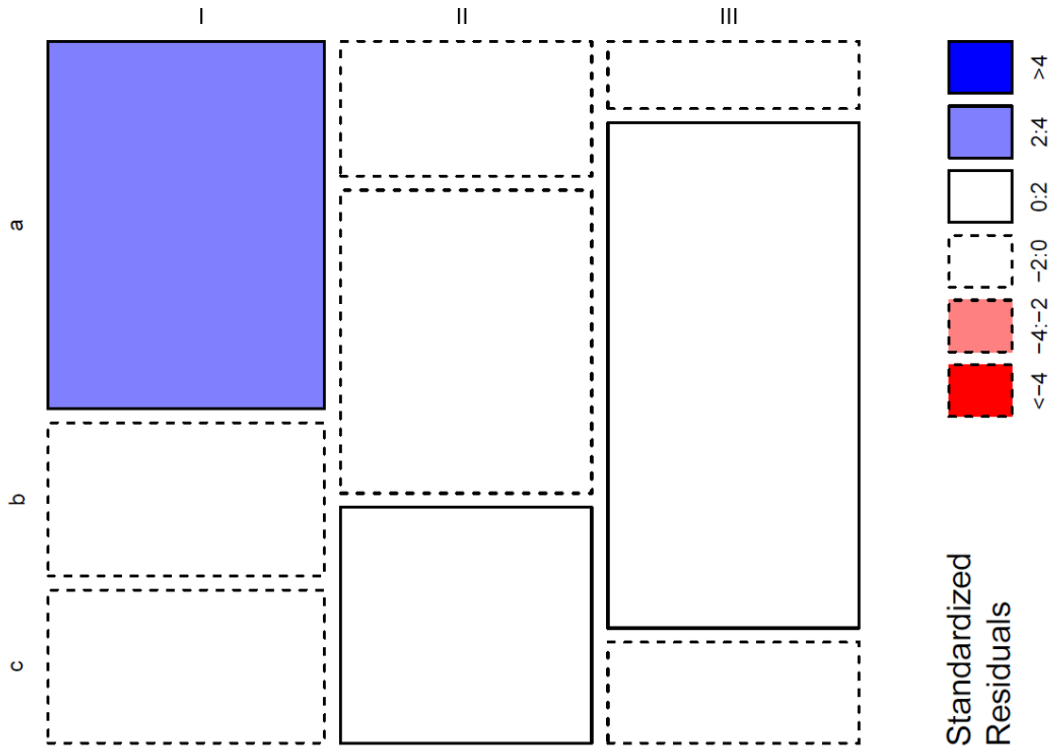

Graph 10 - Distribution of "a", "b" and "c" groups among histological grades I-II-III, standardized residuals analysis (p=0.004). A higher than expected number of subjects in class "a" displayed a histological grade I. "a" = MMP-9=TIMP-2; "b" = MMP-9>TIMP-2; "c" = MMP-9<TIMP-2

Discussion

The present study investigates the expression of matrix metalloproteinases in the complex tumor-matrix interaction underlying malignant progression of FDIM, with specific emphasis on its relationship with well-known histological prognostic criteria.

Sixty-two samples of FDIM were examined in the present study. The median age of diagnosis of FDIM was 10, consistently with previously reported data (Kalishman et al., 1998; Wiggans et al., 2016). Most affected cats were European Shorthair. Among purebred cats, an interesting high number of Persian cats was noted. No similar data are reported in the literature. Definitive conclusions on the possible predisposition of Persian breed cannot be drawn at present, lacking concurrent evaluation of the local distribution of this cat breed.

The expression of selected matrix metalloproteinases was investigated. About 77% of FDIM samples expressed MMP-9, whereas 71% FDIM expressed TIMP-2. FDIM is a malignant, even if slowly progressive, tumor, which may arise as multifocal neoplastic foci on the anterior surface of the iris, and therefore progress over years throughout the iris stroma, up to the posterior surface of the iris and finally infiltrating adjacent structures (filtration angle, ciliary bodies, sclera) (Dubielzig, 2017; Kalishman et al., 1998). The extent of the tumor within the eye is considered an excellent predictor of survival according to the study from Kalishman and colleagues: cats with high grade FDIM have a lower expected survival time (Kalishman et al., 1998). Mitotic index is also a recently established criterion of malignancy (Wiggans et al., 2016).

We considered the activity of metalloproteinases with regard to the MI. Evaluation of MI is considered a prognostic indicator in ocular melanoma in humans (Spencer, 1996), dogs (Wilcock and Peiffer, 1986) and cats (Wiggans et al., 2016). Wiggans and colleagues set 7 mitoses in 10 HPF as parameter of increased metastatic risk in FDIM (Wiggans et al., 2016). In the present study, we found that MMP-9 and TIMP-2 expression significantly increases in cases of FDIM with MI > 7.

We also evaluated MMPs in association with the histological grade of investigated FDIMs. Interestingly, it emerged that increasing percentage of expression of MMP-9 and TIMP-2 is associated with progression of FDIM. While MMP-9 was expressed in more than 50% of neoplastic cells only in 13.6% cases of grade I FDIM, this percentage was of 40% and 35% in grade II and III cases, respectively. In particular, significant difference was noted in grade II and III when compared to grade I, suggesting an higher expression of MMP-9 in more invasive, higher grades tumors.

Similarly, TIMP-2 was detected in most samples, with values that frequently paralleled those of MMP-9, and generally tended to be lower. Only 4.5% of grade I tumors but 20% of both grades II and III expressed TIMP-2 in more than 50% of neoplastic cells. A statistical difference was noted among grade I and II. In general, grade II tumors showed a tendency for higher overall expression of both the investigated enzymes.

In this study, MMP-9 appeared of growing intensity in FDIMs with high MI and intermediate/grade II and advanced/grade III histological grade. MMP-9 is among the most extensively investigated matrix metalloproteinases due to its role in the digestion of basal

membranes and thus in the tumor potential for invasiveness. Highly aggressive human uveal melanomas express high levels of MMPs such as MMP-2, MMP-9, MMP-1 and MT1-MMP (Schnaeker et al., 2004). In particular, MMP-9 in human uveal melanoma is expressed in 50-80% of the neoplastic cells, with a prevalence of epithelioid morphology and a presence of peri-vascular distribution, and in tumor vessels and intravascular leukocytes (El-Shabrawi et al., 2001; Lai et al., 2008). In humans, MMP-9 expression is positively correlated with metastasizing behavior and unfavorable prognosis, whereas TIMP-2 expression is correlated with a better survival rate (El-Shabrawi et al., 2001). On the other hand, selective silencing or downregulation of MMP-9 results in the inhibition of the invasion and migration of murine melanoma cell lines or murine experimental intraocular melanoma (Shi et al., 2015; Tang et al., 2013). The relevant role of MMPs has come to the point that application of MMP-9 inhibitors is currently ongoing research for perspective therapy of human melanoma (Aksenenko and Ruksha, 2013). The present study highlighted that MMP-9 in cats increases in iris diffuse melanoma with unfavorable criteria of malignancy.

Since the balance among the activity of MMPs and TIMPs can be considered an estimate of the overall effect on the ECM remodeling, we calculated the ratio between MMP-9 and TIMP-2. In our cases, classifying the ratio among MMP-9/TIMP-2 simply just in matter of equality or prevalence of the one among the other (referred as classes “a”, “b”, “c”), revealed that cats with balanced levels of MMP-9/TIMP-2 more probably fall in the category of grade I tumors. Contrarily, no differences emerged in comparing the distribution of these classes among groups with different mitotic index. We hypothesized that Kalishman’s histological grade and mitotic index may demonstrate, as prognostic parameters, different features related to the mechanism of malignancy of FDIM neoplastic cells, that are the ability to invade and the ability to replicate, respectively. The invasive ability enhanced by MMPs, indeed, seems to be more involved in the behavior of the tumor toward the extracellular matrix and adjacent connective tissues, as better expressed in the simplified histological grade of Kalishman, which refers to the anatomical invasion of different sectors of the eye from FDIM, than to the intrinsic cytological characteristics of single neoplastic cells.

We also analyzed the statistical correlation among the single values of TIMP-2 and MMP-9: we expected that their distribution deviated from randomness, and instead followed parallel courses

due to an expected increase in TIMP-2 in front of increased MMP-9. In fact, statistical correlation revealed that TIMP-2 expression paralleled MMP-9 in grade I and III, whereas the two investigated proteins were poorly correlated in grade II cases, probably due to higher MMP-9. It is well-known that, in healthy tissues, there is a balance between TIMPs and MMPs, indicating a balance between lysis and deposition of the ECM. An excess of TIMPs may lead toward the inhibition of matrix degradation, up to an excess of matrix deposition. On the other hand, an excess of MMPs leads to degeneration of the ECM, a process generating a favorable environment for tumor invasion (Khokha et al., 2013; Moro et al., 2014; Nagase et al., 2006; Roeb, 2018).

In our FDIM cases, we formulated different hypotheses to justify the observed patterns of MMPs-TIMPs expression. Firstly, we hypothesize that TIMP-2 may increase as an attempt to inhibit increasing levels of MMPs, according to the peculiar and specific inhibitory role of TIMPs as endogenous inhibitors of MMPs (Nagase et al., 2006; Khoka et al., 2013). Secondly, we considered that TIMPs, at low concentrations, may act as activators, rather than inhibitors, of other kind of latent MMPs — eg. pro-MMP-2 — which in turn may activate MMP-9 (Bernardo and Fridman, 2003; Fridman et al., 1995; Lai et al., 2008; Lu et al., 2004). Finally, we speculated that grade II tumors could represent a specific moment in the progression of the neoplasm, when tumor invasion is enhanced by particularly intense activity of matrix metalloproteinases unhampered by low tissue inhibitors. This could stand as a key-moment in the progression of this slowly growing tumor, representing a crucial moment in which FDIM exceeds the confinement to the iris and starts to invade adjacent ocular structures.

Not only grade II FDIMs showed a prevalence of MMPs over TIMPs: grade II tumors also displayed a mixed distribution of cases with low and high mitotic index, and an overall expression of MMP-9 and TIMP-2 not different from grade III tumors, suggesting that this grade represents an overlap among classes difficult to discriminate. Grade II FDIMs could be worth of further investigations, even if, in our experience, they are not the preferred clinical stage of surgical excision, since most ophthalmologists prefer to perform the enucleation of the affected eye either when tumor gives early clinical signs or when the tumor has irreversible extension and secondary glaucoma.

Conclusions

In feline diffuse iris melanoma, MMP-9 and TIMP-2 are highly expressed in high grade tumors. MMPs activity is correlated with histological grade and mitotic index, thus suggesting a relevant role of enzymes involved in tumor-matrix interaction in the progression of the tumor toward invasion.

Results of the present work have been presented as follows:

- *Nordio L., Stornelli V., Franzo G., Giudice C. "Expression of MMP-9 and TIMP-2 in feline diffuse iris melanoma and correlation with histological grade and mitotic index". Manuscript in preparation.*
- *Nordio L., Stornelli V., Giudice C. (2018). "Expression of MMP-9 and TIMP-2 in feline diffuse iris melanoma: correlation with histological grade and mitotic index". Joint ESVP/ECVP European Congress, Cluj-Napoca, 5th-8th September 2018 (poster flash presentation).*
- *Nordio L., Stornelli V., Giudice C. (2018). "MMP-9 immunohistochemical expression is correlated with histologic grade in feline diffuse iris melanoma". Proceeding of Veterinary and Animal Science Days 2018, 6th-8th June 2018, Milano (oral presentation). International Journal of Health, Animal Science and Food safety, 5.*

V. CASE REPORT: EVIDENCES OF VASCULOGENIC MIMICRY IN A PALPEBRAL MELANOCYTOMA IN A DOG

Abstract

A female spayed, 7-year-old Doberman dog was presented to the ophthalmologist with a palpebral nodule on the haired eyelid of the left eye. The nodule was surgically removed and submitted for histopathology. Histologically, the nodule was consistent with eyelid melanocytoma. The neoplasia was also characterized by an unusual histological feature: interspersed throughout the neoplastic melanocytes, numerous lacunar and slit-like spaces filled by erythrocytes were observed. On immunohistochemistry, these spaces were lined by cells PNL2-positive, Factor VIII-negative and CD31 negative, consistent with neoplastic melanocytes without endothelial cell participation. This feature was interpreted as vasculogenic mimicry (VM), a mechanism of tumour angiogenesis well-recognized in human melanomas that, to the authors' best knowledge, has not yet been reported in melanomas in veterinary medicine.

Introduction

Vasculogenic mimicry (VM) is a well-known feature of human melanoma (Maniotis et al., 1999). VM has been defined as the de novo generation of vascular channels by tumour cells and is not considered a strictly vasculogenic event because it does not result in de novo formation of endothelial cell-lined vessels (Spiliopoulos et al., 2015). Rather, these microcirculatory networks or capillary-like structures are made of extracellular matrix and are lined by neoplastic cells instead of endothelium (Spiliopoulos et al., 2015). It is still not well understood if these vascular structures are functional, however these channels can be detected angiographically and red blood cells are histologically recognizable within their lumens (Maniotis et el., 1999). Lining endothelial cells have not been identified by light microscopy, by transmission electron microscopy, or by the use of immunohistochemical endothelial cell markers (Factor VIII-related antigen, CD31, CD34, and KDR[Flk-1]) (Maniotis et el., 1999; Spiliopoulos et al., 2015).

VM was firstly described in human melanoma by Maniotis and coauthors in 1999 (Maniotis et el., 1999) and, thereafter, it has also been reported in different types of human tumour, such as malignant mesothelioma (Pulford et al., 2016), cancer of the liver (Zhao et al., 2015), pancreas (Guo et al., 2014), stomach (Zang et al., 2015), prostate (Wang et al., 2016), ovaries and breast (Hendrix et al., 2003). The presence of VM patterns in patients with malignant tumours, e.g. human uveal and cutaneous melanomas, has been correlated with a worse prognosis and shorter survival than their non-VM-forming counterparts (Spiliopoulos et al., 2015).

To date, in dogs, VM has been reported only in canine inflammatory breast cancer (Clemente et al., 2010; Rasotto et al., 2012) but, to the best of the authors' knowledge, it has not been previously described in canine melanocytic tumours. In the present report, VM pattern is described in a melanocytic neoplasm of the eyelid in a dog.

Case report

A female spayed Doberman 7-year old dog was presented with a 5 mm, brownish, palpebral nodule on the skin of the upper eyelid of the left eye. The nodule had been present for one year and was slowly enlarging. Complete ophthalmic examination was otherwise unremarkable, except for mild bilateral epiphora. Pre-operative diagnostic tests, i.e. complete blood count and serum chemistry, were within normal limits. The nodule was surgically removed with "V" full-thickness excision and submitted for histopathology. The sample was fixed in 10% buffered formalin and routinely processed for histology. Microtomic sections were obtained and stained with hematoxylin and eosin (H&E) for histopathological examination.

Histologically, the dermis of the eyelid was expanded by a multilobular nodular neoplasm, which was moderately well demarcated and not encapsulated. Neoplastic cells were arranged in lobules and nests with multifocal areas of junctional activity. Neoplastic cells were epithelioid or, less commonly, spindle-shaped, with indistinct cell borders and high nucleus/cytoplasmic ratio. Cytoplasm was moderate, granular and eosinophilic, occasionally vacuolated and multifocally filled by melanin pigment. Nuclei were oval, with marginated chromatin and single prominent central nucleolus. Anisocytosis and anisokaryosis were moderate and mitotic count in 10 HPF was 1.

Multifocally, throughout the neoplasm, numerous irregular slit-like or lacunar spaces were observed (Figure 10). These spaces were filled by a moderate number of red blood cells, were supported by fine fibrous stroma and were lined by polygonal, epithelioid or spindle cells with moderate cytoplasm and a round to oval nucleus with a prominent nucleolus. The neoplasm was diagnosed as a mixed-type sparsely pigmented dermal melanocytoma.

With Periodic acid–Schiff (PAS) special staining of serial sections, performed to characterize the lacunar spaces, there was moderately positive staining of the thin fibrous septa delimiting the blood-filled spaces.

Immunohistochemistry (ABC standard method) was also performed to further characterize the cells lining the blood-filled lacunar spaces. The endothelial cell markers Factor VIII (FVIII) and CD31 and the melanocytic marker PNL2 were specifically investigated.

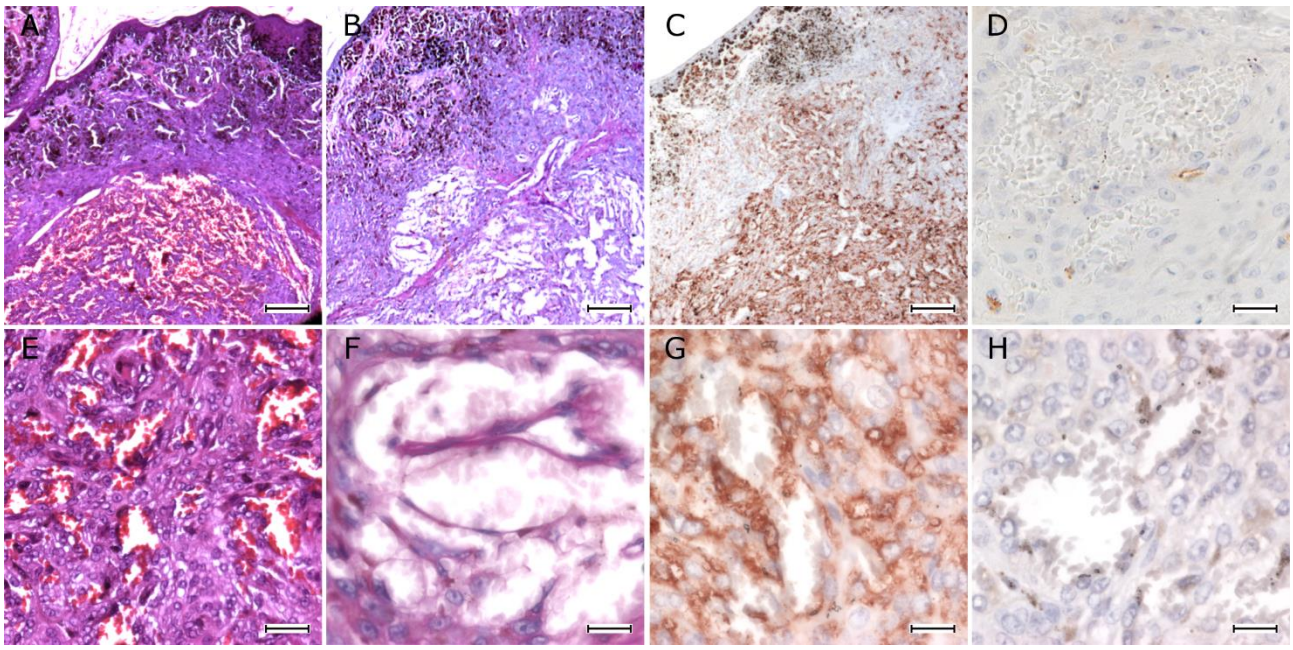

Figure 10 - Eyelid. A) Dermis is expanded by a multilobular melanocytoma admixed with numerous irregular slit-like or lacunar spaces filled by red blood cells. H&E, bar = 100 µm. B) Blood-filled spaces are supported by fine fibrous stroma. PAS stain, bar = 100 µm. C) Spaces are lined by PNL2-positive neoplastic cells. IHC anti-PNL2, AEC chromogen, bar = 100 µm. D) Cells lining blood-filled spaces are CD-31 negative. IHC anti-CD31, DAB chromogen, bar = 12,5 µm. E) Higher magnification of A. H&E, bar = 25 µm. F) Higher magnification of B. PAS stain, bar = 12,5 µm. G) Higher magnification of C. IHC anti-PNL2, AEC chromogen, bar = 12,5 µm. H) Cells lining blood-filled spaces are FVIII negative. IHC anti-FVIII, AEC chromogen, bar = 12,5 µm.

For immunohistochemistry, serial microtomic sections were obtained and mounted on polylysine coated slides (Menzel-Gläser, Braunschweig, Germany). PNL and FVIII labelling were performed by manual staining with standard ABC method. After heat-induced antigen retrieval in EDTA buffer

(PNL2) or enzymatic-retrieval with pepsin (FVIII), slides were immunostained using a mouse monoclonal anti-PNL2 antibody (Monosan, Uden, Netherlands), incubated at 1:25 overnight at 4°C, and a rabbit polyclonal anti-Factor VIII antibody (Dako, Carpinteria, USA), incubated at 1:200 overnight at 4°C, respectively. CD31 labelling was automatically performed with Ventana BenchMarck ULTRA (Ventana Medical System, Roche, Oro Valley, AZ, USA): the sections were unmasked with Benchmark ULTRA CC1 (pH 8.4) at 95°C for 52 minutes and incubated with the primary antibody mouse monoclonal anti-CD31 Endothelial cell (JC70A; Dako, Carpinteria, USA), at 1:20 for 32 minutes at room temperature. DAB (3,3'-diaminobenzidine) (Roche, Oro Valley, AZ, USA) or AEC (3-amino-9-ethylcarbazole) (Vector Laboratories, Burlingame, USA) substrate-chromogen kit were used as chromogen, and sections were counterstained with Mayer's hematoxylin. Negative controls were prepared by replacing the respective primary antibody with normal rabbit or mouse serum (non-immune serum, Dakocytomation). Endothelium of blood vessels served as internal positive control for FVIII and CD31.

The cells lining red blood cell-filled spaces, as well as the neoplastic cells composing the melanocytoma, labelled strongly with antibody against PNL2, whereas they were negative to FVIII and CD31 (Figure 10). Normal endothelium of pre-existing blood vessels within the same section was diffusely and intensely stained with both FVIII and CD31.

Based on histological and immunohistochemical results, lacunar spaces were interpreted as areas of vasculogenic mimicry within an eyelid melanocytoma.

Eight months after surgery, the dog was in good health conditions with no indications of recurrence of the eyelid mass.

Discussion and conclusions

The term vasculogenic mimicry (VM) has been used to describe the ability of aggressive neoplastic cells to acquire an endothelial-like morphology and to form extracellular matrix (ECM)-rich vasculogenic-like networks (Hendrix et al., 2003), which are hypothesized to facilitate tumor perfusion independently from tumor angiogenesis (Maniotis et al., 1999). The present case describes histological evidences of vasculogenic mimicry in a canine cutaneous melanocytoma. The

mass arose on the eyelid and contained widespread microscopic slit-like and lacunar spaces filled with erythrocytes. Histochemical and immunohistochemical staining confirmed the melanocytic origin of the cells lining these lacunar spaces. In fact, these spaces, sustained by PAS-positive fibrous septa, were lined by cells that labelled strongly with antibody against PNL2, marker of melanocytic origin, whereas did not label with antibodies anti FVIII and CD31, markers of endothelial origin. These results confirmed the melanocytic origin of the cells lining the newly formed vascular network and confirmed the presence of a “vasculogenic mimicry” phenomenon.

In VM in human melanoma, it has now been recognized that the deeper layer of melanoma cell-lined microvascular structures is composed of extracellular matrix proteins such as laminin, collagens IV and VI, and heparan sulfate proteoglycans, which provide the PAS-positive supportive fibrous stroma (Spiliopoulos et al., 2015). Currently, there are two hypotheses concerning the origin of VM network-forming melanoma cells: they could either be tumor cells that have undergone de-differentiation, resulting in a primitive cell-type which encompasses tumor cell, stem cell, and endothelial cell characteristics, or they may arise from cancer stem cells (Spiliopoulos et al., 2015).

VM in melanoma involves several signaling molecules that are also involved in embryonic vasculogenesis, including for example vascular endothelial (VE)-cadherin, erythropoietin-producing hepatocellular carcinoma-A2 (EPHA2), phosphatidylinositol 3-kinase, focal adhesion kinase, matrix metalloproteinases and laminin 5 γ2-chain (Hendrix et al., 2003). Identification of the pathways that regulate this undifferentiated and highly plastic phenotype may be strategic in the development of new therapies for human cancer. In fact, even though the biological implications of VM in vivo are still unclear, tumor VM is associated with a poor prognosis (Hendrix et al., 2016). Thus, VM in tumors of human patients with a poor clinical outcome suggests a functionally relevant role in the survival of tumor cells (Hendrix et al., 2016). VM in human melanomas is correlated with a high mitotic index and prevalence of epithelioid morphology, which is associated with worse prognosis (Spiliopoulos et al., 2017).

Nevertheless, VM has also been described in benign melanocytic nevi (Demitsu et al., 1998; Spiliopoulos et al., 2017). In a study by Spiliopoulos and co-authors on human melanocytic tumors of the eye and the periocular area, 10% of benign nevi, mostly arising in the conjunctiva, included

areas of VM, without any other atypical features, suggesting the absence of an association with malignant potential. However, in human medicine, conjunctival nevi can occasionally also behave as pre-cancerous lesions and progress into melanomas. The prognostic implication of VM in benign nevi has not yet been elucidated (Spiliopoulos et al., 2017).

There are few reports in the veterinary literature of VM in dogs. VM has been reported in canine mammary carcinoma: specifically, VM has a higher frequency in inflammatory mammary cancer compared to non-inflammatory mammary cancer (Clemente et al., 2010), although VM is not considered predictive of invasion of the lymphatic system (Rasotto et al., 2012).

To the best of the authors' knowledge, VM has not been previously reported in canine melanocytic tumors. To date, there are insufficient cases in the veterinary literature on VM in canine melanocytic tumors to draw prognostic considerations on the significance of VM in dogs, yet it would be interesting to assess if this phenomenon may bear a role in the behavior and invasiveness of this tumor, thus resembling the human cases. The incidence, role and prognostic significance of VM in veterinary species is a field worthy of further investigation.

Results of the present work have been presented as follows:

- *Nordio L., Fattori S., Vascellari M., Giudice C (2018). "Evidence of vasculogenic mimicry in a palpebral melanocytoma in a dog". Journal of Comparative Pathology, 162, 43-46.*

GENERAL CONCLUSIONS

The present PhD project investigated molecules involved in the pathogenesis and prognosis of canine and feline spontaneous models of non-UV induced melanoma, that are canine oral melanoma and feline diffuse iris melanoma (FDIM).

After the preliminarily technical validation for the use of anti-FXR1 antibodies in the canine species, the normal distribution of FXR1 protein was illustrated in normal canine tissues, being present in at least one tissue or cellular population in all the organs, with a particularly intense expression in skeletal muscle and interstitial cells of Leydig of the testis. As a preliminary analysis for further investigations, FXR1 was also detected in a small caseload of different types of canine melanocytic tumors.

FXR1 and LTA4H proteins were detected in the majority of the investigated canine oral melanomas. Although these proteins seemed not to have significant associations with the relative expression of their codifying genes, the known indicators of tumor malignant behavior (i.e. mitotic index and Ki-67 index) or the clinical outcome, the expression of this two molecules has been verified at both gene and protein levels. This data encourage further investigation on a possible role of FXR1 and LTA4H in the pathogenesis of canine oral melanoma, possibly on a larger cohort of cases.

Hypothesizing, as per literature, that FXR1 could be associated with the expression of MMP-9, we tested MMP9 and TIMP2 expression in canine oral melanomas. In our cohort of cases we did not find any significant association FXR1-MMP-9 in canine oral melanomas. Anyway, despite not significant, a trend for higher levels of expression of MMP-9 and its inhibitor TIMP-2 was observed in cases with high expression of FXR1 and in cases with an unfavorable clinical outcome. These preliminary results warrant more investigations on the role of matrix metalloproteinases in the progression of canine oral melanoma.

In FDIM, intense expression of both MMP-9 and TIMP-2 was significantly associated with high histological grades and high mitotic index, well-known prognostic parameters in this tumor. These

results suggest that MMPs have a relevant role in neoplastic progression in FDIM, presumably creating a microenvironment favorable to invasion through the digestion of the extracellular matrix.

ACKNOWLEDGMENT

Department of Veterinary Medicine (DIMEVET), Università degli Studi di Milano, Milano

Prof. Chiara Bazzocchi

Dr. Francesca Genova

Dr. Valentina Serra

Prof. Maria Lina Longeri

Dr. Andreia Marques

Dr. Cristina Lecchi

Prof. Fabrizio Ceciliani

Prof. Damiano Stefanello

Prof. Chiara Giudice

All the colleagues and technical staff of the Service of Anatomic Pathology

Department of Health, Animal Science and Food Safety (VESPA), Università degli Studi di Milano, Milano

Prof. Alberto Luciano

Private veterinary practitioners

Dr. Valentina Stornelli

Dr. Sabina Fattori

Department of Animal Medicine, Production and Health (MAPS), Università degli Studi di Padova, Padova

Dr. Giovanni Franzo

Laboratorio Privato San Marco, Padova

Dr. Marco Rondena

REFERENCES

- Agulhon, C., Blanchet, P., Kobetz, A., Marchant, D., Faucon, N., Sarda, P., Moraine, C., Sittler, A., Biancalana, V., Malafosse, A., Abitbol, M., 1999. Expression of FMR1, FXR1, and FXR2 genes in human prenatal tissues. J. Neuropathol. Exp. Neurol. 58, 867–80.
- Aksenenko, M.B., Ruksha, T.G., 2013. Analysis of the application of MMP-9 inhibitor in skin melanoma: experimental study. Bull. Exp. Biol. Med. 154, 594–6.
- Arguello, M., Paz, S., Hernandez, E., Corriveau-Bourque, C., Fawaz, L.M., Hiscott, J., Lin, R., 2006. Leukotriene A4 Hydrolase Expression in PEL Cells Is Regulated at the Transcriptional Level and Leads to Increased Leukotriene B4 Production. J. Immunol. 176, 7051–7061.
- Ashton, N., 1964. Primary Tumours Of The Iris. Br. J. Ophthalmol. 48, 650–68.
- Atherton, M.J., Morris, J.S., McDermott, M.R., Lichty, B.D., 2016. Cancer immunology and canine malignant melanoma: A comparative review. Vet. Immunol. Immunopathol. 169, 15–26.
- Ballester Sanchez, R., de Unamuno Bustos, B., Navarro Mira, M., Botella Estrada, R., 2015. Mucosal melanoma: an update. Actas Dermosifiliogr. 106, 96–103.
- Bardoni, B., Schenck, a, Mandel, J.L., 2001. The Fragile X mental retardation protein. Brain Res. Bull. 56, 375–82.
- Batioğlu, F., Günalp, I., 1998. Malignant melanomas of the iris. Jpn. J. Ophthalmol. 42, 281–5.
- Bergin, I.L., Smedley, R.C., Esplin, D.G., Spangler, W.L., Kiupel, M., 2011. Prognostic evaluation of ki67 threshold value in canine oral melanoma. Vet. Pathol. 48, 41–53.
- Bergman, P.J., 2007. Canine Oral Melanoma. Clin. Tech. Small Anim. Pract. 22, 55–60.
- Bernardo, M.M., Fridman, R., 2003. TIMP-2 (tissue inhibitor of metalloproteinase-2) regulates MMP-2 (matrix metalloproteinase-2) activity in the extracellular environment after pro-MMP-2 activation by MT1 (membrane type 1)-MMP. Biochem. J. 374, 739–45.
- BLAST, 2017. Basic Local Alignement Search Tool, available online at https://blast.ncbi.nlm.nih.gov/Blast.cgi#359323779, retrieved on November 14, 2017.

- Bolon, B., Calderwood Mays, M.B., Hall, B.J., 1990. Characteristics of canine melanomas and comparison of histology and DNA ploidy to their biologic behavior. Vet. Pathol. 27, 96–102.
- Breton, J., Woolf, D., Young, P., Chabot-Fletcher, M., 1996. Human keratinocytes lack the components to produce leukotriene B4. J. Invest. Dermatol. 106, 162–167.
- Callender, G.R., 1931. Malignant melanocytic tumors of the eye. A study of histologic types in 111 cases. Trans. Am. Acad. Ophthalmol. Otolaryngol. 36, 131.
- Candrea, E., Senila, S., Tatomir, C., Cosgarea, R., 2014. Active and inactive forms of matrix metalloproteinases 2 and 9 in cutaneous melanoma. Int. J. Dermatol. 53, 575–80.
- Castagnola, S., Bardoni, B., Maurin, T., 2017a. The search for an effective therapy to treat Fragile X Syndrome: Dream or reality? Front. Synaptic Neurosci.
- Chen, X., Li, N., Wang, S., Wu, N., Hong, J., Jiao, X., Krasna, M.J., Beer, D.G., Yang, C.S., 2003. Leukotriene A4 hydrolase in rat and human esophageal adenocarcinomas and inhibitory effects of bestatin. J. Natl. Cancer Inst. 95, 1053–1061.
- Chen, X., Wang, S., Wu, N., Yang, C., 2004. Leukotriene A4 Hydrolase as a Target for Cancer Prevention and Therapy. Curr. Cancer Drug Targets 4, 267–283.
- Chen, Y., Chen, Y., Huang, L., Yu, J., 2012. Evaluation of heparanase and matrix metalloproteinase-9 in patients with cutaneous malignant melanoma. J. Dermatol. 39, 339–343.
- Clemente, M., Pérez-Alenza, M.D., Illera, J.C., Peña, L., 2010. Histological, immunohistological, and ultrastructural description of vasculogenic mimicry in canine mammary cancer. Vet. Pathol. 47, 265–74.
- Comtesse, N., Keller, A., Diesinger, I., Bauer, C., Kayser, K., Huwer, H., Lenhof, H.P., Meese, E., 2007. Frequent overexpression of the genes FXR1, CLAPM1 and EIF4G located on amplicon 3q26-27 in squamous cell carcinoma of the lung. Int. J. Cancer 120, 2538–2544.
- Coy, J.F., Sedlacek, Z., Bächner, D., Hameister, H., Joos, S., Lichter, P., Delius, H., Poustka, A., 1995. Highly conserved 3’ UTR and expression pattern of FXR1 points to a divergent gene regulation of FXR1 and FMR1. Hum. Mol. Genet. 4, 2209–18.
- Davidovic, L., Durand, N., Khalfallah, O., Tabet, R., Barbry, P., Mari, B., Sacconi, S., Moine, H.,

Bardoni, B., 2013. A Novel Role for the RNA-Binding Protein FXR1P in Myoblasts Cell-Cycle Progression by Modulating p21/Cdkn1a/Cip1/Waf1 mRNA Stability. PLoS Genet. 9.

- Demirci, H., Reed, D., Elner, V.M., 2013. Tissue-based microarray expression of genes predictive of metastasis in uveal melanoma and differentially expressed in metastatic uveal melanoma. J. Ophthalmic Vis. Res. 8, 303–307.
- Demirci, H., Shields, C.L., Shields, J.A., Eagle, R.C., Honavar, S.G., 2002. Diffuse iris melanoma: a report of 25 cases. Ophthalmology 109, 1553–60.
- Demitsu, T., Kakurai, M., Yamada, T., Kiyosawa, T., Yaoita, H., 1998. The vascular space-like structure in melanocytic nevus is not an injection artifact: report of a case and an experimental study. J. Dermatol. 25, 143–9.
- Dieci, C., Lodde, V., Franciosi, F., Lagutina, I., Tessaro, I., Modina, S.C., Albertini, D.F., Lazzari, G., Galli, C., Luciano, A.M., 2013. The effect of cilostamide on gap junction communication dynamics, chromatin remodeling, and competence acquisition in pig oocytes following parthenogenetic activation and nuclear transfer. Biol. Reprod. 89, 68.
- Docampo, M.-J., Cabrera, J., Rabanal, R.M., Bassols, A., 2011. Expression of matrix metalloproteinase-2 and -9 and membrane-type 1 matrix metalloproteinase in melanocytic tumors of dogs and canine melanoma cell lines. Am. J. Vet. Res. 72, 1087–96.
- Dubielzig, R., 2017. Tumors of the Eye; 902-907. In “Tumors in Domestic Animals”, fifth edition, edited by D.J. Meuten. Wiley-Blackwell, Hoboken, USA.
- Dubois, R.N., 2003. Leukotriene A 4 Signaling , Inflammation , and Cancer. Cancer 95, 4–5.
- Duncan, D.E., Peiffer, R.L., 1991. Morphology and prognostic indicators of anterior uveal melanomas in cats. Prog. Vet. Comp. Ophthalmol. 1,25.
- Edbauer, D., Neilson, J.R., Foster, K.A., Wang, C.-F., Seeburg, D.P., Batterton, M.N., Tada, T., Dolan, B.M., Sharp, P.A., Sheng, M., 2010. Regulation of Synaptic Structure and Function by FMRP-Associated MicroRNAs miR-125b and miR-132. Neuron 65, 373–384.
- El-Shabrawi, Y., Ardjomand, N., Radner, H., Ardjomand, N., 2001. MMP-9 is predominantly expressed in epithelioid and not spindle cell uveal melanoma. J. Pathol. 194, 201–6. h
- Esplin, D.G., 2008. of the Mucous Membranes of the Lips and Oral Cavity Survival of Dogs

Following Surgical Excision of Histologically Well-differentiated Melanocytic Neoplasms Survival of Dogs Following Surgical Excision of Histologically Well-differentiated Melanocytic Neo 896, 889–896.

- Fan, Y., Yue, J., Xiao, M., Han-Zhang, H., Wang, Y.V., Ma, C., Deng, Z., Li, Y., Yu, Y., Wang, X., Niu, S., Hua, Y., Weng, Z., Atadja, P., Li, E., Xiang, B., 2017. FXR1 regulates transcription and is required for growth of human cancer cells with TP53/FXR2 homozygous deletion. Elife 6.
- Fridman, R., Toth, M., Peña, D., Mobashery, S., 1995. Activation of progelatinase B (MMP-9) by gelatinase A (MMP-2). Cancer Res. 55, 2548–55.
- Garnon, J., Lachance, C., Di Marco, S., Hel, Z., Marion, D., Ruiz, M.C., Newkirk, M.M., Khandjian, E.W., Radzioch, D., 2005. Fragile X-related protein FXR1P regulates proinflammatory cytokine tumor necrosis factor expression at the post-transcriptional level. J. Biol. Chem. 280, 5750–5763.
- Geisse, L.J., Robertson, D.M., 1985. Iris melanomas. Am. J. Ophthalmol. 99, 638–48.
- Gillard, M., Cadieu, E., De Brito, C., Abadie, J., Vergier, B., Devauchelle, P., Degorce, F., Dréano, S., Primot, A., Dorso, L., Lagadic, M., Galibert, F., Hédan, B., Galibert, M.D., André, C., 2014. Naturally occurring melanomas in dogs as models for non-UV pathways of human melanomas. Pigment Cell Melanoma Res. 27, 90–102.
- Giudice, C., Ceciliani, F., Rondena, M., Stefanello, D., Grieco, V., 2010. Immunohistochemical investigation of PNL2 reactivity of canine melanocytic neoplasms and comparison with Melan A. J. Vet. Diagnostic Investig. 22, 389–394.
- Goldschmidt, M.H., Goldschmidt, K.H., 2017. Epithelial and Melanocytic Tumors of the Skin; 125-131. In “Tumors in Domestic Animals”, fifth edition, edited by D.J. Meuten. Wiley-Blackwell, Hoboken, USA.
- Guo, J.-Q., Zheng, Q.-H., Chen, H., Chen, L., Xu, J.-B., Chen, M.-Y., Lu, D., Wang, Z.-H., Tong, H.-F., Lin, S., 2014. Ginsenoside Rg3 inhibition of vasculogenic mimicry in pancreatic cancer through downregulation of VE-cadherin/EphA2/MMP9/MMP2 expression. Int. J. Oncol. 45, 1065–1072.
- Guo, Y., Wang, X., Zhang, X., Sun, Z., Chen, X., 2011. Ethanol Promotes Chemically Induced

Oral Cancer in Mice through Activation of the 5-Lipoxygenase Pathway of Arachidonic Acid Metabolism. Cancer Prev. Res. 4, 1863–1872.

- Guriec, N., Le Jossic- Corcos, C., Simon, B., Ianotto, J.C., Tempescul, A., Dréano, Y., Salaün, J.P., Berthou, C., Corcos, L., 2014. The arachidonic acid-LTB4-BLT2 pathway enhances human B-CLL aggressiveness. Biochim. Biophys. Acta - Mol. Basis Dis. 1842, 2096–2105.
- Henderson, E., Margo, C.E., 2008. Iris melanoma. Arch. Pathol. Lab. Med. 132, 268–72.
- Hendrix, M.J.C., Seftor, E.A., Kirschmann, D.A., Quaranta, V., Seftor, R.E.B., 2003. Remodeling of the microenvironment by aggressive melanoma tumor cells. Ann. N. Y. Acad. Sci. 995, 151–61.
- Hendrix, M.J.C., Seftor, E.A., Seftor, R.E.B., Chao, J.-T., Chien, D.-S., Chu, Y.-W., 2016. Tumor cell vascular mimicry: Novel targeting opportunity in melanoma. Pharmacol. Ther. 159, 83–92.
- Henriquez, F., Janssen, C., Kemp, E.G., Roberts, F., 2007. The T1799A *BRAF* Mutation Is Present in Iris Melanoma. Investig. Opthalmology Vis. Sci. 48, 4897.
- Human Protein Atlas, 2017. Tissue expression of FXR1 – The Human Protein Atlas, available online at https://www.proteinatlas.org/ENSG00000114416-FXR1/tissue, retrieved on November 14, 2017.
- Jakobiec, F.A., Silbert, G., 1981. Are most iris "melanomas' really nevi? A clinicopathologic study of 189 lesions. Arch. Ophthalmol. (Chicago, Ill. 1960) 99, 2117–32.
- Jakobsson, P., Odlander, B., Claesson, H., 1991. Effects of monocyte-lymphocyte interaction on the synthesis of leukotriene B4 400, 395–400.
- Jeong, C.H., Bode, A.M., Pugliese, A., Cho, Y.Y., Kim, H.G., Shim, J.H., Jeon, Y.J., Li, H., Jiang, H., Dong, Z., 2009. [6]-Gingerol suppresses colon cancer growth by targeting leukotriene A 4 hydrolase. Cancer Res. 69, 5584–5591.
- Jin, X., Zhai, B., Fang, T., Guo, X., Xu, L., 2016. FXR1 is elevated in colorectal cancer and acts as an oncogene. Tumor Biol. 37, 2683–2690.
- Kalishman, Chappell, Flood, Dubielzig, 1998. A matched observational study of survival in cats with enucleation due to diffuse iris melanoma. Vet. Ophthalmol. 1, 25–29.

- Khan, S., Finger, P.T., Yu, G.-P., Razzaq, L., Jager, M.J., de Keizer, R.J.W., Sandkull, P., Seregard, S., Gologorsky, D., Schefler, A.C., Murray, T.G., Kivelä, T., Giuliari, G.P., McGowan, H., Simpson, E.R., Corriveau, C., Coupland, S.E., Damato, B.E., 2012. Clinical and Pathologic Characteristics of Biopsy-Proven Iris Melanoma. Arch. Ophthalmol. 130, 57.
- Khera, T.K., Dick, A.D., Nicholson, L.B., 2010a. Fragile X-related protein FXR1 controls post-transcriptional suppression of lipopolysaccharide-induced tumour necrosis factor-α production by transforming growth factor-β1. FEBS J. 277, 2754–2765.
- Khera, T.K., Dick, A.D., Nicholson, L.B., 2010b. Mechanisms of TNFα regulation in uveitis: Focus on RNA-binding proteins. Prog. Retin. Eye Res. 29, 610–621.
- Khokha, R., Murthy, A., Weiss, A., 2013. Metalloproteinases and their natural inhibitors in inflammation and immunity. Nat. Rev. Immunol. 13, 649–65.
- Kirkpatrick, L.L., McIlwain, K.A., Nelson, D.L., 1999. Alternative splicing in the murine and human FXR1 genes. Genomics 59, 193–202.
- Kondratiev, S., Gnepp, D.R., Yakirevich, E., Sabo, E., Annino, D.J., Rebeiz, E., Laver, N. V., 2008. Expression and prognostic role of MMP2, MMP9, MMP13, and MMP14 matrix metalloproteinases in sinonasal and oral malignant melanomas. Hum. Pathol. 39, 337–343.
- Kumar, V., Abbas, A.K., Aster, J.C., 2015. Inflammation and repair; 83-86. In: “Pathologic Basis of Disease”, ninth edition. Elsevier Saunders, Philadelphia, USA.
- Lai, K., Conway, R.M., Crouch, R., Jager, M.J., Madigan, M.C., 2008. Expression and distribution of MMPs and TIMPs in human uveal melanoma. Exp. Eye Res. 86, 936–941.
- Le Tonqueze, O., Kollu, S., Lee, S., Al-Salah, M., Truesdell, S.S., Vasudevan, S., 2016. Regulation of monocyte induced cell migration by the RNA binding protein, FXR1. Cell Cycle 15, 1874–1882. 0
- Lee, N., Zakka, L.R., Mihm, M.C., Schatton, T., 2016. Tumour-infiltrating lymphocytes in melanoma prognosis and cancer immunotherapy. Pathology 48, 177–187.
- Lee, W.R., 2002. “Opthalmic Histopathology”, second edition; 131-138. Springer, New York, USA.
- Lepetit, H., Eddahibi, S., Fadel, E., Frisdal, E., Munaut, C., Noel, A., Humbert, M., Adnot, S.,

D'Ortho, M.-P., Lafuma, C., 2005. Smooth muscle cell matrix metalloproteinases in idiopathic pulmonary arterial hypertension. Eur. Respir. J. 25, 834–42.

- Liotta, L.A., Stetler-Stevenson, W.G., 1991. Tumor invasion and metastasis: an imbalance of positive and negative regulation. Cancer Res. 51, 5054s–5059s.
- Lu, K. V, Jong, K.A., Rajasekaran, A.K., Cloughesy, T.F., Mischel, P.S., 2004. Upregulation of tissue inhibitor of metalloproteinases (TIMP)-2 promotes matrix metalloproteinase (MMP)-2 activation and cell invasion in a human glioblastoma cell line. Lab. Investig. 84, 8–20.
- Ma, Y., Wang, C., Li, B., Qin, L., Su, J., Yang, M., He, S., 2014. Bcl-2-associated transcription factor 1 interacts with fragile X-related protein 1. Acta Biochim. Biophys. Sin. (Shanghai). 46, 119–127.
- Malho, P., Dunn, K., Donaldson, D., Dubielzig, R.R., Birand, Z., Starkey, M., 2013. Investigation of prognostic indicators for human uveal melanoma as biomarkers of canine uveal melanoma metastasis. J. Small Anim. Pract. 54, 584–593.
- Maniotis, A.J., Folberg, R., Hess, A., Seftor, E.A., Gardner, L.M.G., Pe'er, J., Trent, J.M., Meltzer, P.S., Hendrix, M.J.C., 1999. Vascular Channel Formation by Human Melanoma Cells in Vivo and in Vitro: Vasculogenic Mimicry. Am. J. Pathol. 155, 739–752.
- McLean, I.W., Foster, W.D., Zimmerman, L.E., Gamel, J.W., 1983. Modifications of Callender's classification of uveal melanoma at the Armed Forces Institute of Pathology. Am. J. Ophthalmol. 96, 502–9.
- Mignatti, P., Rifkin, D.B., 1993. Biology and biochemistry of proteinases in tumor invasion. Physiol. Rev. 73, 161–195.
- Mihajlovic, M., Vlajkovic, S., Jovanovic, P., Stefanovic, V., 2012. Primary mucosal melanomas: A comprehensive review. Int. J. Clin. Exp. Pathol. 5, 739–753.
- Momose, M., Ota, H., Hayama, M., 2011. Re-evaluation of melanin bleaching using warm diluted hydrogen peroxide for histopathological analysis. Pathol. Int. 61, 345–50.
- Moro, N., Mauch, C., Zigrino, P., 2014. Metalloproteinases in melanoma. Eur. J. Cell Biol. 93, 23–9.

- Munday, J.S., Löhr, C.V., Kiupel, M., 2017. Tumors of the Alimentary Tract; 500-523. In "Tumors in Domestic Animals", fifth edition, edited by D.J. Meuten. Wiley-Blackwell, Hoboken, USA.
- Myung, J.K., Jeong, J.B., Han, D., Song, C.S., Moon, H.J., Kim, Y.A., Kim, J.E., Byun, S.J., Kim, W.H., Chang, M.S., 2011. Well-differentiated liposarcoma of the oesophagus: Clinicopathological, immunohistochemical and array CGH analysis. Pathol. Oncol. Res. 17, 415–420.
- Nagase, H., Visse, R., Murphy, G., 2006. Structure and function of matrix metalloproteinases and TIMPs. Cardiovasc. Res. 69, 562–573.
- Nakaichi, M., Yunuki, T., Okuda, M., Une, S., Taura, Y., 2007. Activity of matrix metalloproteinase-2 (MMP-2) in canine oronasal tumors. Res. Vet. Sci. 82, 271–9.
- NCBI, 2017. FXR1 FMR1 autosomal homolog 1 [Homo sapiens (human)] – Gene – NCBI, available online at https://www.ncbi.nlm.nih.gov/gene/8087, retrieved October 2, 2017.
- Nikkola, J., Vihinen, P., Vuoristo, M.-S., Kellokumpu-Lehtinen, P., Kähäri, V.-M., Pyrhönen, S., 2005. High Serum Levels of Matrix Metalloproteinase-9 and Matrix Metalloproteinase-1 Are Associated with Rapid Progression in Patients with Metastatic Melanoma. Clin. Cancer Res. 11, 5158–5166.
- Nordio, L., Marques, A.T., Lecchi, C., Luciano, A.M., Stefanello, D., Giudice, C., 2018. Immunohistochemical Expression of FXR1 in Canine Normal Tissues and Melanomas. J. Histochem. Cytochem.
- Ohishi, N., Minami, M., Kobayashi, J., Seyama, Y., Hata, J., Yotsumoto, H., Takaku, F., Shimizu, T., 1990. Immunological quantitation and immunohistochemical localization of leukotriene A4 hydrolase in guinea pig tissues. J. Biol. Chem. 265, 7520–5.
- Oi, N., Jeong, C.H., Nadas, J., Cho, Y.Y., Pugliese, A., Bode, A.M., Dong, Z., 2010. Resveratrol, a red wine polyphenol, suppresses pancreatic cancer by inhibiting leukotriene A4 hydrolase. Cancer Res. 70, 9755–9764.
- Okano-Mitani, H., Ikai, K., Imamura, S., 1997. Human melanoma cells generate leukotrienes B4 and C4 from leukotriene A4. Arch. Dermatol. Res. 289, 347–351.

- Onken, M.D., Worley, L. a, Ehlers, J.P., Harbour, J.W., 2004. Gene Expression Profiling in Uveal Melanoma Reveals Two Molecular Classes and Predicts Metastatic Death Advances in Brief Gene Expression Profiling in Uveal Melanoma Reveals Two Molecular Classes and Predicts Metastatic Death. Cancer Res 7205–7209. h
- Onken, M.D., Worley, L.A., Tuscan, M.D., Harbour, J.W., 2010. An accurate, clinically feasible multi-gene expression assay for predicting metastasis in uveal melanoma. J. Mol. Diagnostics 12, 461–468.
- Panek, A.N., Bader, M., 2006. Matrix reloaded: the matrix metalloproteinase paradox. Hypertens. (Dallas, Tex. 1979) 47, 640–1. 4
- Patnaik, A.K., Mooney, S., 1988. Feline Melanoma: A Comparative Study of Ocular, Oral, and Dermal Neoplasms. Vet. Pathol. 25, 105–112.
- Poorman, K., Borst, L., Moroff, S., Roy, S., Labelle, P., Motsinger-Reif, A., Breen, M., 2015. Comparative cytogenetic characterization of primary canine melanocytic lesions using array CGH and fluorescence in situ hybridization. Chromosom. Res. 23, 171–186.
- Porcellato, I., Giontella, A., Mechelli, L., Del Rossi, E., Brachelente, C., 2014. Feline eosinophilic dermatoses: a retrospective immunohistochemical and ultrastructural study of extracellular matrix remodelling. Vet. Dermatol. 25, 86–94, e26.
- Pulford, E., Hocking, A., Griggs, K., McEvoy, J., Bonder, C., Henderson, D.W., Klebe, S., 2016. Vasculogenic mimicry in malignant mesothelioma: an experimental and immunohistochemical analysis. Pathology 48, 650–659.
- Qian, J., Hassanein, M., Hoeksema, M.D., Harris, B.K., Zou, Y., Chen, H., Lu, P., Eisenberg, R., Wang, J., Espinosa, A., Ji, X., Harris, F.T., Rahman, S.M.J., Massion, P.P., 2015. The RNA binding protein FXR1 is a new driver in the 3q26-29 amplicon and predicts poor prognosis in human cancers. Proc. Natl. Acad. Sci. 112, 3469–3474.
- Raffetto, J.D., Khalil, R.A., 2008. Matrix metalloproteinases and their inhibitors in vascular remodeling and vascular disease. Biochem. Pharmacol. 75, 346–359.
- Ramos-DeSimone, N., Hahn-Dantona, E., Sipley, J., Nagase, H., French, D.L., Quigley, J.P., 1999. Activation of matrix metalloproteinase-9 (MMP-9) via a converging

plasmin/stromelysin-1 cascade enhances tumor cell invasion. J. Biol. Chem. 274, 13066–76.

- Ramos-Vara, J.A., Beissenherz, M.E., Miller, M.A., Johnson, G.C., Pace, L.W., Fard, A., Kottler, S.J., 2000. Retrospective study of 338 canine oral melanomas with clinical, histologic, and immunohistochemical review of 129 cases. Vet. Pathol. 37, 597–608.
- Rasotto, R., Zappulli, V., Castagnaro, M., Goldschmidt, M.H., 2012. A retrospective study of those histopathologic parameters predictive of invasion of the lymphatic system by canine mammary carcinomas. Vet. Pathol. 49, 330–40.
- Reinhard, S.M., Razak, K., Ethell, I.M., 2015. A delicate balance: role of MMP-9 in brain development and pathophysiology of neurodevelopmental disorders. Front. Cell. Neurosci. 9, 280.
- Remmele, W., Stegner, H.E., 1987. Recommendation for uniform definition of an immunoreactive score (IRS) for immunohistochemical estrogen receptor detection (ER-ICA) in breast cancer tissue. Pathologe 8, 138–40.
- Rimoldi, D., Salvi, S., Liénard, D., Lejeune, F.J., Speiser, D., Zografos, L., Cerottini, J.-C., 2003. Lack of BRAF mutations in uveal melanoma. Cancer Res. 63, 5712–5.
- Roeb, E., 2018. Matrix metalloproteinases and liver fibrosis (translational aspects). Matrix Biol. 68–69, 463–473.
- Rushton, J.G., Ertl, R., Klein, D., Nell, B., 2017. Mutation analysis and gene expression profiling of ocular melanomas in cats. Vet. Comp. Oncol. 15, 1403–1416.
- Schnaeker, E.-M., Ossig, R., Ludwig, T., Dreier, R., Oberleithner, H., Wilhelmi, M., Schneider, S.W., 2004. Microtubule-Dependent Matrix Metalloproteinase-2/Matrix Metalloproteinase-9 Exocytosis. Cancer Res. 64, 8924–8931.
- Shain, A.H., Bastian, B.C., 2016. From melanocytes to melanomas. Nat. Rev. Cancer 16, 345–358.
- Shellman, Y.G., Makela, M., Norris, D.A., 2006. Induction of secreted matrix metalloproteinase-9 activity in human melanoma cells by extracellular matrix proteins and cytokines. Melanoma Res. 16, 207–211.
- Shi, H., Liu, L., Liu, L., Geng, J., Chen, L., 2015. Inhibition of tumor growth by β-elemene

through downregulation of the expression of uPA, uPAR, MMP-2, and MMP-9 in a murine intraocular melanoma model. Melanoma Res. 25, 15–21.

- Shields, C.L., Kaliki, S., Hutchinson, A., Nickerson, S., Patel, J., Kancherla, S., Peshtani, A., Nakhoda, S., Kocher, K., Kolbus, E., Jacobs, E., Garoon, R., Walker, B., Rogers, B., Shields, J.A., 2013. Iris Nevus Growth into Melanoma: Analysis of 1611 Consecutive Eyes. Ophthalmology 120, 766–772.
- Shureiqi, I., Lippman, S.M., 2001. Perspectives in Cancer Research Lipoxygenase Modulation to Reverse Carcinogenesis 1 6307–6312.
- Singh, A.D., Sisley, K., Xu, Y., Li, J., Faber, P., Plummer, S.J., Mudhar, H.S., Rennie, I.G., Kessler, P.M., Casey, G., Williams, B.G., 2007. Reduced expression of autotaxin predicts survival in uveal melanoma. Br. J. Ophthalmol. 91, 1385–1392.
- Siomi, M.C., Siomi, H., Sauer, W.H., Srinivasan, S., Nussbaum, R.L., Dreyfuss, G., 1995. FXR1, an autosomal homolog of the fragile X mental retardation gene. EMBO J. 14, 2401–8.
- Smedley, R.C., Spangler, W.L., Esplin, D.G., Kitchell, B.E., Bergman, P.J., Ho, H.Y., Bergin, I.L., Kiupel, M., 2011. Prognostic markers for canine melanocytic neoplasms: A comparative review of the literature and goals for future investigation. Vet. Pathol. 48, 54–72.
- Smith, S.H., Goldschmidt, M.H., McManus, P.M., 2002. A Comparative Review of Melanocytic Neoplasms. Vet. Pathol. 39, 651–678.
- Sorensen, K.C., Kitchell, B.E., Schaeffer, D.J., Mardis, P.E., 2004. Expression of matrix metalloproteinases in feline vaccine site-associated sarcomas. Am. J. Vet. Res. 65, 373–9.
- Spangler, W.L., Kass, P.H., 2006. The histologic and epidemiologic bases for prognostic considerations in canine melanocytic neoplasia. Vet. Pathol. 43, 136–149.
- Spencer, K.R., Mehnert, J.M., 2016. Melanoma 167.
- Spencer, W.H., 1996. “Opthalmic Pathology: an atlas and textbook”, fourth edition; 2121-2168. Saunders, Philadelphia, USA.
- Spiliopoulos, K., Peschos, D., Batistatou, A., Ntountas, I., Agnantis, N., Kitsos, G., 2015. Vasculogenic mimicry: lessons from melanocytic tumors. In Vivo 29, 309–17.
- Spiliopoulos, K., Peschos, D., Batistatou, A., Ntountas, I., Papoudou-Bai, A., Zioga, A.,

Agnantis, N., Kitsos, G., 2017. Immunohistochemical Study of Vasculogenic Mimicry and Angiogenesis in Melanocytic Tumors of the Eye and the Periocular Area. Anticancer Res. 37, 1113–1120.

- Starr, O.D., Patel, D. V, Allen, J.P., McGhee, C.N., 2004. Iris melanoma: pathology, prognosis and surgical intervention. Clin. Exp. Ophthalmol. 32, 294–296.
- Sun, Z., Sood, S., Li, N., Ramji, D., Yang, P., Newman, R.A., Yang, C.S., Chen, X., 2006. Involvement of the 5-lipoxygenase/leukotriene A4 hydrolase pathway in 7,12-dimethylbenz[a]anthracene (DMBA)-induced oral carcinogenesis in hamster cheek pouch, and inhibition of carcinogenesis by its inhibitors. Carcinogenesis 27, 1902–1908.
- Sveinbjörnsson, B., Rasmuson, A., Baryawno, N., Wan, M., Pettersen, I., Ponthan, F., Orrego, A., Haeggström, J.Z., Johnsen, J.I., Kogner, P., 2008. Expression of enzymes and receptors of the leukotriene pathway in human neuroblastoma promotes tumor survival and provides a target for therapy. FASEB J. 22, 3525–3536.
- Tang, Z.-Y., Liu, Y., Liu, L.-X., Ding, X.-Y., Zhang, H., Fang, L.-Q., 2013. RNAi-mediated MMP-9 silencing inhibits mouse melanoma cell invasion and migration in vitro and in vivo. Cell Biol. Int. 37, 849–54.
- Tímár, J., Vizkeleti, L., Doma, V., Barbai, T., Rásó, E., 2016. Genetic progression of malignant melanoma. Cancer Metastasis Rev. 35, 93–107.
- van der Velden, P.A., Zuidervaart, W., Hurks, M.H.M.H., Pavey, S., Ksander, B.R., Krijgsman, E., Frants, R.R., Tensen, C.P., Willemze, R., Jager, M.J., Gruis, N.A., 2003. Expression profiling reveals that methylation of TIMP3 is involved in uveal melanoma development. Int. J. cancer 106, 472–9.
- van der Weyden, L., Patton, E.E., Wood, G.A., Foote, A.K., Brenn, T., Arends, M.J., Adams, D.J., 2016. Cross-species models of human melanoma. J. Pathol. 238, 152–65.
- Van Raamsdonk, C.D., Griewank, K.G., Crosby, M.B., Garrido, M.C., Vemula, S., Wiesner, T., Obenauf, A.C., Wackernagel, W., Green, G., Bouvier, N., Sozen, M.M., Baimukanova, G., Roy, R., Heguy, A., Dolgalev, I., Khanin, R., Busam, K., Speicher, M.R., O'Brien, J., Bastian, B.C., 2010. Mutations in GNA11 in uveal melanoma. N. Engl. J. Med. 363, 2191–9.

- Uzal, F.A., Plattner, B.L., Hostetter, J.M., 2016. Alimentary System; 26-27. In “Pathology of Domestic Animals”, sixth edition, edited by M. Grant Maxie. Elsevier, New York, USA.
- Visse, R., Nagase, H., 2003. Matrix metalloproteinases and tissue inhibitors of metalloproteinases: structure, function, and biochemistry. Circ. Res. 92, 827–39.
- Wang, H., Lin, H., Pan, J., Mo, C., Zhang, F., Huang, B., Wang, Z., Chen, X., Zhuang, J., Wang, D., Qiu, S., 2016. Vasculogenic Mimicry in Prostate Cancer: The Roles of EphA2 and PI3K. J. Cancer 7, 1114–1124.
- Wiggans, K.T., Reilly, C.M., Kass, P.H., Maggs, D.J., 2016. Histologic and immunohistochemical predictors of clinical behavior for feline diffuse iris melanoma. Vet. Ophthalmol. 19, 44–55.
- Wilcock, B.P., Peiffer, R.L., 1986. Morphology and Behavior of Primary Ocular Melanomas in 91 Dogs. Vet. Pathol. 23, 418–424.
- Yadav, L., Puri, N., Rastogi, V., Satpute, P., Ahmad, R., Kaur, G., 2014. Matrix metalloproteinases and cancer - roles in threat and therapy. Asian Pac. J. Cancer Prev. 15, 1085–91.
- Zachary, J.S., 2016. Inflammation and Healing; 73-131. In: “Pathologic Basis of Veterinary Disease”, sixth edition. Elsevier, New York, USA.
- Zang, M., Zhang, Y., Zhang, B., Hu, L., Li, J., Fan, Z., Wang, H., Su, L., Zhu, Z., Li, C., Yan, C., Gu, Q., Liu, B., Yan, M., 2015. CEACAM6 promotes tumor angiogenesis and vasculogenic mimicry in gastric cancer via FAK signaling. Biochim. Biophys. Acta 1852, 1020–8.
- Zhang, Y., O’Connor, J.P., Siomi, M.C., Srinivasan, S., Dutra, A., Nussbaum, R.L., Dreyfuss, G., 1995. The fragile X mental retardation syndrome protein interacts with novel homologs FXR1 and FXR2. EMBO J. 14, 5358–66.
- Zhao, N., Sun, B.-C., Zhao, X.-L., Wang, Y., Meng, J., Che, N., Dong, X.-Y., Gu, Q., 2015. Role of Bcl-2 and its associated miRNAs in vasculogenic mimicry of hepatocellular carcinoma. Int. J. Clin. Exp. Pathol. 8, 15759–68.

LIST OF PHD ACTIVITIES AND PUBLICATIONS

Attendance to courses, seminars, workshops and scientific meetings

III year

Congresses:

- ESVP-ECVP annual Congress, 5th-8th September 2018, Cluj-Napoca, Romania

- Veterinary and Animal Science Days 2018, 6th - 8th June 2018, Milan, Italy

Seminars, meetings and courses:

- Seminar “Le produzioni di montagna: una risorsa dal territorio”, Bosco Chiesanuova (VR), 12th May 2018 (5 h)

- PhD courses: Medical statistic 3, Communication 3; Transferrable skill courses.

II year

Congresses:

- Congress Veterinary and Animal Science Days 2017, 6th - 8th June 2017, Milan, Italy.

Seminars, meetings and courses:

- Seminar “Strumentazioni innovative a supporto della ricerca nazionale”, ThermoFisher Scientific, Milano, 13th December 2016 (8 h)

- Meeting “Il diploma di specializzazione veterinaria – I colleges europei e come diventare specialista europeo”, Milano, 28th September 2017

- ECVP/ESVP Summer school in Veterinary Pathology, Berlin, 17th-28th July 2017, (88 h), attendance sponsored by ESVP summer school stipend

- Courses: “Pathology of laboratory animals” (8 hr) and “Zoo animal pathology” (6 hr), followed by final examination, at the Ohio State University, March-May 2017

- PhD courses: Medical statistic 2, Communication 2; Transferrable skill courses.

I year

Congresses:

- Congress 34th ESVP – 27th ECVP Annual Meeting, Bologna, 7th-10th September 2016, attendance sponsored by the Journal of Comparative Pathology Educational Trust travel bursary

- Congress Veterinary and Animal Science Days 2016, 8th - 10th June 2016, Milan, Italy.

Seminars, meetings and courses:

- Course Sistema Bibliotecario di Ateneo "PubMed", Milano, 17th December 2015, (6 h)

- Seminar "Correlative and super-resolution microscopy", Pavia, 4th February 2016

- ECVP/ESVP Summer school in Veterinary Pathology, Berlin, 18th -29th July 2016, (88 h), attendance sponsored by ECVP summer school stipend

- Davis Thompson Foundation European Symposium, Bologna, 6th-7th September 2016, (13 h)

- PhD courses: Medical statistic 1, Communication 1, Digital imaging and image integrity in scientific publication, Genomics of pathology; Transferrable skill courses.

Visit to external laboratories

III year

- Visitor at Dipartimento di Scienze Agroalimentari, Ambientali e Animali, Università di Udine, Udine, 30th October – 3rd November 2017.

II year

- Visitor at Molecular Biology Laboratory, Institute for Pharmacological Research "Mario Negri", Milano, 15th-16th-17th November 2016.

- Visitor at the Service of Applied Pathology, Department of Veterinary Biosciences, the Ohio State University, Columbus (OH), United States, 13th March-12th May 2017.

Publications and conference presentations

2017-2018

Full papers

- Nordio L., Stornelli V., Franzo G., Giudice C. "Expression of MMP-9 and TIMP-2 in feline diffuse iris melanoma and correlation with histological grade and mitotic index". *Manuscript in preparation.*

- Nordio L., Bazzocchi C., Genova F., Serra V., Longeri M.L., Rondena M., Stefanello D., Giudice C. "Molecular and immunohistochemical expression of LTA4H and FXR1 in canine oral melanomas". *Manuscript in preparation.*

- Nordio L., Perelli M., Multari D., Giudice C. "Lacrimal gland tumors in dogs: a histological and immunohistochemical study". *Manuscript in preparation.*

- Nordio L., Fattori S., Vascellari M., Giudice C. (2018). "Evidence of vasculogenic mimicry in a palpebral melanocytoma in a dog". *Journal of Comparative Pathology*, 162, 43-46.

- Nordio L., Marques A. T., Lecchi C., Stefanello D., Giudice C. (2018). "Immunohistochemical expression of FXR1 in canine normal tissues and melanomas". *Journal of Histochemistry and Cytochemistry*, 66:585-593.

Conference presentations

- Nordio L., Stornelli V., Giudice C. (2018). "Expression of MMP-9 and TIMP-2 in feline diffuse iris melanoma: correlation with histological grade and mitotic index". Joint ESVP/ECVP European Congress, Cluj-Napoca, 5th-8th September 2018 (poster flash presentation).

- Nordio L., Parker V.J., Martinez M., Lorbach J.N., Jennings R., Cianciolo R.E. (2018). "Co-occurence of calcinosis cutis and calcinosis circumscripta in a young Boxer dog". Joint ESVP/ECVP European Congress, Cluj-Napoca, 5th-8th September 2018 (poster presentation).

- Nordio L., Stornelli V., Giudice C. (2018). "MMP-9 immunohistochemical expression is correlated with histologic grade in feline diffuse iris melanoma". Proceeding of Veterinary and Animal Science Days 2018, 6th-8th June 2018, Milano (oral presentation). *International Journal of Health, Animal Science and Food safety*, 5.

- Nordio L. (2018). "The veterinary specialization training in the United States: an experience as visiting resident at The Ohio State University", invited oral presentation at the seminar "Le produzioni di montagna: una risorsa dal territorio", Bosco Chiesanuova (VR), 12th May 2018.

- Multari D., Giudice C., Nuti M., Nordio L., Falzone C. (2018). "A case of third eyelid hibernoma in a dog". European College of Veterinary Opthalmology (ECVO) Conference, 10th-13th May 2018, Florence, Italy (poster presentation).

2016-2017

Full papers

- Barzago M.M., Kurosaki M., Fratelli M., Bolis M., Giudice C., Nordio L., Cerri E., Domenici L., Terao M., Garattini E. (2017) “Generation of a new mouse model of glaucoma characterized by reduced expression of the AP-2β and AP-2δ proteins". *Scientific Reports*, 7: 11140.

- Marques A.T., Nordio L., Lecchi C., Grilli G., Giudice C., Ceciliani F. (2017). “Widespread extrahepatic expression of acute-phase proteins in healthy chicken (Gallus gallus) tissues”. *Veterinary Immunology and Immunopathology,* 190: 10-17.

- Nordio L., Fattori S., Giudice C. (2017). “Fibrosarcoma of the eyelid in two sibling Czech wolfdogs”. *Open Veterinary Journal*, 7(2): 95-99.

Conference presentations

- Nordio L., Genova F., Serra V., Bazzocchi C., Longeri M.L., Stefanello D., Rondena M., Giudice C. (2017). “LTA4H and FXR1 gene and protein expression in canine oral melanoma”. 3rd Joint European Congress of the ESVP, ESTP and ECVP, Lyon, 30th August-2nd September 2017 (poster presentation).

- Nordio L., Perelli N., Multari D, Giudice C. (2017). “Lacrimal gland tumors in dogs: a histological and immunohistochemical study”. 3rd Joint European Congress of the ESVP, ESTP and ECVP, Lyon, 30th August-2nd September 2017 (poster presentation).

- Nordio L., Marques A. F. T. (2017). “Validation of anti-FXR1 antibodies in the canine species and application to an immunohistochemical study of canine oral melanomas”. Proceeding of Veterinary and Animal Science Days 2017, 6th-8th June 2017, Milano (oral presentation). *International Journal of Health, Animal Science and Food safety,* 4.

2015-2016

Full papers

- Nordio L., Vascellari M., Berto G., Bano L. (2016). “Squamous cell carcinoma of the oropharynx and esophagus with pulmonary metastasis in a backyard laying hen”. *Avian Diseases*, 60, 694-697

Conference presentations

- Nordio L., Genova F., Serra V., Bazzocchi C., Longeri M.L., Stefanello D., Giudice C. (2016). "LTA4H expression in canine oral melanomas: preliminary results". 34th ESVP – 27th ECVP Annual Meeting, Bologna, 7th-10th September 2016 (poster presentation), *Journal of Comparative Pathology* 2017, Vol. 156, 54-141, ESVP and ECVP Proceedings 2016.

- Nordio L., Genova F., Serra V., Giudice C. (2016). "LTA4H expression in canine oral melanomas: methodological set up and preliminary results". Proceeding of Veterinary and Animal Science Days 2016, 8th - 10th June 2016, Milan, Italy (oral presentation). *International Journal of Health, Animal Science and Food safety*, 3.

- Marques A.T., Lecchi C., Nordio L., Giudice C., Grillli G., Ariño-Bassols H., Ceciliani F. (2016) "Widespread extrahepatic expression of acute phase proteins in chicken (Gallus gallus) tissues". Proceeding of Veterinary and Animal Science Days 2016, 8th - 10th June 2016, Milan, Italy. *International Journal of Health, Animal Science and Food safety*, 3.

Bursaries and awards

- Scholarship Award from Associazione Giovanni Vincenzi, Verona, for the report "Il training di specializzazione veterinaria negli Stati Uniti: esperienza come visiting resident in anatomia patologica alla Ohio State University", May 2018

- ESVP summer school stipend for the attendance of ESVP/ECVP summer school, July 2017

-Journal of Comparative Pathology Educational Trust travel bursary for the attendance of ESVP/ECVP Annual Meeting, September 2016

- ECVP summer school stipend for the attendance of ESVP/ECVP summer school, July 2016

Any other relevant activity

- Instructor of Practical lectures on Neuropathology of Domestic Animals, within the course "Morphological and molecular basis of the Central Nervous System and its Pathologies – Degree course in Veterinary Biotechnology Sciences" (held by Prof. Fabrizio Ceciliani); April-May 2018 (8 h).

- Involvement in the Anatomic Pathology laboratory diagnostic activity (necropsy and histopathology) related to the Veterinary Hospital (2016-2018; 1 week on duty every 4 weeks for necropsy, 2 weeks/month for histopathology).

- Weekly training post lauream European Board of Veterinary Specialisation: approved and registered residency training program by ECVP - European College of Veterinary Pathologists, Tutor: Prof. Chiara Giudice, Head of the program: Prof. Paola Roccabianca (5 h every Friday); 2015 – 2018.

- Organizer of the Anatomic Pathology Weekly Journal Club 2017-2018, included in the ECVP training program (2015-2018).

- Co-supervision of the degree thesis “Ghiandole lacrimali orbitali nella specie canina e felina: frequenza, distribuzione, caratteristiche istologiche ed immunoistochimiche dei tumori ghiandolari delle ghiandole lacrimale principale e nittitante”, candidate Novella Perelli, supervisor Dr. Chiara Giudice, co-supervisor Dr. Laura Nordio, October 2016.

ATTACHED PAPERS

i. **Nordio L**., Fattori S., Vascellari M., Giudice C (2018). “Evidence of vasculogenic mimicry in a palpebral melanocytoma in a dog*”. Journal of Comparative Pathology*, 162: 43-46.

ii. **Nordio L**., Marques A.T., Lecchi C., Luciano A.M., Stefanello D., Giudice C. (2018). “Immunohistochemical Expression of FXR1 in Canine Normal Tissues and Melanomas”. *Journal of Histochemistry & Cytochemistry*, 66: 585 – 593.

iii. Barzago M.M., Kurosaki M., Fratelli M., Bolis M., Giudice C., **Nordio L**., Cerri E., Domenici L., Terao M., Garattini E. (2017) “Generation of a new mouse model of glaucoma characterized by reduced expression of the AP-2β and AP-2δ proteins". *Scientific Reports*, 7: 11140

iv. Marques A.T., **Nordio L**., Lecchi C., Grilli G., Giudice C., Ceciliani F. (2017). “Widespread extrahepatic expression of acute-phase proteins in healthy chicken (Gallus gallus) tissues”. *Veterinary Immunology and Immunopathology*, 190: 10-17.

v. **Nordio L**., Fattori S., Giudice C. (2017). “Fibrosarcoma of the eyelid in two sibling Czech wolfdogs”. *Open Veterinary Journal*, 7(2): 95-99.

vi. **Nordio L.,** Vascellari M., Berto G., Bano L. (2016). “Squamous cell carcinoma of the oropharynx and esophagus with pulmonary metastasis in a backyard laying hen”. *Avian Diseases*, 60, 694-697.